Interdisciplinary Physics of the Sun
Spanish-German WE-Heraeus-Seminar
29 June – 04 July 2025, Bad Honnef

Solar magnetohydrodynamics: Paradigmatic liquid-metal experiments and some theoretical aspects

Frank Stefani

With thanks to:

Agris Gailitis (Riga), Gunter Gerbeth, André Giesecke, Thomas Gundrum, Rainer Hollerbach (Leeds), Laurène Jouve (Toulouse), George Mamatsashvili, Ashish Mishra, Günther Rüdiger (Potsdam), Martin Seilmayer, Rodion Stepanov (Perm), Tom Weier…

HZDR
HELMHOLTZ ZENTRUM DRESDEN ROSSENDORF

Motivation and schedule

1) Alfvén waves

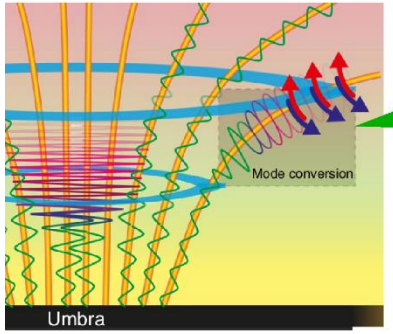

2) Convection

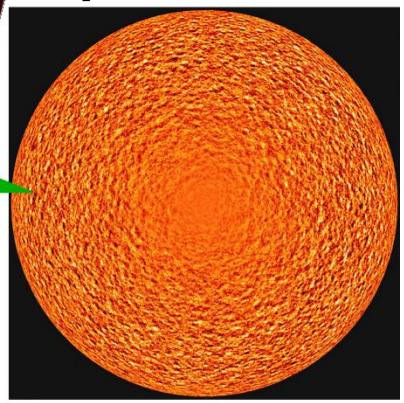

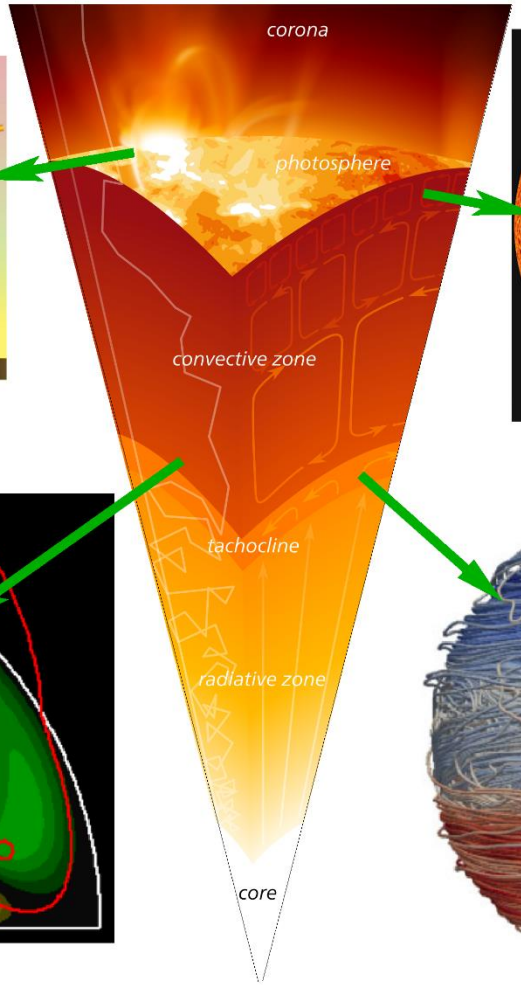

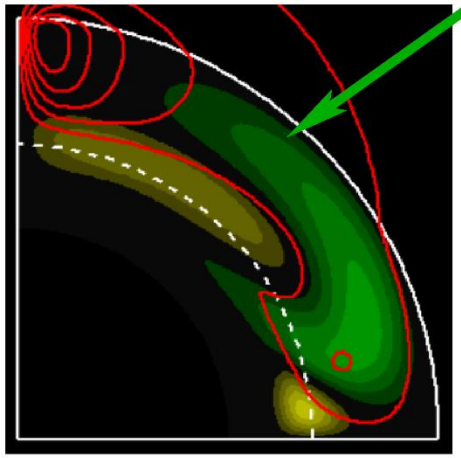

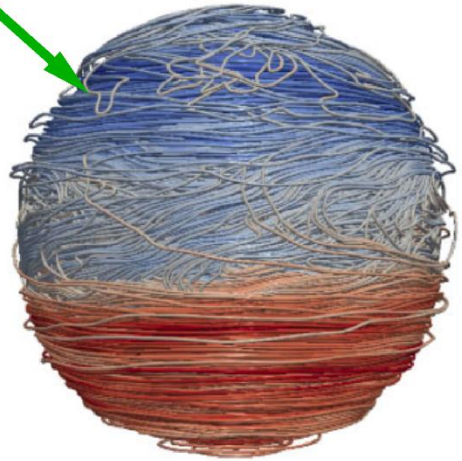

4) Dynamo:

Theory and Experiment

3) Magnetorotational instability etc…

Motivation and schedule

1) Alfvén waves

2) Convection

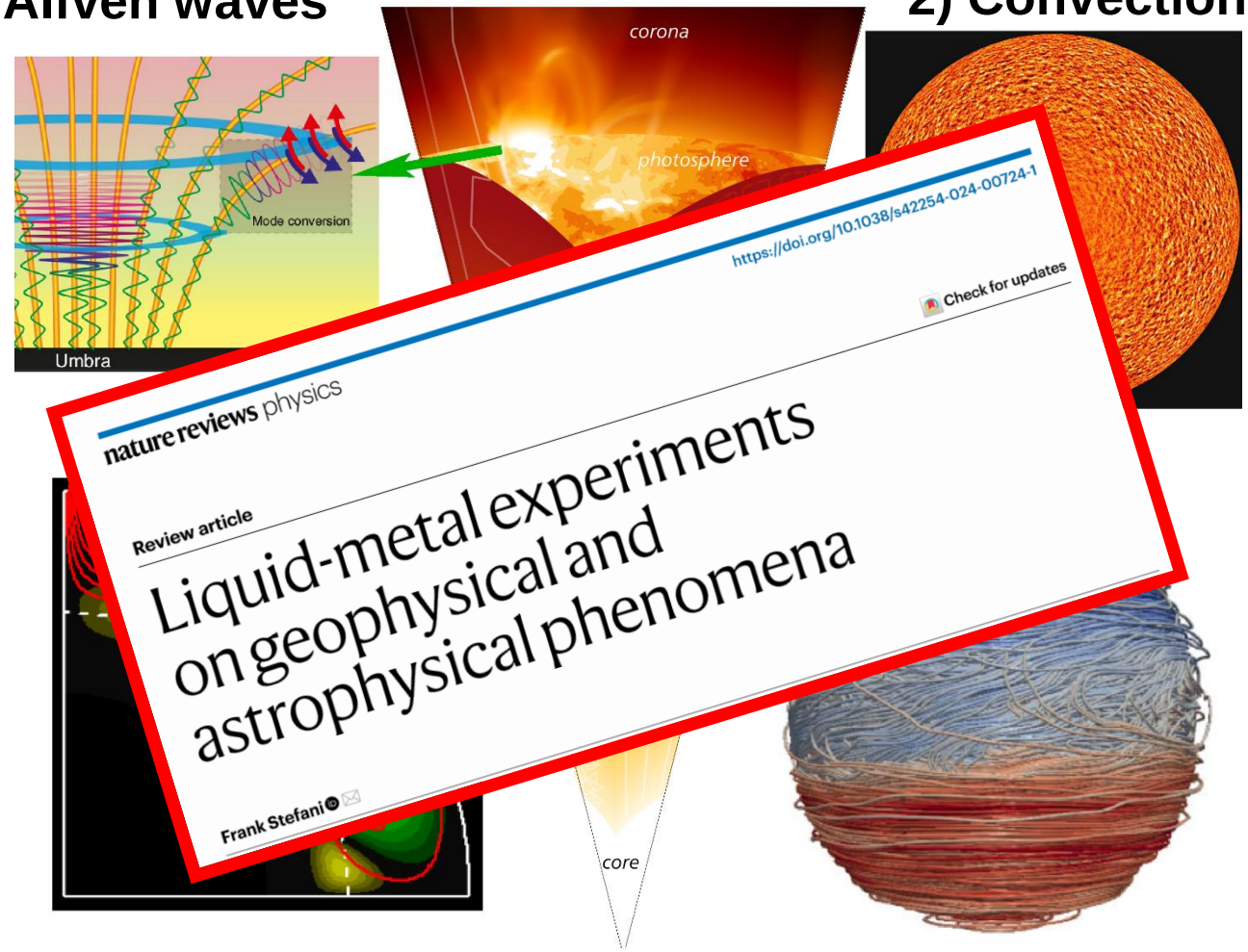

nature reviews physics

Review article

https://doi.org/10.1038/s42254-024-00724-1

Check for updates

Liquid-metal experiments on geophysical and astrophysical phenomena

Frank Stefani

4) Dynamo:

Theory and Experiment

3) Magnetorotational instability etc…

DRESDEN concept

HZDR

Magnetohydrodynamics: Basic theory

Induction equation for magnetic field **B**

$$\frac{\partial \mathbf{B}}{\partial t} = \nabla \times (\mathbf{v} \times \mathbf{B}) + \frac{1}{\mu_0 \sigma} \Delta \mathbf{B}$$

Governing parameter:
Magnetic Reynolds number

$$Rm = \mu_0 \sigma L V$$

Navier-Stokes equation for velocity field **v**

$$\frac{\partial \mathbf{v}}{\partial t} + (\mathbf{v} \cdot \nabla)\mathbf{v} = -\frac{\nabla p}{\rho} + \frac{1}{\mu_0 \rho}(\nabla \times \mathbf{B}) \times \mathbf{B} + \nu \Delta \mathbf{v} + \mathbf{f}_{extern}$$

Governing parameters:
Reynolds, Hartmann

$$\mathrm{Re} = \frac{LV}{\nu}$$

$$Ha = BL\sqrt{\frac{\sigma}{\rho \nu}}$$

Alternatively: Lundquist number

$$Lu = Pm^{1/2}\, Ha$$

…using the magnetic Prandtl number

$$Pm = \nu\, \mu_0\, \sigma$$

Alfvén waves

Alfvén waves: Prediction by H. Alfvén 1942 (Nobel prize 1970)

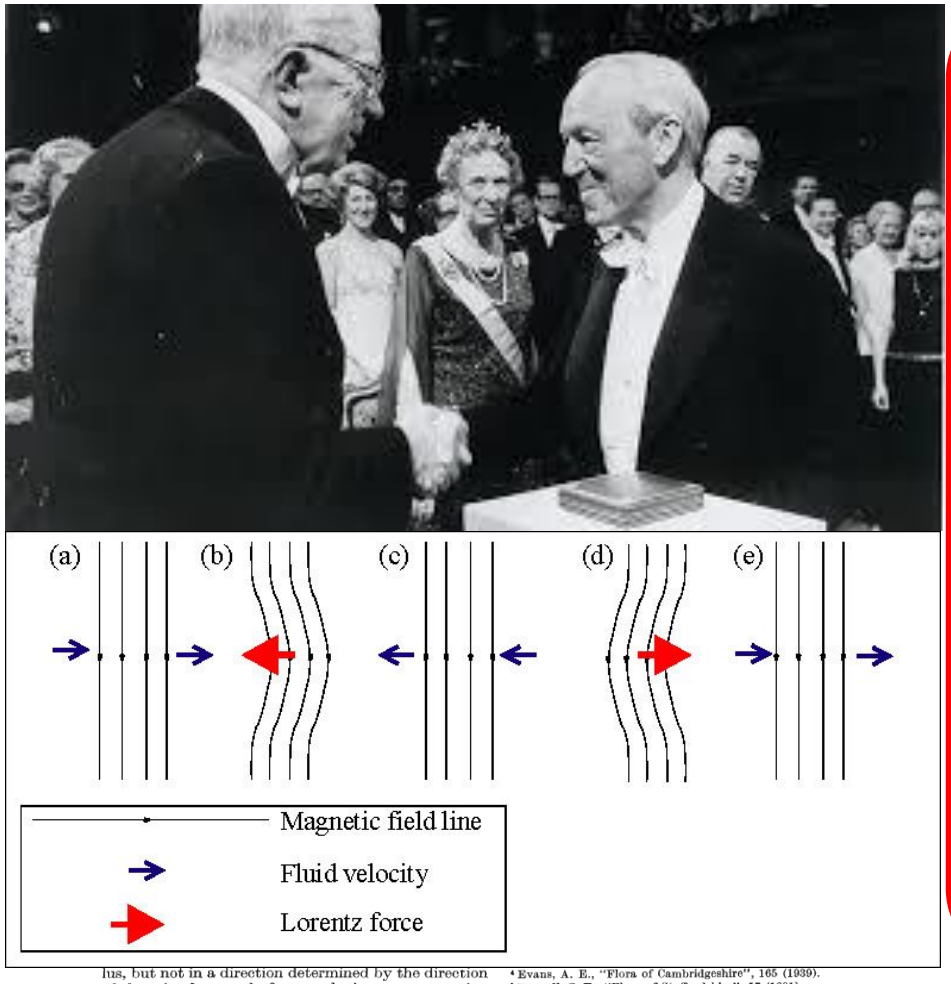

lus, but not in a direction determined by the direction of the stimulus—and often producing an aggregating effect superficially similar to that of a taxis; and an *orientation*, which is the placing of the body (usually if not always animal) in a direction determined by the direction of the stimulus. To these three classes many of the cases can be referred.

But the responses of sessile plant organs do not seem to be so conveniently classified. The thigmotropism of Clematis tendrils appears to warrant that name, for the response is a directional one. But the same cannot be said of the so-called 'thigmotropism' of Mimosa leaflets, Mimulus stigma or Berberis

[4] Evans, A. E., "Flora of Cambridgeshire", 165 (1939).
[5] Bagnall, J. E., "Flora of Staffordshire", 57 (1901).
[6] Britton, C. E., *J. Bot.*, **48**, 186 (1910).

Existence of Electromagnetic-Hydrodynamic Waves

If a conducting liquid is placed in a constant magnetic field, every motion of the liquid gives rise to an E.M.F. which produces electric currents. Owing to the magnetic field, these currents give mechanical forces which change the state of motion of the liquid.

Thus a kind of combined electromagnetic-hydrodynamic wave is produced which, so far as I know, has as yet attracted no attention.

The phenomenon may be described by the electrodynamic equations

$$\text{rot } H = \frac{4\pi}{c} i$$

$$\text{rot } E = -\frac{1}{c}\frac{dB}{dt}$$

$$B = \mu H$$

$$i = \sigma(E + \frac{v}{c} \times B);$$

together with the hydrodynamic equation

$$\partial \frac{dv}{dt} = \frac{1}{c}(i \times B) - \text{grad } p,$$

where σ is the electric conductivity, μ the permeability, ∂ the mass density of the liquid, i the electric current, v the velocity of the liquid, and p the pressure.

Consider the simple case when $\sigma = \infty$, $\mu = 1$ and the imposed constant magnetic field H_0 is homogeneous and parallel to the z-axis. In order to study a plane wave we assume that all variables depend upon the time t and z only. If the velocity v is parallel to the x-axis, the current i is parallel to the y-axis and produces a variable magnetic field H' in the x-direction. By elementary calculation we obtain

$$\frac{d^2H'}{dz^2} = \frac{4\pi\partial}{H_0^2}\frac{d^2H'}{dt^2},$$

which means a wave in the direction of the z-axis with the velocity

$$V = \frac{H_0}{\sqrt{4\pi\partial}}.$$

Waves of this sort may be of importance in solar phy[illegible] field, and as solar matter is a good conductor, the conditions for the existence of electromagnetic-hydrodynamic waves are satisfied. If in a region of the sun we have $H_0 = 15$ gauss and $\partial = 0{\cdot}005$ gm. cm.$^{-3}$, the velocity of the waves amounts to

$$V \sim 60 \text{ cm. sec.}^{-1}.$$

This is about the velocity with which the sunspot zone moves towards the equator during the sunspot cycle. The above values of H_0 and ∂ refer to a distance of about 10^{10} cm. below the solar surface where the original cause of the sunspots may be found. Thus it is possible that the sunspots are associated with a magnetic and mechanical disturbance proceeding as an electromagnetic-hydrodynamic wave.

The matter is further discussed in a paper which will appear in *Arkiv för matematik, astronomi och fysik*.

H. Alfvén.

Kgl. Tekniska Högskolan,
Stockholm.

Energy of Dissociation of Carbon Monoxide

The energies of dissociation of a number of diatomic molecules have been determined from spectroscopic data, apparently with high accuracy, by the observation of predissociation limits. During the last few years the following values have been proposed for CO: $D(\text{CO}) = 6{\cdot}92$ [1], $8{\cdot}41$ [3], $9{\cdot}14$ [3], $10{\cdot}45$ [4] e.v.; while values of $9{\cdot}85$ and $11{\cdot}11$ also appear possible[3]. Controlled electron experiments suggest $9{\cdot}6$ [5].

The value obtained by extrapolation of the vibrational levels of the ground state is about 11, and support for this value has been given by Kynch and Penney[6]. Herzberg[7] has recently summarized evidence favouring $9{\cdot}14$.

At first sight, the strongest argument for $9{\cdot}14$ is the observation by Faltings, Groth and Harteck[8] that CO is decomposed by the xenon line at 1295 A., but not by that at 1470 A., from which they conclude that $8{\cdot}44 < D(\text{CO}) < 9{\cdot}57$. This conclusion is not based on an examination of the initial act of absorption. The only known absorption in the 1295 A. region is that corresponding to the fourth positive bands. The origins of the (9,0) and (10,0) bands lie at 76,839 cm.$^{-1}$ and 78,010 cm.$^{-1}$. The xenon line 1295 A. = 77,172 cm.$^{-1}$ falls between these bands and, if absorbed from the lowest vibrational level of CO, would correspond approximately to the line $P(35)$ of (10,0). This gives as the upper limit of $D(\text{CO})$ (when the rotational energy is taken into account) a value of 79,722 cm.$^{-1}$ = 9·88 e.v. (not 9·57 e.v. as stated by Herzberg[7]). Actually, it is doubtful whether such a high rotational line as $P(35)$ would be observed at room temperature, and absorption, if it is due to CO, would probably occur from a higher vibrational level, corresponding perhaps to the (13,2) band, in which case the dissociation limit may be placed as high as $10{\cdot}1$.

Taking the first act of absorption as

$$\text{CO}(X^1\Sigma) + h\nu = \text{CO}(A^1\Pi),$$

and assuming a life not less than 10^{-8} sec. for $A^1\Pi$, when at atmospheric pressure each molecule experiences at least 100 collisions before radiating. It seems to us that this gives a reasonable chance for a reaction such as

$$\text{CO}(A^1\Pi) + \text{CO}(X^1\Sigma) = \text{CO}_2 + \text{C}$$

to proceed with quantum efficiency approaching unity. The state of the carbon atom might be either ^1D or ^1P; the former if spin is to be conserved, the latter if not. In either case the reaction is strongly exothermic. The failure of the xenon line 1470 to induce photodissociation may be due to the reaction requiring an activation energy.

Estimates of $D(\text{CO})$ less than 10 take no account of the non-crossing rule of Hund, and Neumann and Wigner[9]. This rule states that potential energy curves of molecular states of identical species cannot cross. Whether the rule is rigorous when the nuclear and electronic motions are not separated needs further examination, but at least we see no reason for anticipating a failure of the rule in the lowest energy curve of CO. If this curve has only one turning point then the non-crossing rule requires unequivocally that $D(\text{CO}) > 10{\cdot}3$, and would agree well with the predissociation limit at $11{\cdot}11$ e.v.

The dissociation energy of CO+ is $2{\cdot}6$ e.v. less than that of CO ($D(\text{CO}^+) = D(\text{CO}) + I(\text{C}) - I(\text{CO})$). Three electronic states of CO+ are known, namely, $X^2\Sigma^+$, $A^2\Pi$ and $B^2\Sigma^+$, extrapolating to dissociation limits of about 9·8 (a very long extrapolation), 9·2 and 9·4 e.v. respectively. Since the two $^2\Sigma^+$ states must give different products of dissociation, it would appear, on the evidence of the $B^2\Sigma^+$ state, that $D(\text{CO}^+)$ is 7·4, and $D(\text{CO})$ is about 10, and on the evidence of the $A^2\Pi$ state that $D(\text{CO}^+)$ is 9·2 and $D(\text{CO})$ is 11·8. All that may fairly be deduced from present evidence on CO+ is that $D(\text{CO})$ is unlikely to be much less than 10.

We have also re-examined nitrogen. The accepted value $D(\text{N}_2) = 7{\cdot}38$ is based on the identification of the upper state of the Vegard–Kaplan bands with the

Alfvén waves: Prediction by H. Alfvén 1942 (Nobel prize 1970)

Many experiments in liquid metal and plasma

S. Lundquist, Nature **164**, 146 (1949)
B. Lehnert, Phys.Rev. **94** (1954), 815
A. Jameson, J. Fluid Mech. **19** (1964), 513
K. Iwai et al, Magnetohydrodynamics 39, 245 (2003)
T. Alboussiere et al., Phys. Fluids **23** (2011), 096601
Z. Tigrine et al., Geophys. J. Int. **219**, S83 (2019)
S. Lalloz et al., J.Fluid Mech**. 1003**, *A19 (2025)*

W. Gekelman et al., Phys. Plasmas **18** (2011), 055501

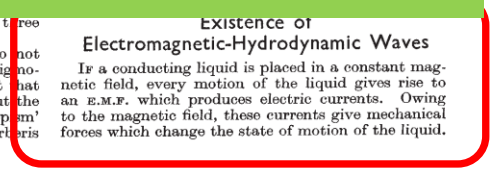

by the direction of the stimulus. To these three classes many of the cases can be referred.

But the responses of sessile plant organs do not seem to be so conveniently classified. The thigmotropism of Clematis tendrils appears to warrant that name, for the response is a directional one. But the same cannot be said of the so-called 'thigmotropism' of Mimosa leaflets, Mimulus stigma or Berberis

Existence of Electromagnetic-Hydrodynamic Waves

If a conducting liquid is placed in a constant magnetic field, every motion of the liquid gives rise to an E.M.F. which produces electric currents. Owing to the magnetic field, these currents give mechanical forces which change the state of motion of the liquid.

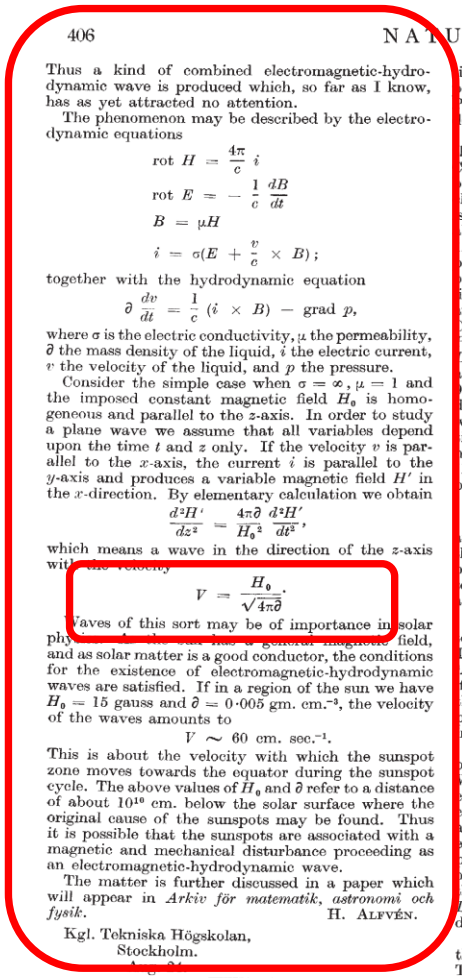

406 NATURE OCTOBER 3, 1942, Vol. 150

Thus a kind of combined electromagnetic-hydrodynamic wave is produced which, so far as I know, has as yet attracted no attention.

The phenomenon may be described by the electrodynamic equations

$$\text{rot } H = \frac{4\pi}{c} i$$

$$\text{rot } E = -\frac{1}{c}\frac{dB}{dt}$$

$$B = \mu H$$

$$i = \sigma(E + \frac{v}{c} \times B);$$

together with the hydrodynamic equation

$$\partial \frac{dv}{dt} = \frac{1}{c}(i \times B) - \text{grad } p,$$

where σ is the electric conductivity, μ the permeability, ∂ the mass density of the liquid, i the electric current, v the velocity of the liquid, and p the pressure.

Consider the simple case when $\sigma = \infty$, $\mu = 1$ and the imposed constant magnetic field H_0 is homogeneous and parallel to the z-axis. In order to study a plane wave we assume that all variables depend upon the time t and z only. If the velocity v is parallel to the x-axis, the current i is parallel to the y-axis and produces a variable magnetic field H' in the x-direction. By elementary calculation we obtain

$$\frac{d^2H'}{dz^2} = \frac{4\pi\partial}{H_0^2}\frac{d^2H'}{dt^2},$$

which means a wave in the direction of the z-axis with the velocity

$$V = \frac{H_0}{\sqrt{4\pi\partial}}.$$

Waves of this sort may be of importance in solar phy[illegible] field, and as solar matter is a good conductor, the conditions for the existence of electromagnetic-hydrodynamic waves are satisfied. If in a region of the sun we have $H_0 = 15$ gauss and $\partial = 0{\cdot}005$ gm. cm.$^{-3}$, the velocity of the waves amounts to

$$V \sim 60 \text{ cm. sec.}^{-1}.$$

This is about the velocity with which the sunspot zone moves towards the equator during the sunspot cycle. The above values of H_0 and ∂ refer to a distance of about 10^{10} cm. below the solar surface where the original cause of the sunspots may be found. Thus it is possible that the sunspots are associated with a magnetic and mechanical disturbance proceeding as an electromagnetic-hydrodynamic wave.

The matter is further discussed in a paper which will appear in *Arkiv för matematik, astronomi och fysik*.

H. Alfvén.

Kgl. Tekniska Högskolan,
Stockholm.

Energy of Dissociation of Carbon Monoxide

The energies of dissociation of a number of diatomic molecules have been determined from spectroscopic data, apparently with high accuracy, by the observation of predissociation limits. During the last few years the following values have been proposed for CO: $D(\text{CO}) = 6{\cdot}92$ [1], $8{\cdot}41$ [3], $9{\cdot}14$ [3], $10{\cdot}45$ [4] e.v.; while values of $9{\cdot}85$ and $11{\cdot}11$ also appear possible[3]. Controlled electron experiments suggest $9{\cdot}6$ [5].

The value obtained by extrapolation of the vibrational levels of the ground state is about 11, and support for this value has been given by Kynch and Penney[6]. Herzberg[7] has recently summarized evidence favouring $9{\cdot}14$.

At first sight, the strongest argument for $9{\cdot}14$ is the observation by Faltings, Groth and Harteck[8] that CO is decomposed by the xenon line at 1295 A., but not by that at 1470 A., from which they conclude that $8{\cdot}44 < D(\text{CO}) < 9{\cdot}57$. This conclusion is not based on an examination of the initial act of absorption. The only known absorption in the 1295 A. region is that corresponding to the fourth positive bands. The origins of the (9,0) and (10,0) bands lie at 76,839 cm.$^{-1}$ and 78,010 cm.$^{-1}$. The xenon line 1295 A. = 77,172 cm.$^{-1}$ falls between these bands and, if absorbed from the lowest vibrational level of CO, would correspond approximately to the line $P(35)$ of (10,0). This gives as the upper limit of $D(\text{CO})$ (when the rotational energy is taken into account) a value of 79,722 cm.$^{-1}$ = 9·88 e.v. (not $9{\cdot}57$ e.v. as stated by Herzberg[7]). Actually, it is doubtful whether such a high rotational line as $P(35)$ would be observed at room temperature, and absorption, if it is due to CO, would probably occur from a higher vibrational level, corresponding perhaps to the (13,2) band, in which case the dissociation limit may be placed as high as $10{\cdot}1$.

Taking the first act of absorption as

$$\text{CO}(X^1\Sigma) + h\nu = \text{CO}(A^1\Pi),$$

and assuming a life not less than 10^{-8} sec. for $A^1\Pi$, when at atmospheric pressure each molecule experiences at least 100 collisions before radiating. It seems to us that this gives a reasonable chance for a reaction such as

$$\text{CO}(A^1\Pi) + \text{CO}(X^1\Sigma) = \text{CO}_2 + \text{C}$$

to proceed with quantum efficiency approaching unity. The state of the carbon atom might be either ^1D or ^3P; the former if spin is to be conserved, the latter if not. In either case the reaction is strongly exothermic. The failure of the xenon line 1470 to induce photodissociation may be due to the reaction requiring an activation energy.

Estimates of $D(\text{CO})$ less than 10 take no account of the non-crossing rule of Hund, and Neumann and Wigner[9]. This rule states that potential energy curves of molecular states of identical species cannot cross. Whether the rule is rigorous when the nuclear and electronic motions are not separated needs further examination, but at least we see no reason for anticipating a failure of the rule in the lowest energy curve of CO. If this curve has only one turning point then the non-crossing rule requires unequivocally that $D(\text{CO}) > 10{\cdot}3$, and would agree well with the predissociation limit at $11{\cdot}11$ e.v.

The dissociation energy of CO+ is $2{\cdot}6$ e.v. less than that of CO ($D(\text{CO}^+) = D(\text{CO}) + I(\text{C}) - I(\text{CO})$). Three electronic states of CO+ are known, namely, $X^2\Sigma^+$, $A^2\Pi$ and $B^2\Sigma^+$, extrapolating to dissociation limits of about 9·8 (a very long extrapolation), 9·2 and 9·4 e.v. respectively. Since the two $^2\Sigma^+$ states must give different products of dissociation, it would appear, on the evidence of the $B^2\Sigma^+$ state, that $D(\text{CO}^+)$ is 7·4, and $D(\text{CO})$ is about 10, and on the evidence of the $A^2\Pi$ state that $D(\text{CO}^+)$ is 9·2 and $D(\text{CO})$ is 11·8. All that may fairly be deduced from present evidence on CO+ is that $D(\text{CO})$ is unlikely to be much less than 10.

We have also re-examined nitrogen. The accepted value $D(\text{N}_2) = 7{\cdot}38$ is based on the identification of the upper state of the Vegard–Kaplan bands with the

An underexplored aspect of Alfvén waves…

…is related to the heating of the solar corona which relies on transformation of sound waves into Alfvén waves via parametric resonance, or swing Excitation, at a point where **sound speed = Alfvén speed** (plasma β~1

T. Zaqarashvili, ApJ 552 (2001) L81

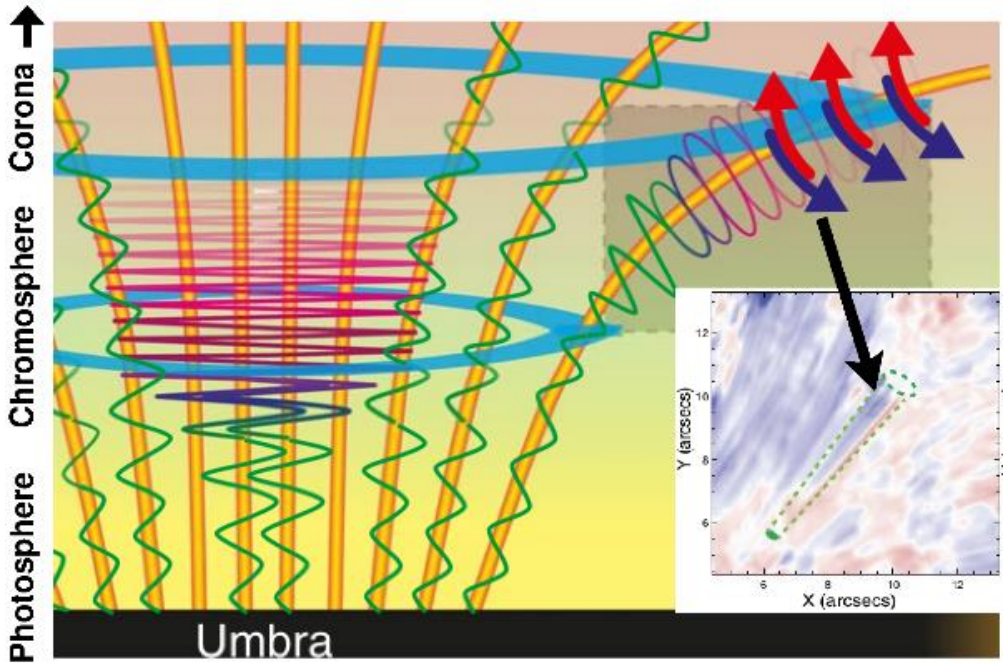

Lecture by van Doorsselaere on Friday

Grant et al., Nature Phys. 14 (2018), 480;
Srivastava et al., Sci. Rep. 7 (2017), 43147

Alfvén wave experiments at High Magnetic Field Lab at HZDR

For liquid Rubidium (dangerous!!!) we obtain Sound speed = Alfvén speed (plasma β=1) at B=54 T

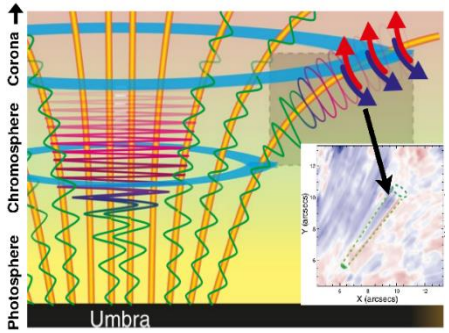

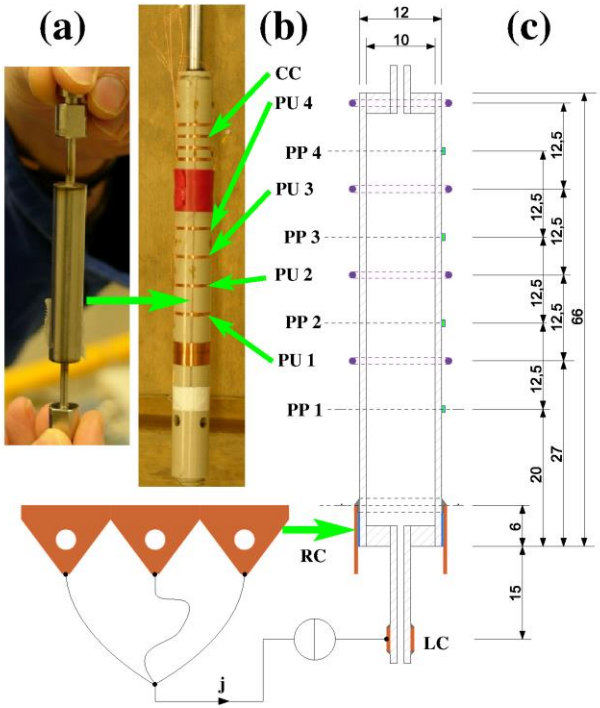

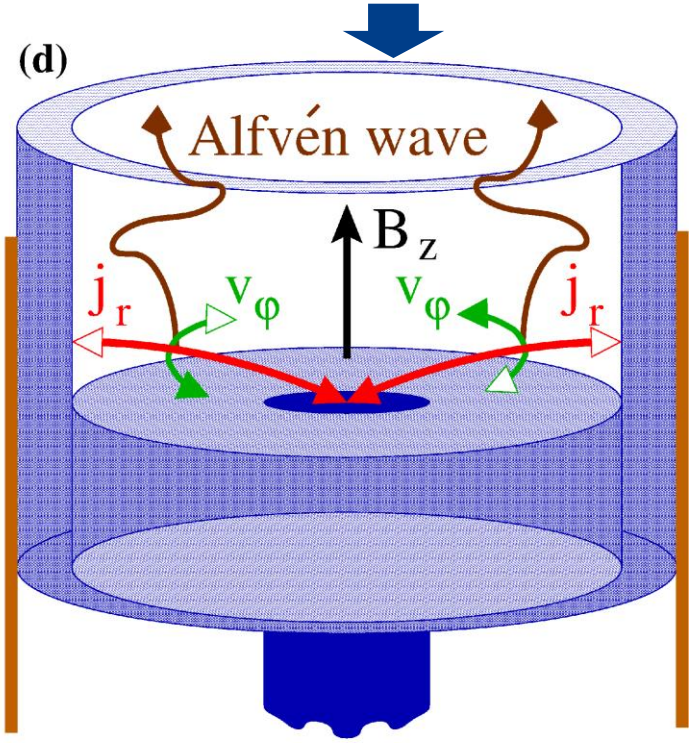

jxB excitation of torsional Alfvén waves in B up to 63 T

Alfvén wave experiments at High Magnetic Field Lab at HZDR

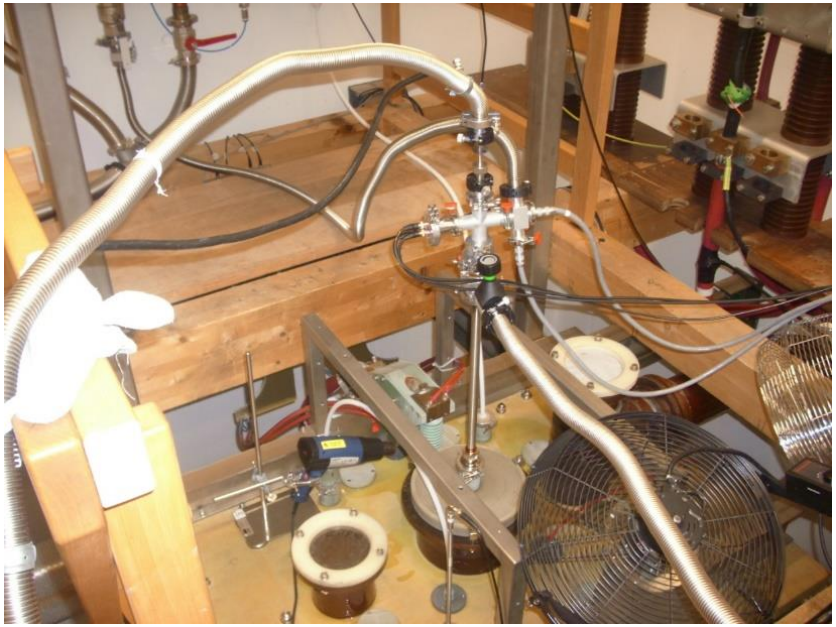

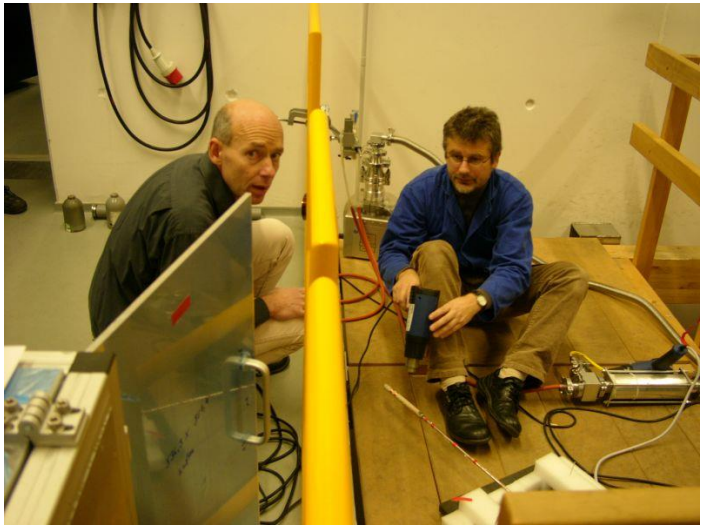

CW excitation: Voltage over bottom contact

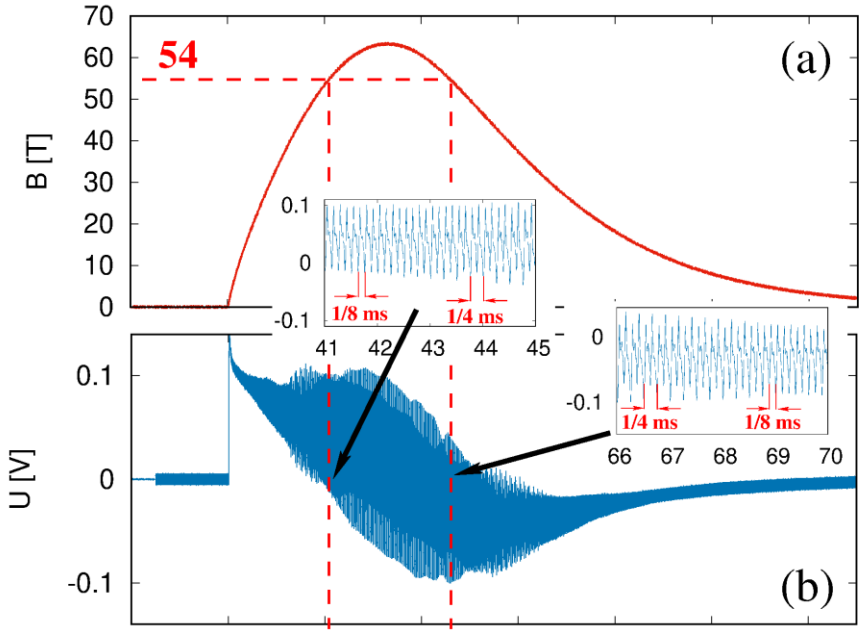

Some rough estimates:

- Excitation current: 5 A, 8 kHz CW
- Current density: ~ 100 kA/m^2
- Azimuthal acceleration: j B/ρ ~ 3000 m/s^2
- Flow velocity: ~a T/2 ~ 20 cm/s
- Induced voltage: ~vBr~50 mV

F.S. et al, Phys. Rev. Lett. 127 (2021), 275001

CW excitation: Voltage over bottom contact

- Gabor transform (short time Fourier) with von Hann window 5 ms
- PSD of 8 kHz stripe is very smooth and roughly ~ B^2
- PSD of 4 kHz stripe appears only for B=54 T (and larger)

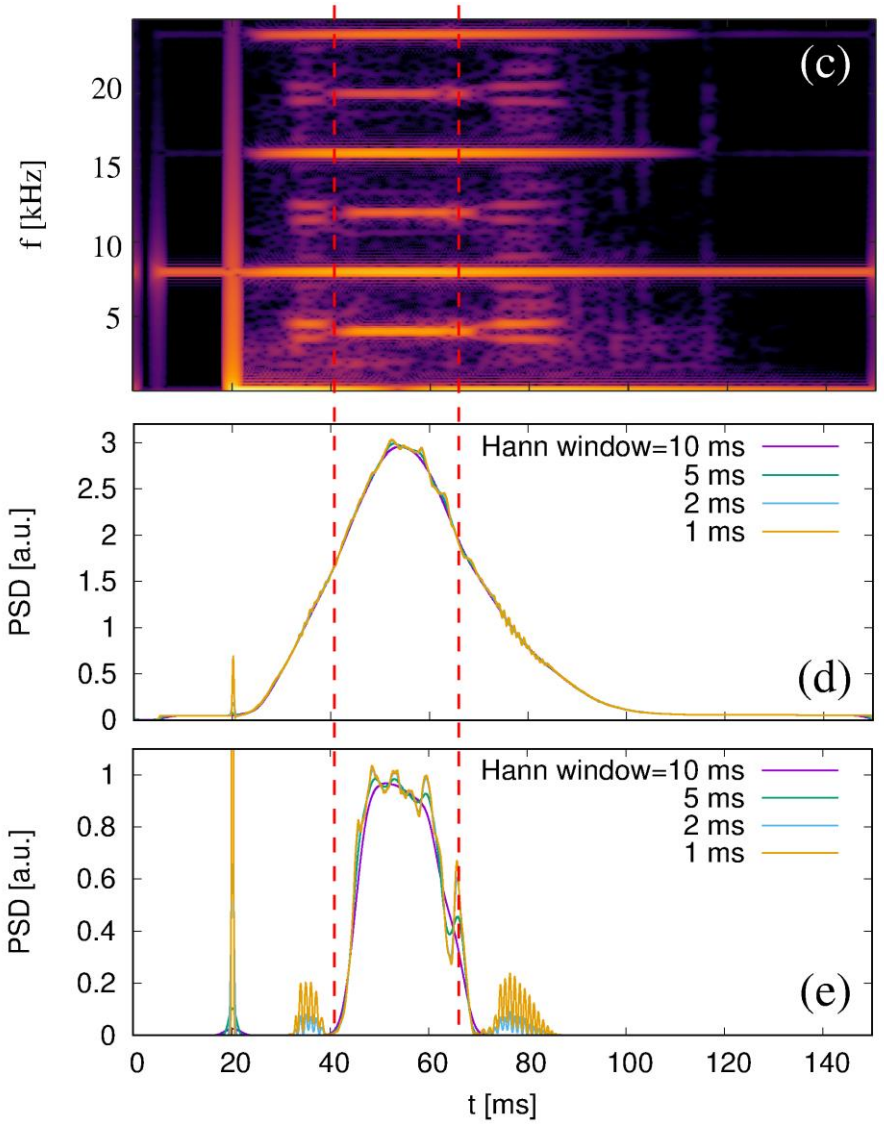

CW excitation: Dependence on magnetic field

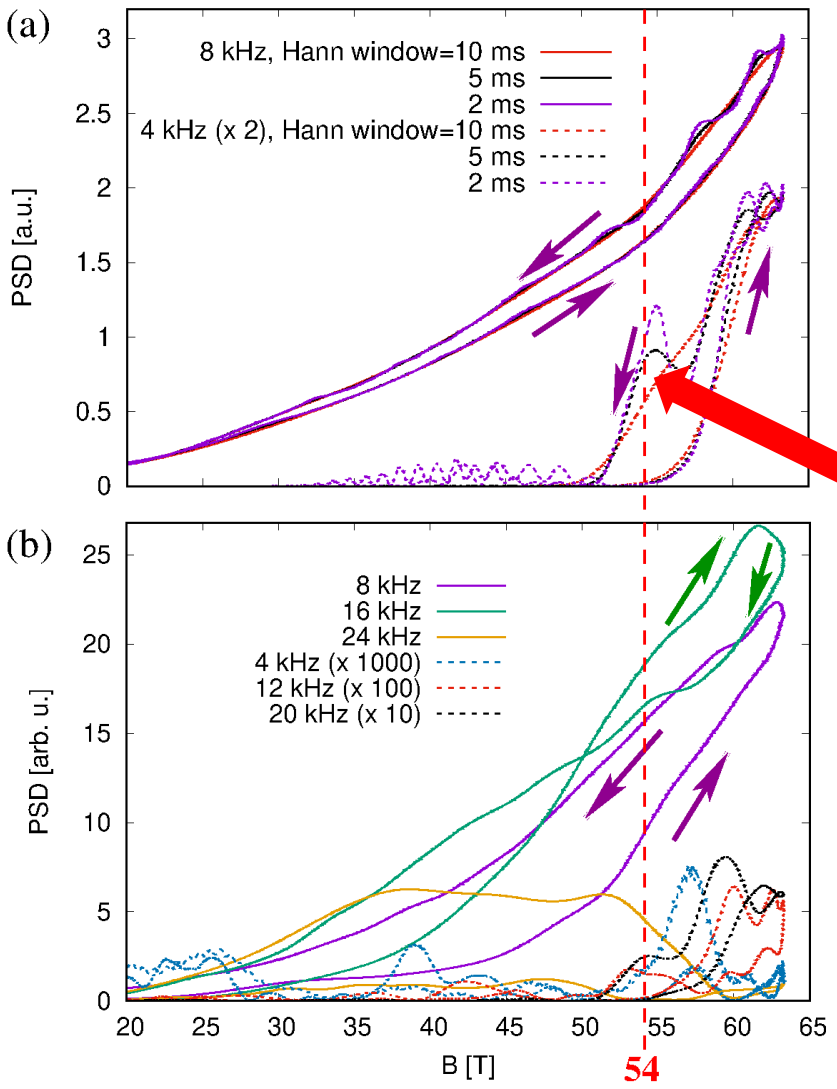

Voltage over bottom contact (indicative of Alfvén wave): PSD's for 8 kHz and 4 kHz

Period doubling due to parametric resonance (swing excitation)!!!

Voltage at pick-up coil 2 (indicative of magnetosonic waves): PSD's for n*4 kHz

Numerical simulations of parametric resonance at β=1

Density

Velocity

Magnetic field

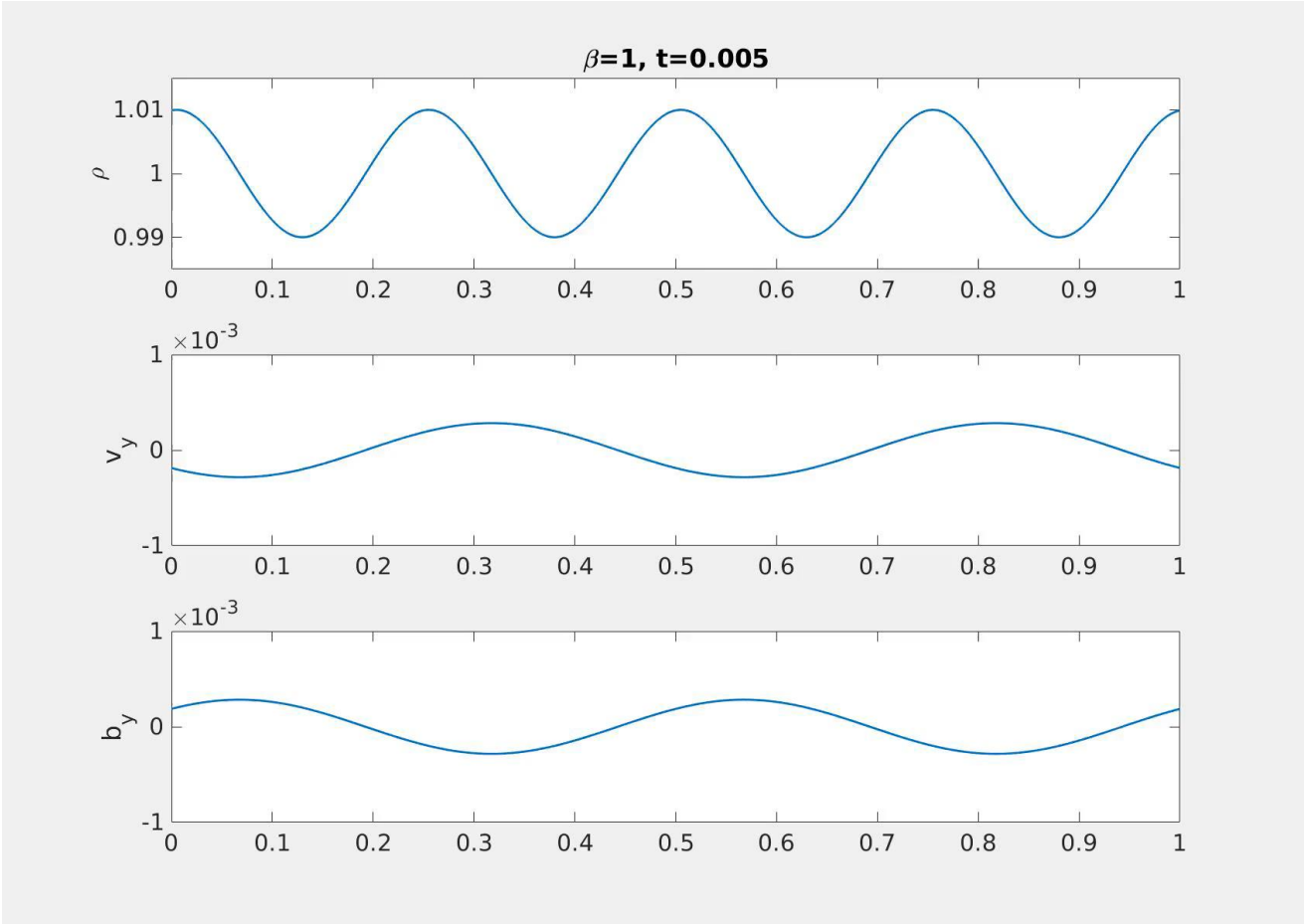

T. Zaqarashvili, ApJ 552 (2001) L81

G. Mamatsashvili et al., in preparation

Convection

Convection at small Prandtl numbers

Turbulent superstructures in shallow geometry

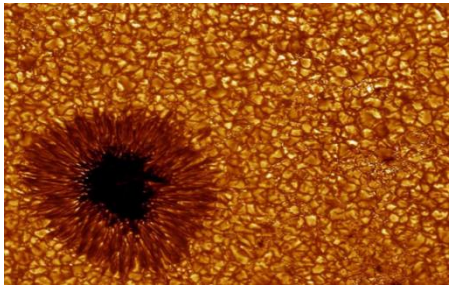

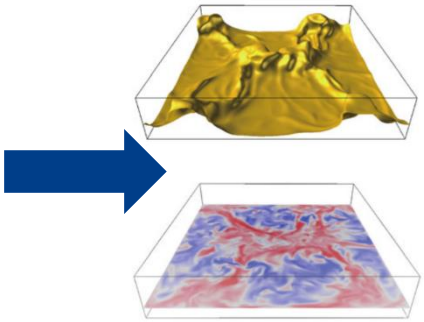

Akashi et al., J. Fluid Mech. 932, A27 (2022)

Jump rope vortex, detected first in…

Vogt et al., PNAS 115, 12674 (2018)

…turns out to be a **universal feature**

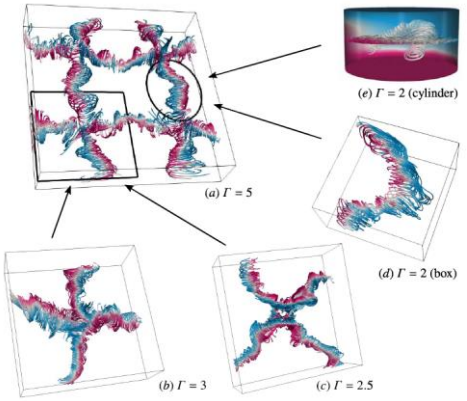

New experiment with Γ=25

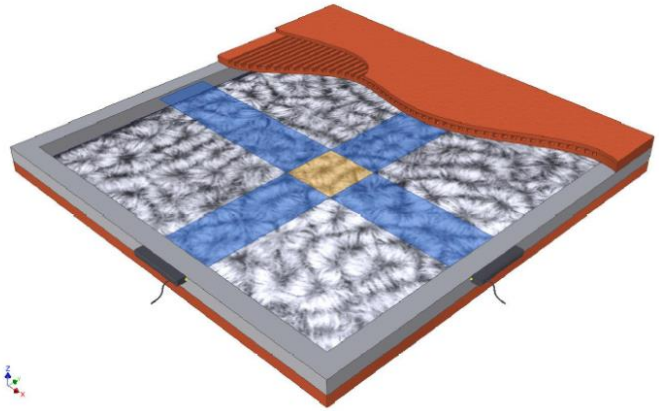

Convection at Γ=0.5

Collaps of large-scale coherent flow

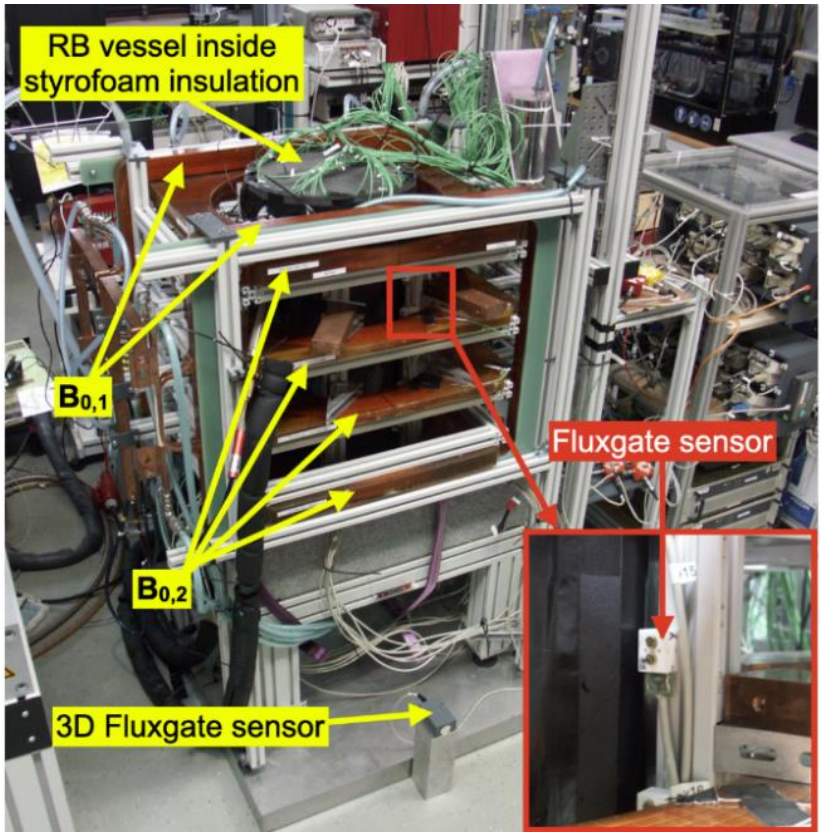

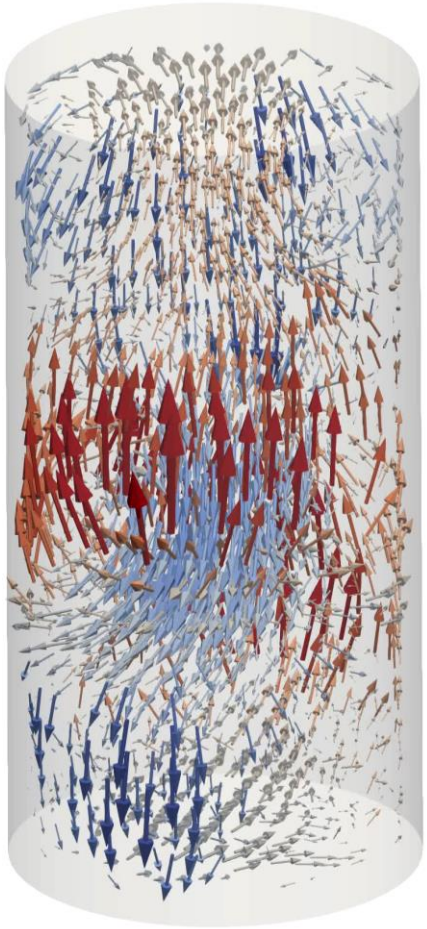

Chaotic transitions between single, double, and triple rolls

T. Wondrak et al., J. Fluid Mech. **974**, A48 (2023)

R. Mitra et al., Flow Meas. Instr. **100**, 102709 (2024)

Application of **Contactless Inductive Flow Tomography** for flow reconstruction using 6x7=42 fluxgate sensors

Oscillations of helicity

Helicity density:

h=**u**•rot **u**

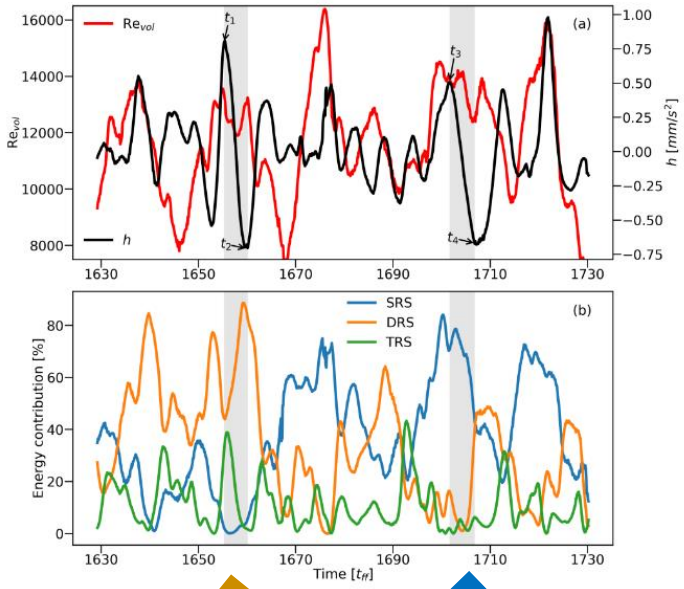

Chaotic transitions between single, double, and triple rolls

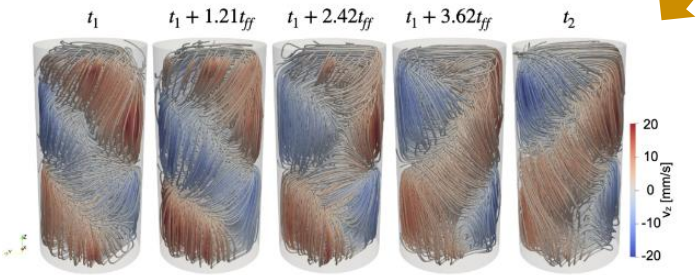

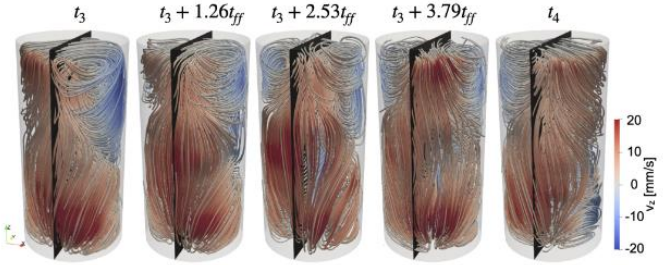

Helicity oscillations (with nearly no energy change) occur for Double Roll Structure and Single Roll Structure

R. Mitra et al., Phys. Fluids 36, 066611(2024)

Magnetorotational Instability (MRI)
and
Tayler Instability (TI)

MRI: From accretion disks….

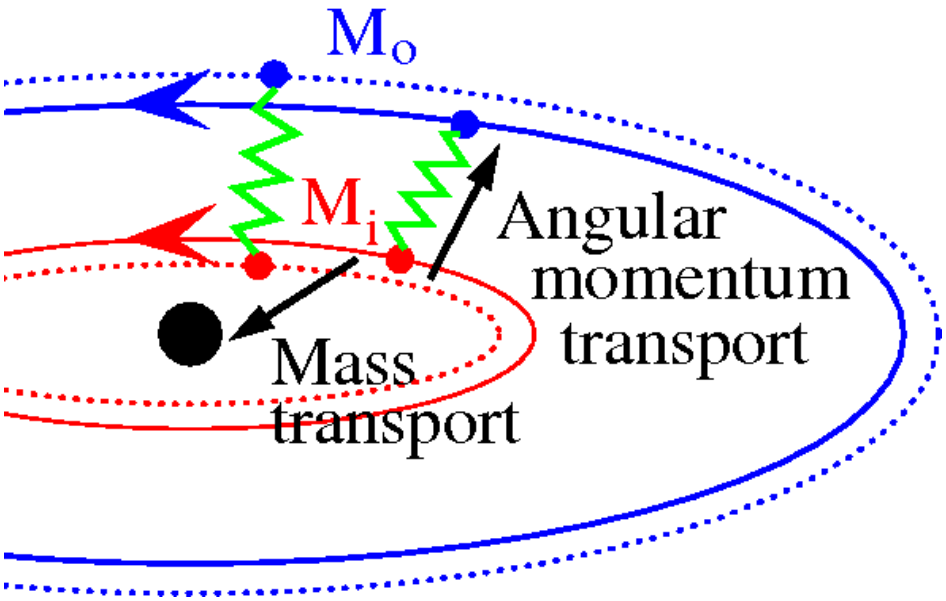

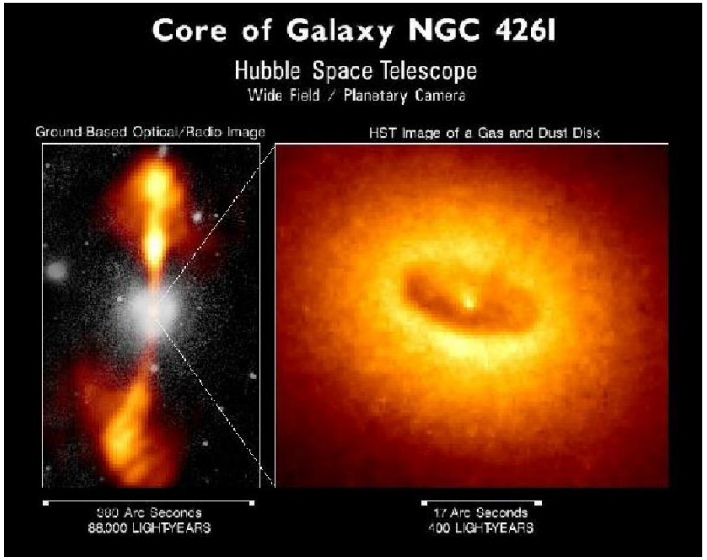

Problem: Outward angular momentum transport is not explainable by normal viscosity, and Keplerian rotation is hydrodynamically stable. So, where does the turbulence come from?

Solution: Magnetic fields act like springs and trigger angular momentum transport in accretion disks around protostars and black holes.

…to the Sun?

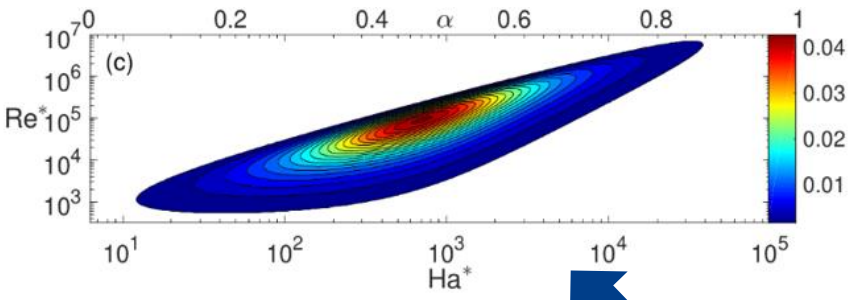

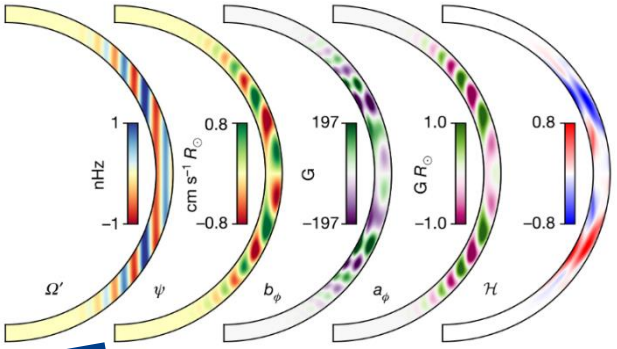

G.M. Vasil et al., Nature 628, 769 (2024)

G. Mamatsashvili, F.S., R. Hollerbach, G. Rüdiger, Phys. Rev. Fluids 4 (2019), 103905

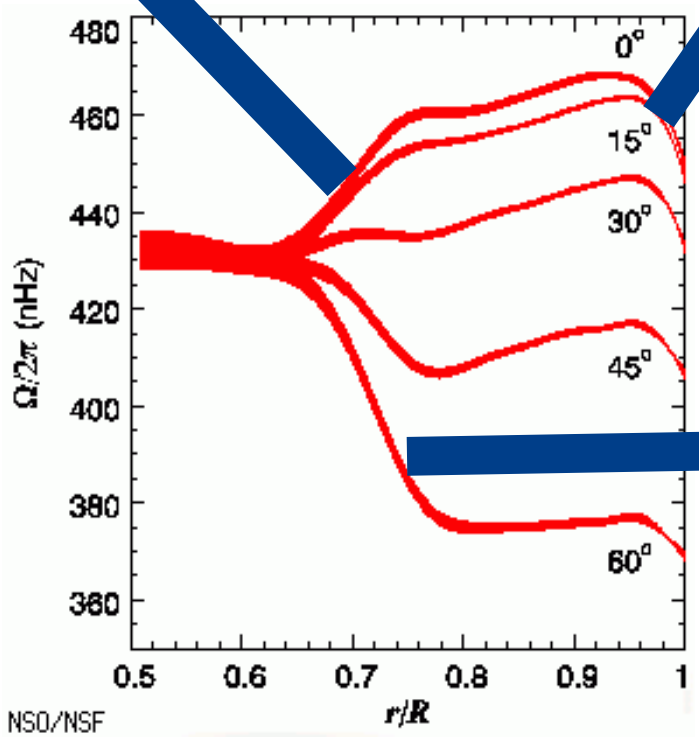

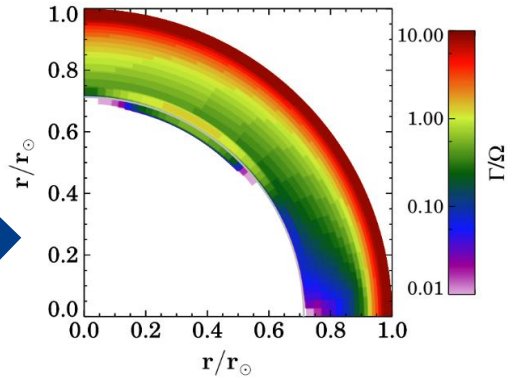

D. Kagan, G.C. Wheeler, ApJ 782, 21 (2014)

A quick guide through the MRI zoo

HMRI

$\Omega_{out} < \Omega_{in}$

$B_\varphi \sim B_z$

m=0

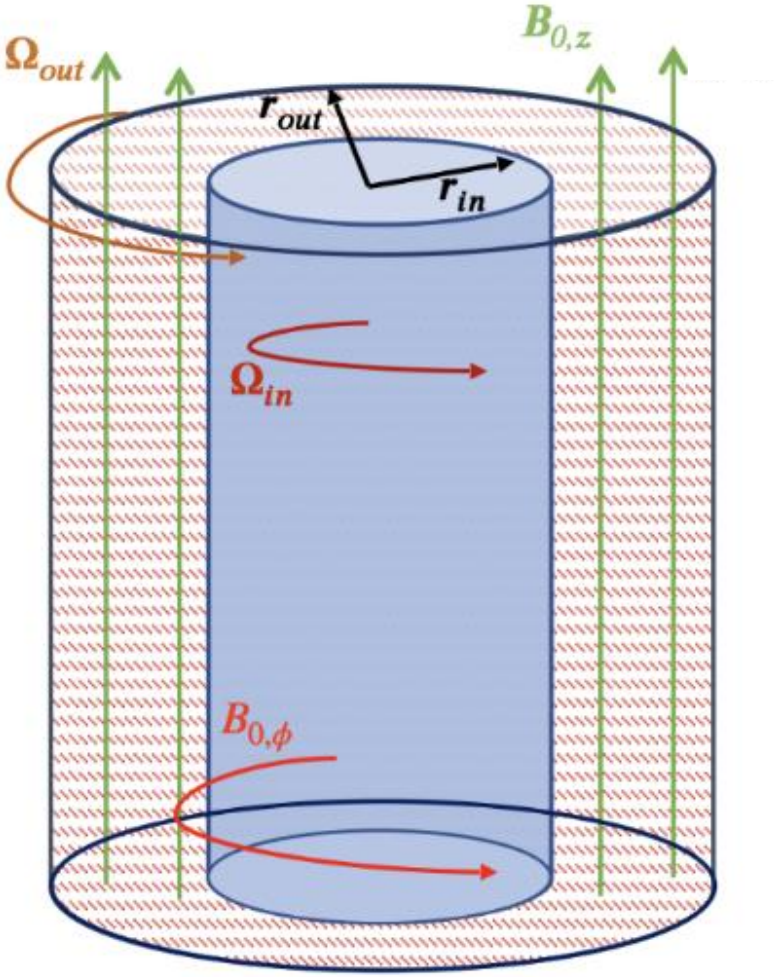

AMRI

$\Omega_{out} < \Omega_{in}$

$B_\varphi >> B_z$

m=1

SMRI

$\Omega_{out} < \Omega_{in}$

$B_\varphi << B_z$

m=0

Super-HMRI

$\Omega_{out} > \Omega_{in}$

$B_\varphi \sim B_z$

m=0

A quick guide through the MRI (and TI) zoo

HMRI

$\Omega_{out} < \Omega_{in}$

$B_\varphi \sim B_z$

m=0

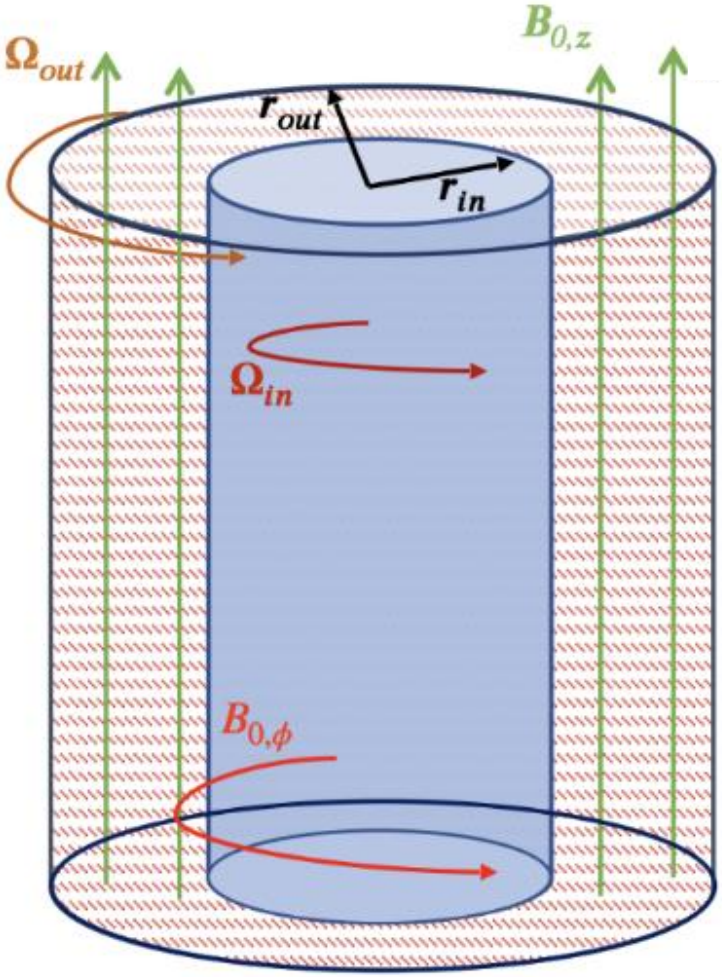

AMRI

$\Omega_{out} < \Omega_{in}$

$B_\varphi >> B_z$

m=1

TI

$B_\varphi \sim r$

m=1

SMRI

$\Omega_{out} < \Omega_{in}$

$B_\varphi << B_z$

m=0

Super-HMRI

$\Omega_{out} > \Omega_{in}$

$B_\varphi \sim B_z$

m=0

TI (and/or AMRI) in the Sun

- ^{7}Li is destroyed by proton capture at high temperatures (2.5x10^{6} K).
- Its observed continuous decrease suggests a transport process from the convection zone into the radiation zone, where it is burned.
- TI and/or AMRI are promising candidates to **explain simultaneously effective angular momentum transport and mild ^{7}Li mixing**

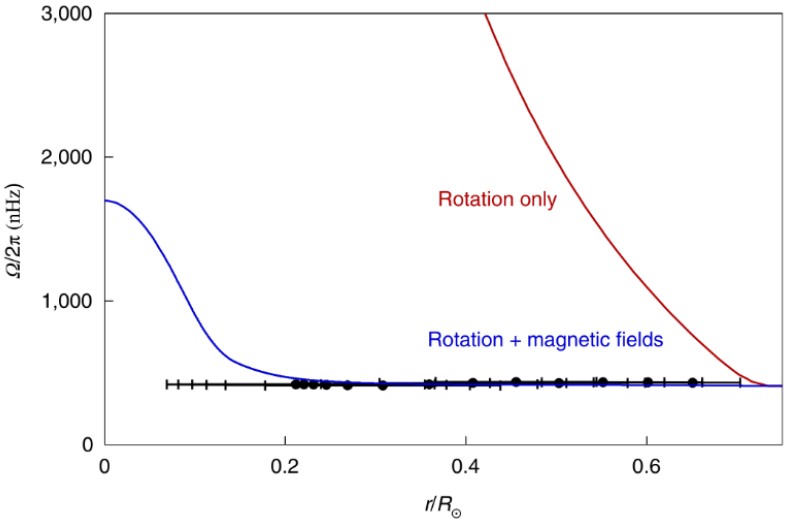

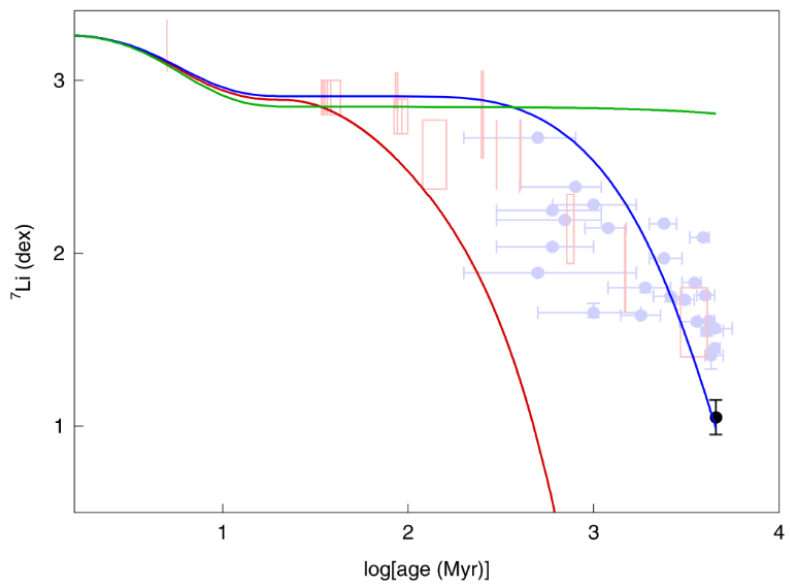

P. Eggenberger et al., Nature Astron. 6, 788 (2022)

Lecture by G. Buldgen on Monday

Helical MRI, Azimuthal MRI and in the liquid metal lab

2006: HMRI

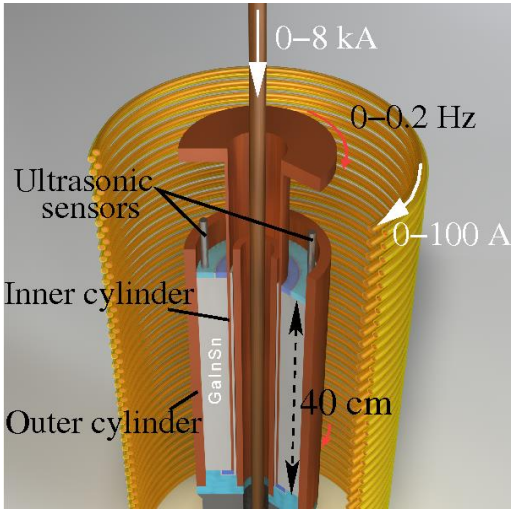

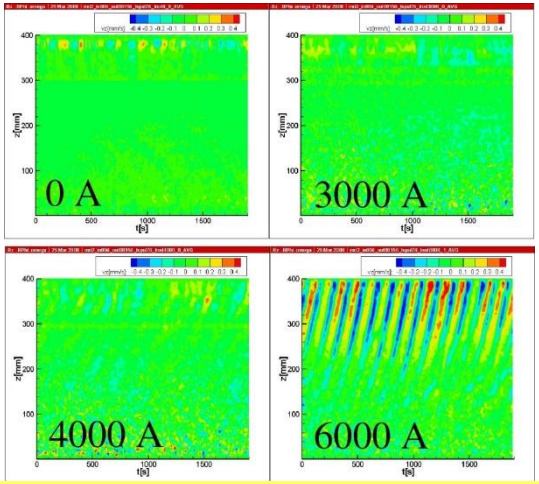

F.S. et al., PRL 97 (2006), 184502;
PRE 80 (2009), 066303

2014: AMRI

Seilmayer et al., PRL113 (2014), 024505

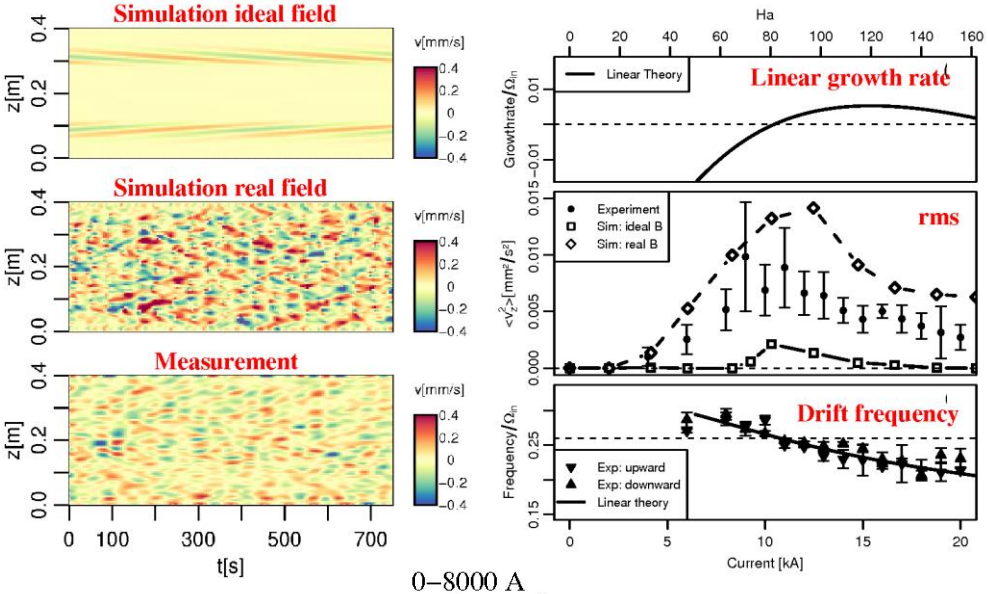

2012: TI

Seilmayer et al., PRL 108 (2012), 244501

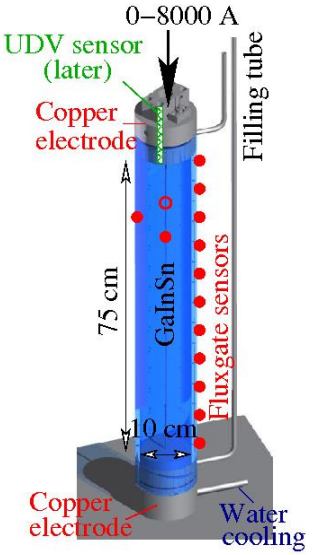

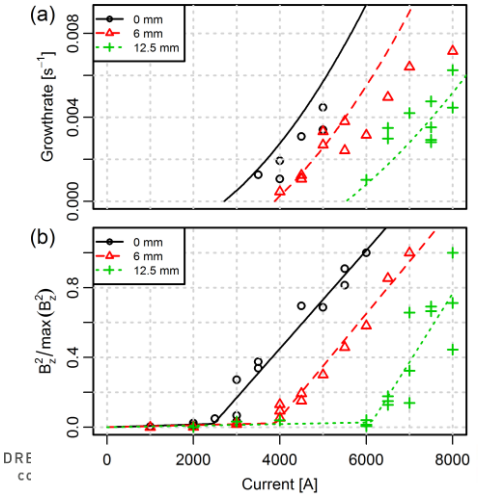

New results for AMRI+Convection: „One-winged butterflies“

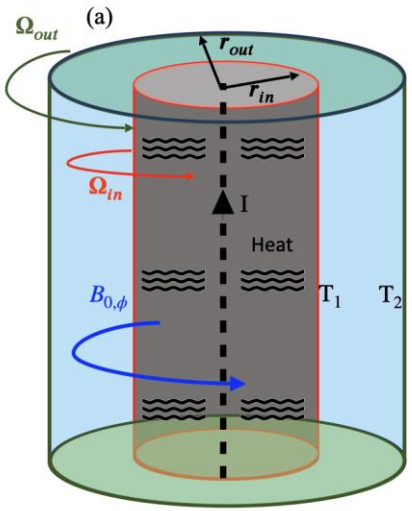

Experiment with changing radial heat flux

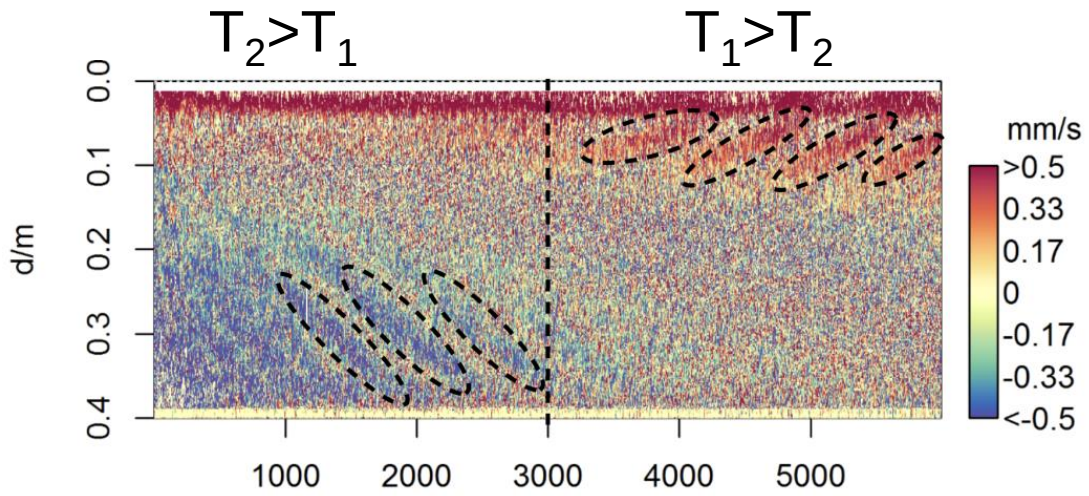

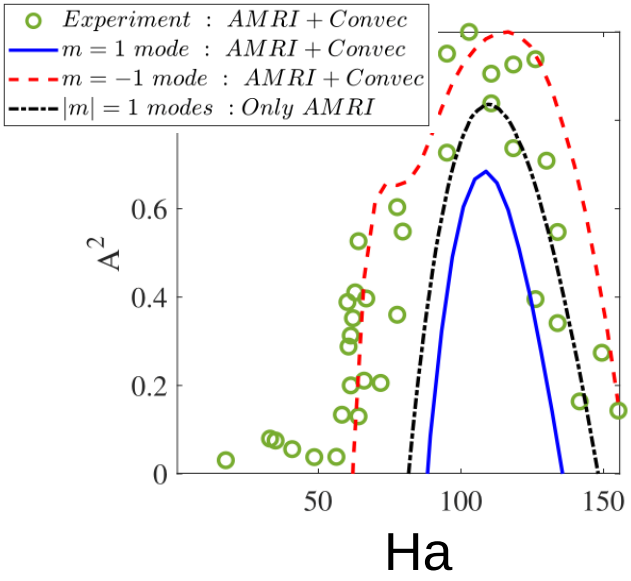

Simulation

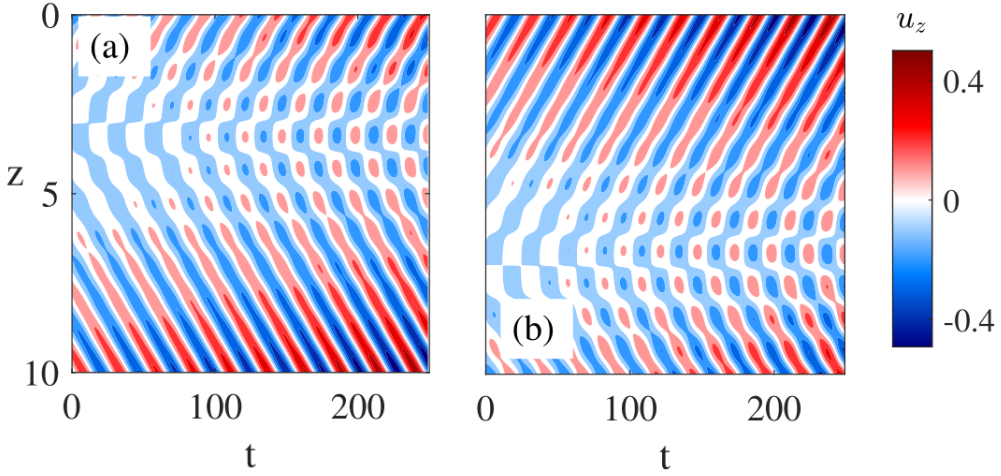

Seilmayer et al., Magnetohydrodyn. 56 (2020), 225; Mishra et al., J. Fluid Mech. 992, R1 (2024)

Planned experiment for SMRI, HMRI, AMRI, Super-HMRI and TI

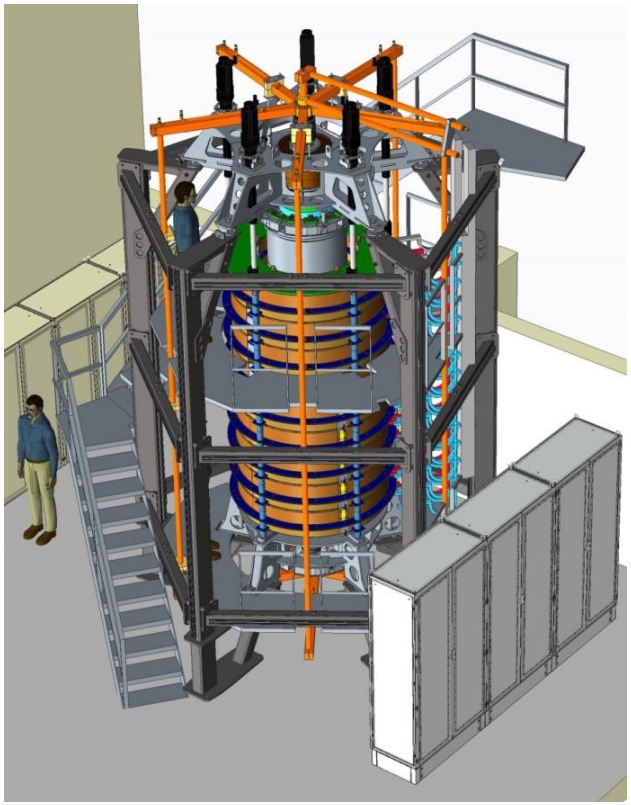

Design of the planned MRI/TI-experiment

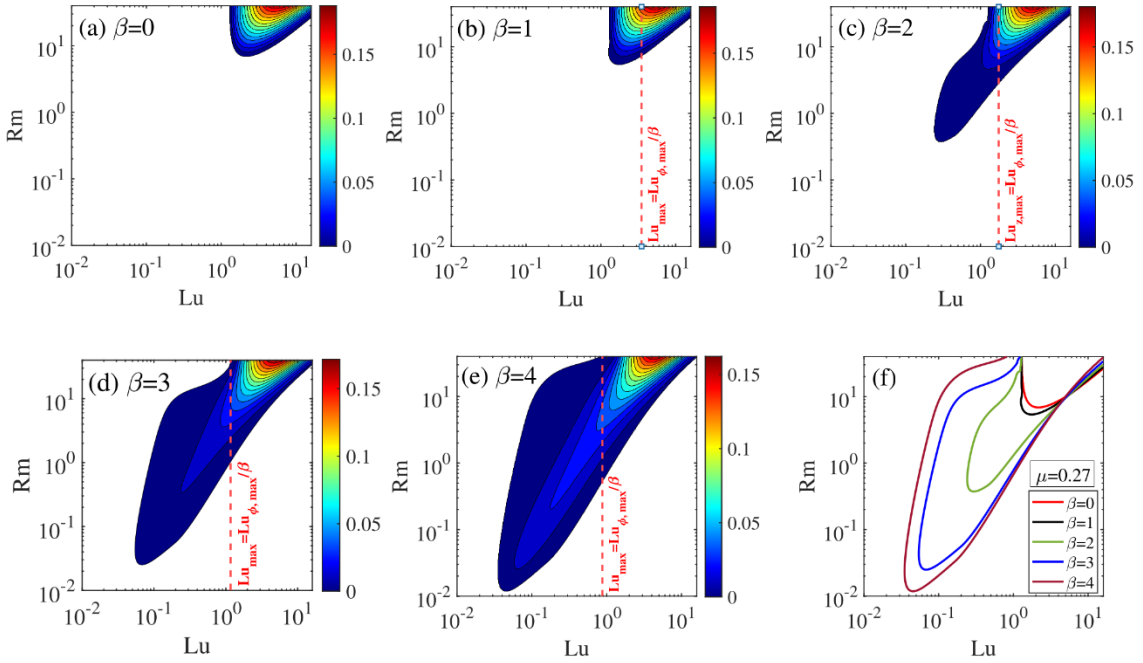

Main goal: follow the monotonic transition from HMRI to SMRI for decreasing $\beta = B_\varphi / B_z$

Mishra et al., Phys. Rev. Fluids 7 (2022), 064802

Preparations of MRI experiment: nonlinear simulations for m=0

Saturation of MRI via magnetic reconnection

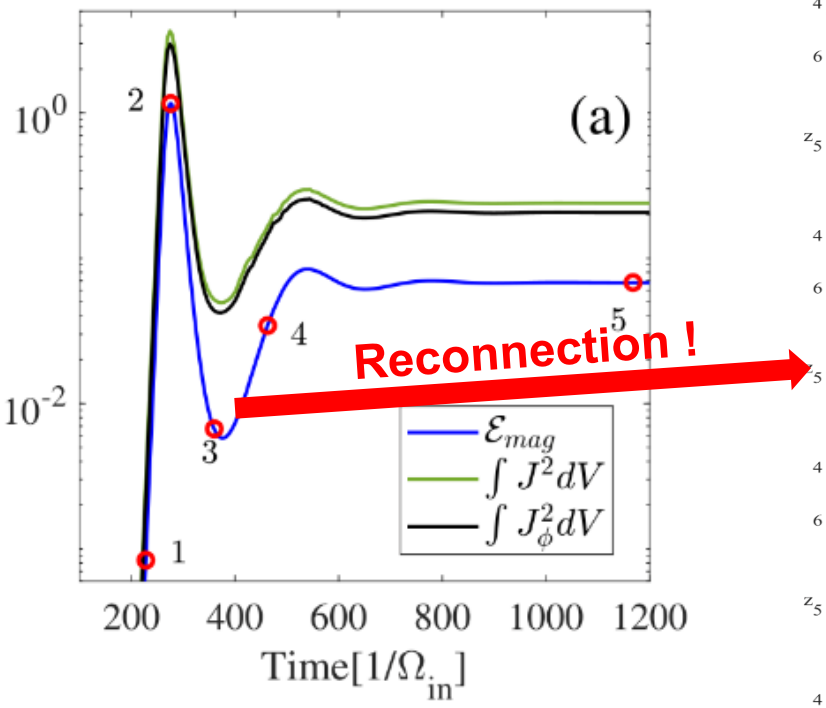

Reconnection !

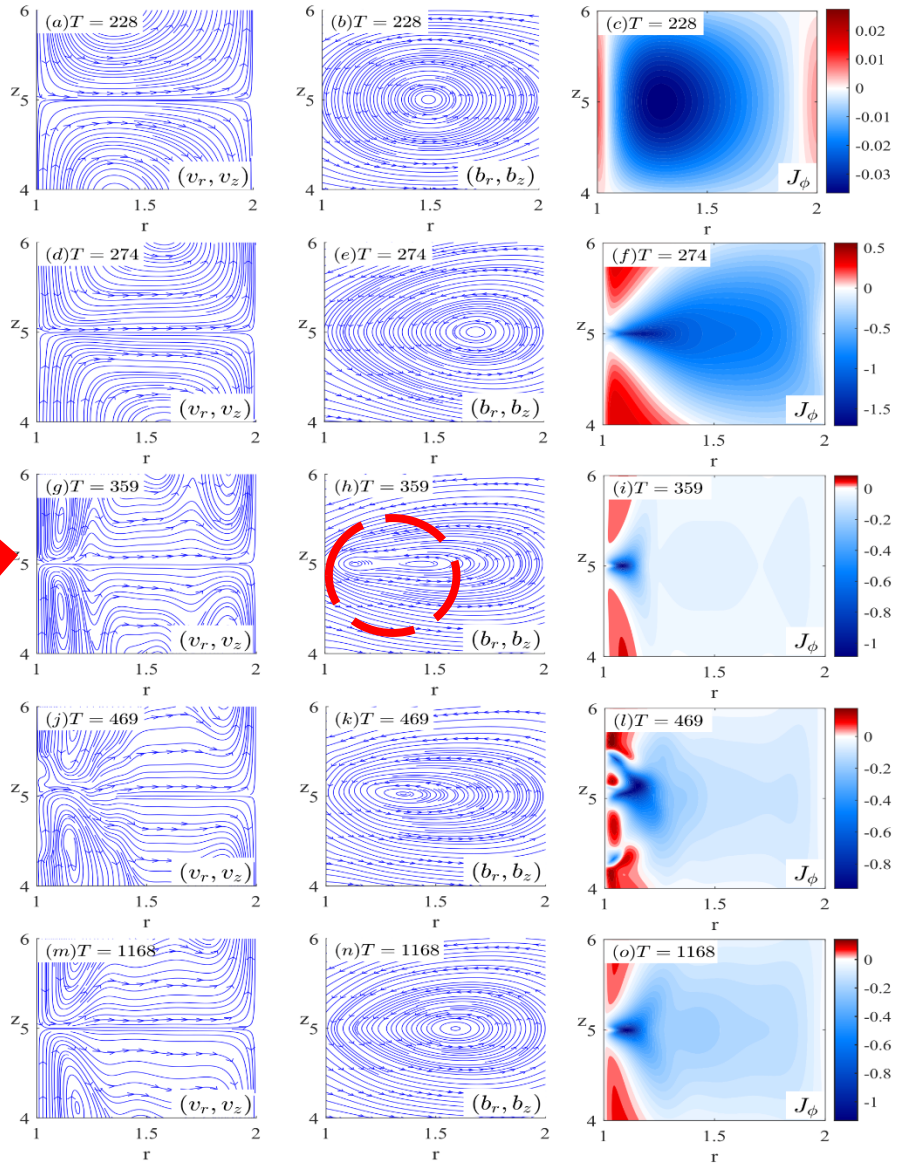

A. Mishra et al, Phys. Rev. Fluids 8, 083902 (2023)

Poster pitch by A. Mishra on Tuesday

Dynamos

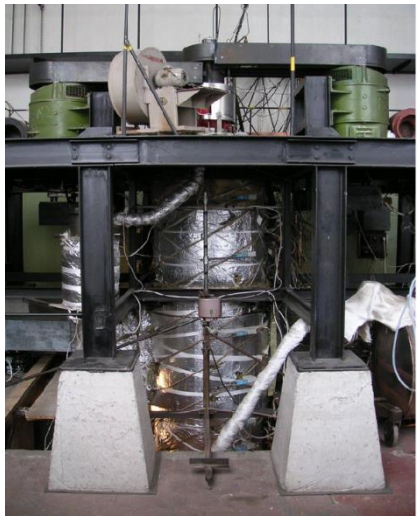

Riga

Karlsruhe

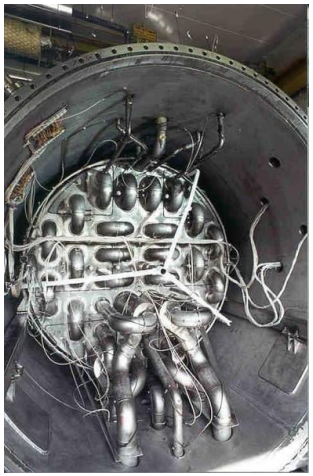

Dynamos

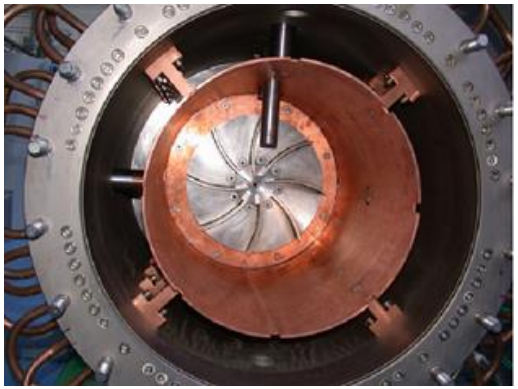

VKS

DRESDYN

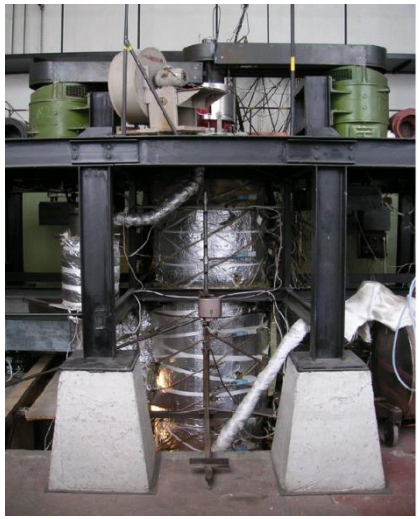

Riga

Karlsruhe

Dynamos

VKS

DRESDYN

Riga dynamo experiment

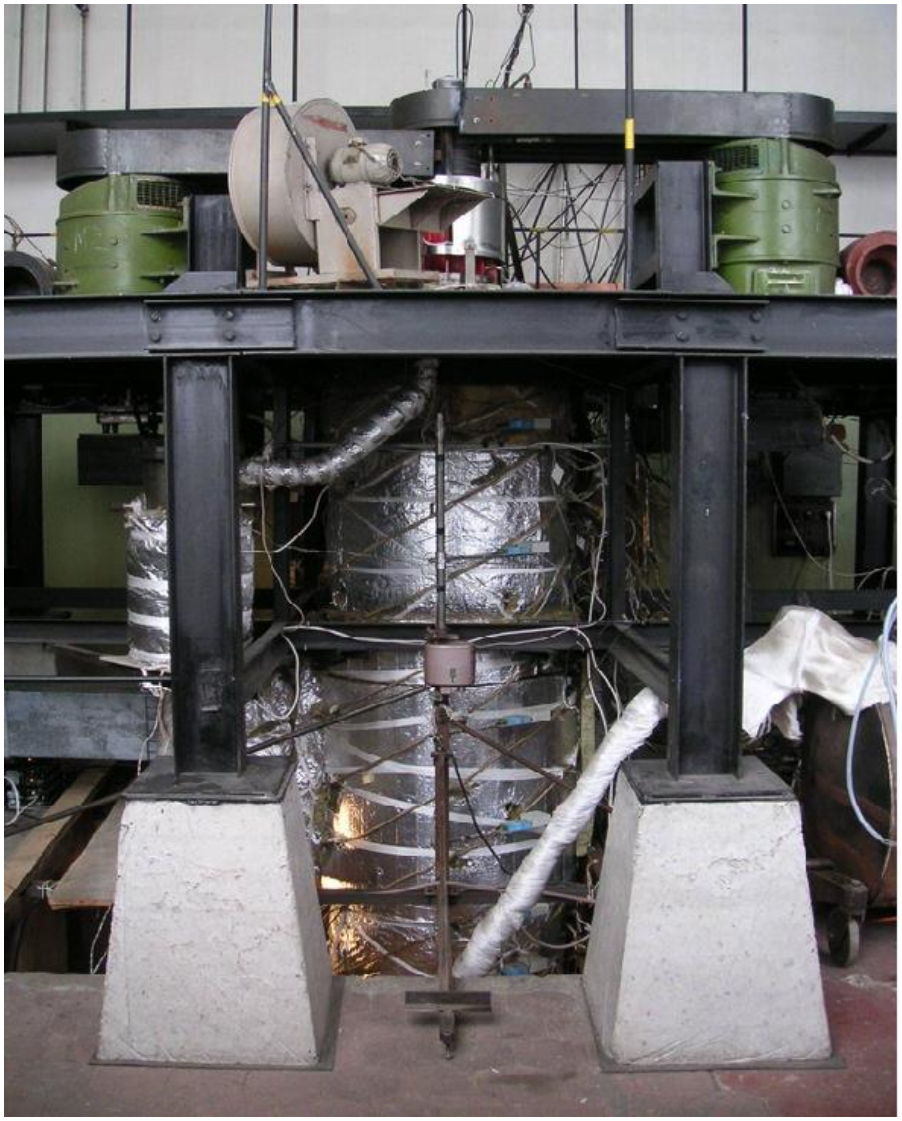

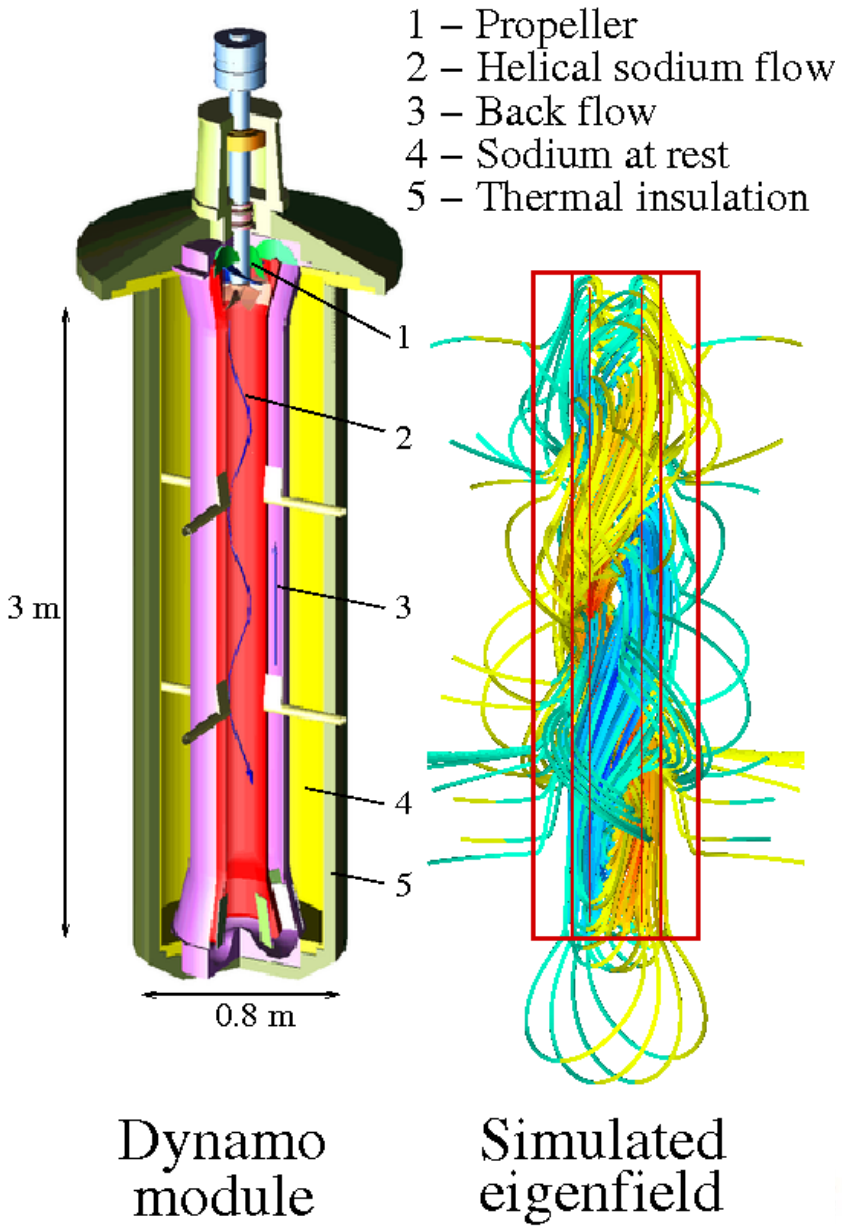

Riga dynamo experiment

First experimental realization of magnetic field self-excitation in a liquid metal flow (11 November 1999)

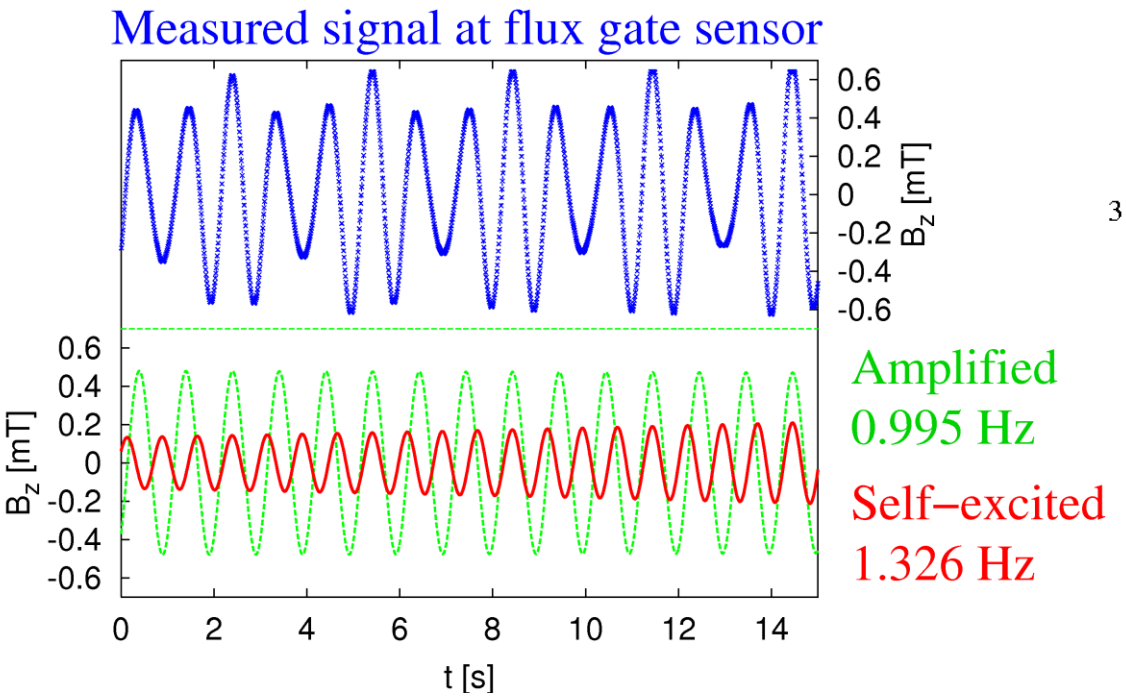

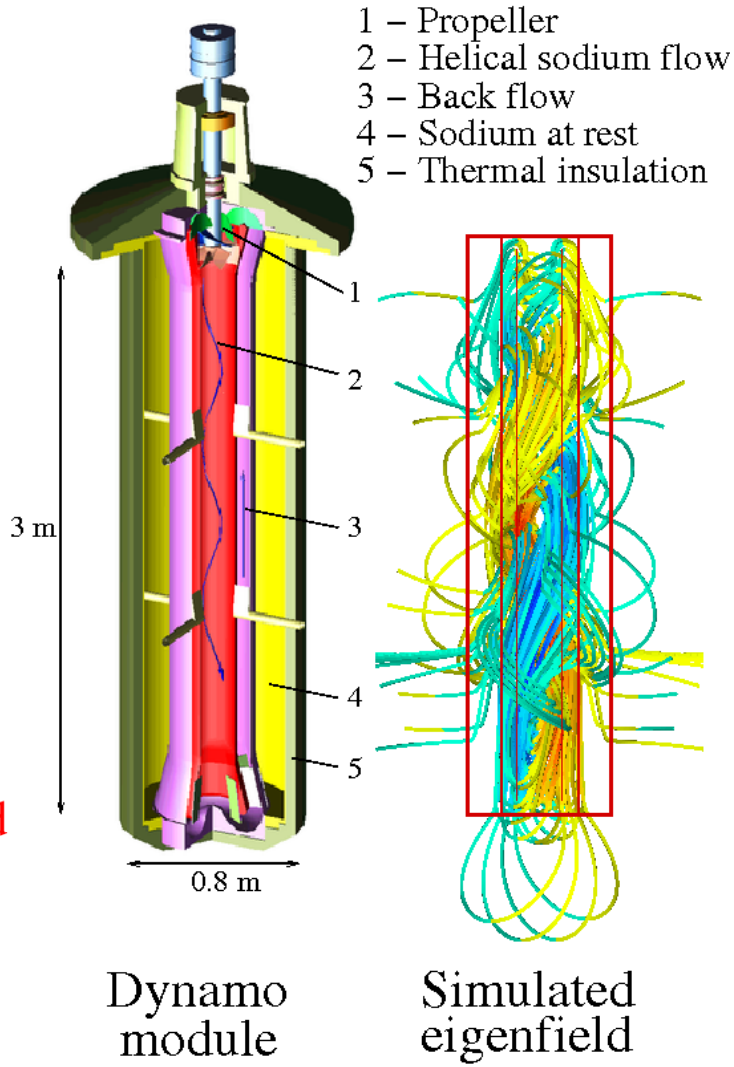

Gailitis et al., Phys. Rev. Lett. 84 (2000) 4365

Come on baby light my SODIUM fire…

Evening of 11th November 1999

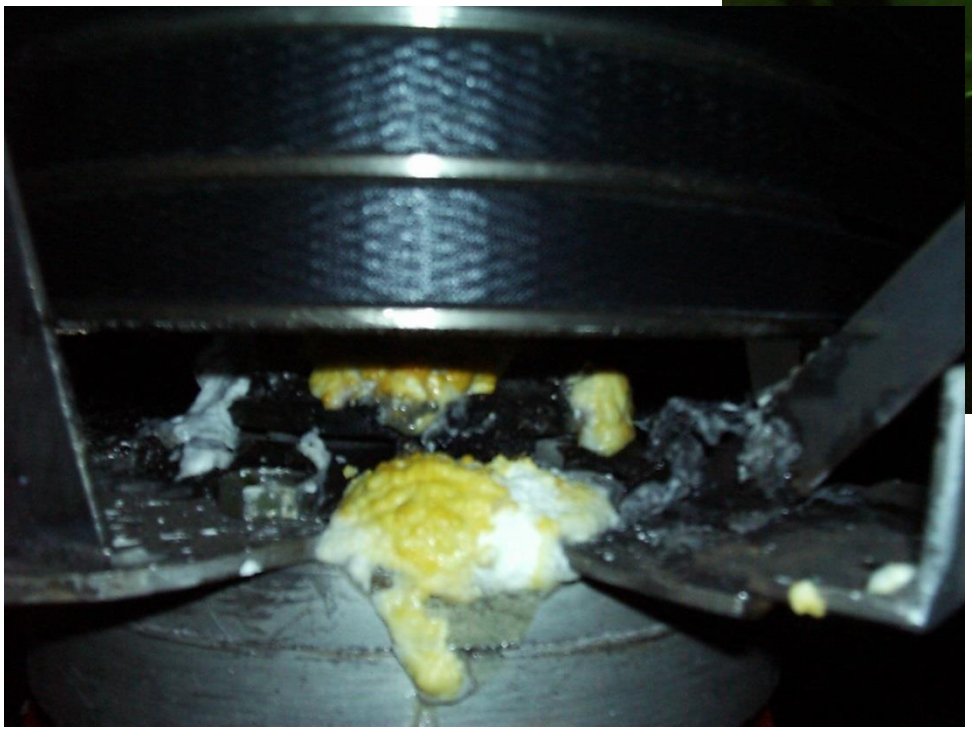

…and the day after…

Riga dynamo experiment

From the kinematic to the saturated regime (July 2000)

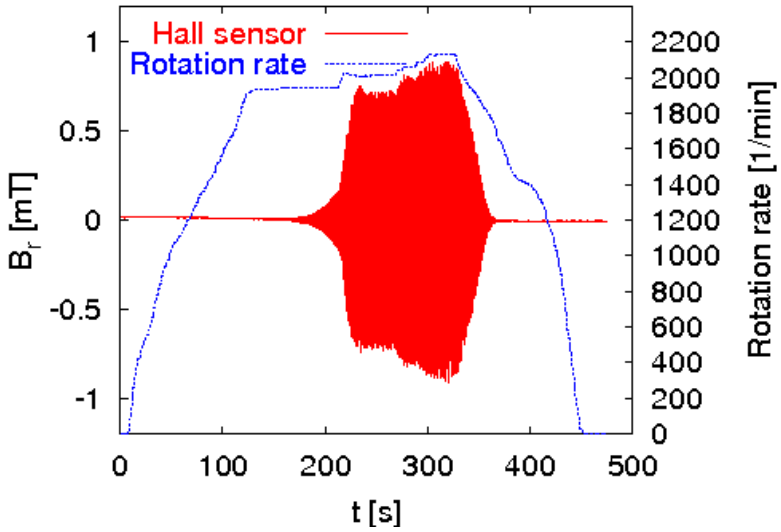

Switching the dynamo on and off (February 2005)

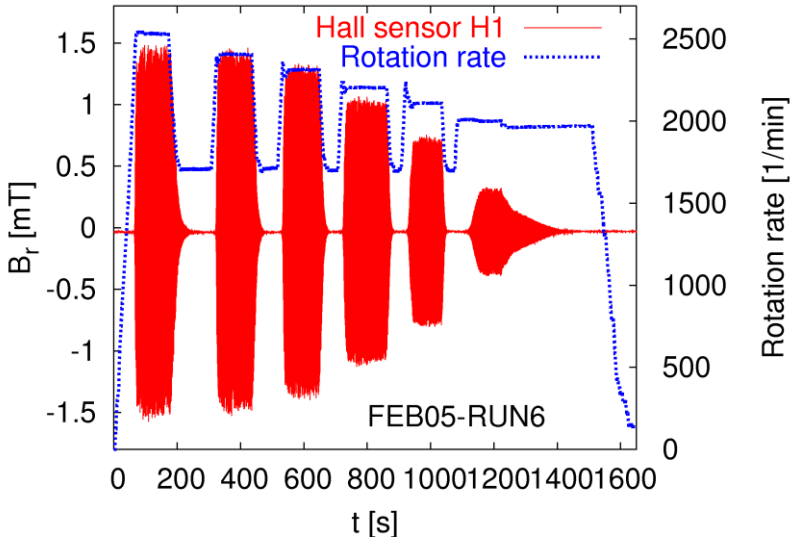

Gailitis et al., Phys. Rev. Lett. 84 (2000) 4365; Phys. Rev. Lett. 86 (2001) 3024; Rev. Mod. Phys. 74 (2002) 973 ; Phys. Plasmas 11 (2004) 2838; Compt. Rend. Phys. 9 (2008), 721; **J. Plasma Phys. 84, 735840301 (2018)**

Riga dynamo experiment: Back-reaction illustrates Lenz´s rule

Lorentz force components resulting from self-excited eigenfield

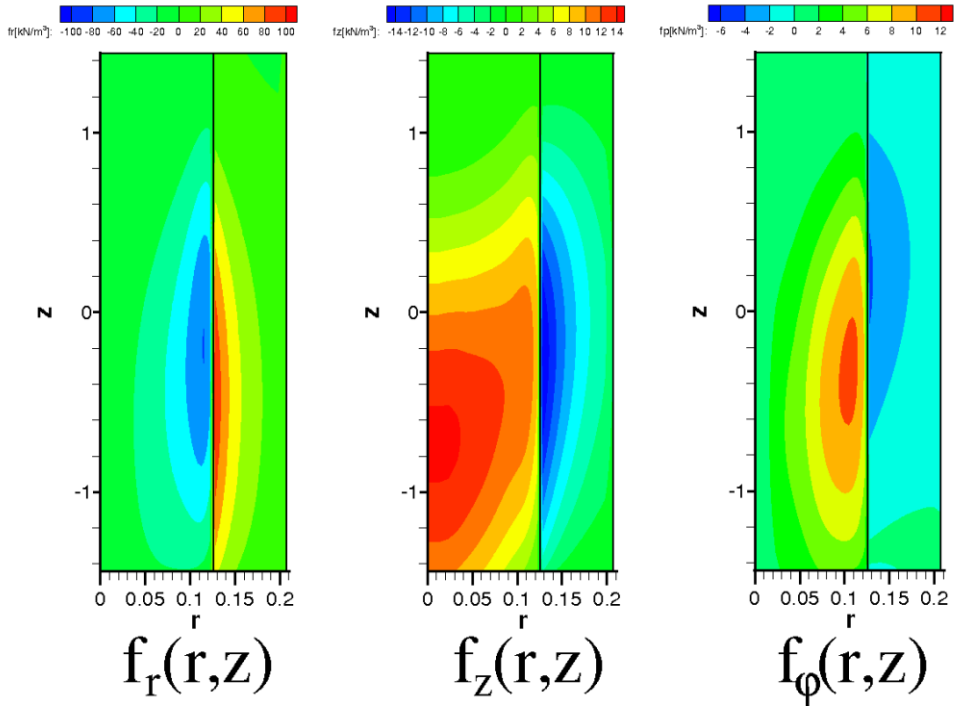

$$\frac{\partial \mathbf{B}}{\partial t} = \nabla \times (\mathbf{v} \times \mathbf{B}) + \frac{1}{\mu_0 \sigma} \Delta \mathbf{B}$$

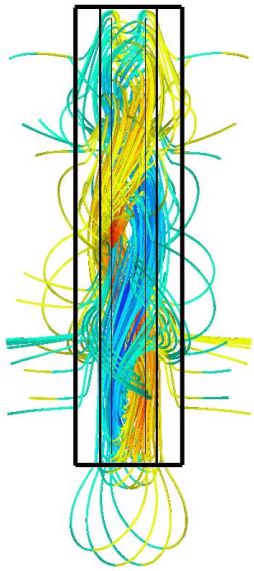

$$\frac{\partial \mathbf{v}}{\partial t} + (\mathbf{v} \cdot \nabla)\mathbf{v} = -\frac{\nabla p}{\rho} + \frac{1}{\mu_0 \rho}(\nabla \times \mathbf{B}) \times \mathbf{B} + \nu \Delta \mathbf{v} + \mathbf{f}_{extern}$$

Riga dynamo experiment: Growth rates and frequencies

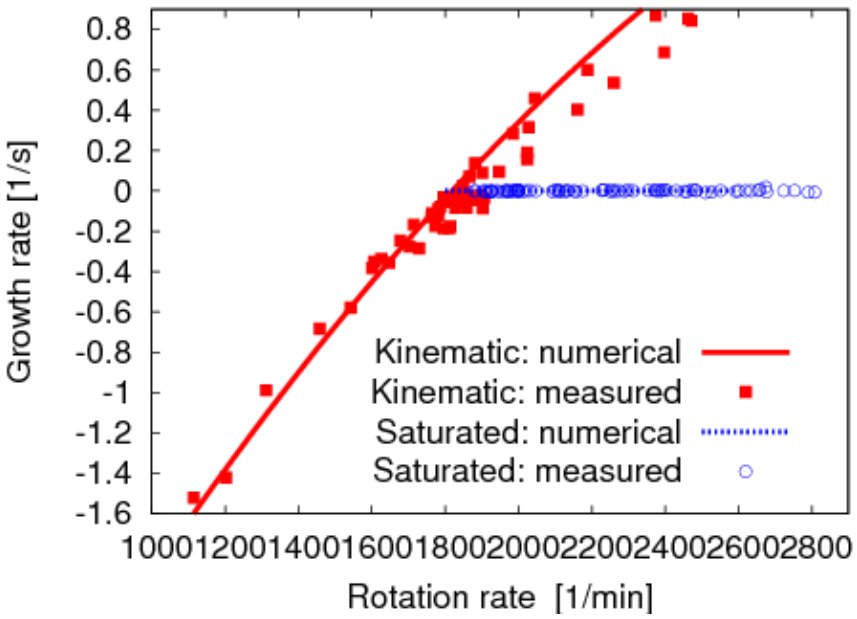

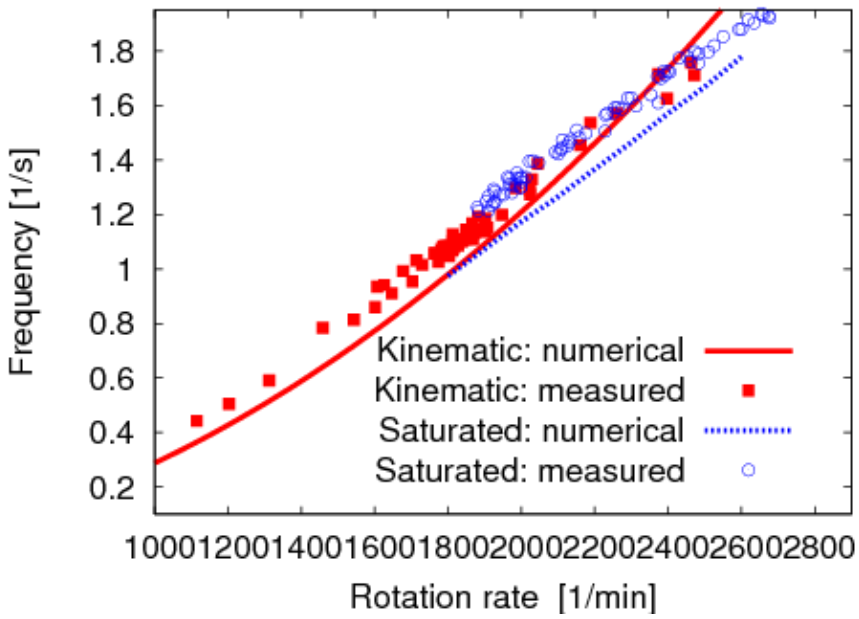

Numerical predictions (with correct vacuum boundary conditions) of the kinematic dynamo were accurate to some 5 per cent

Simplified back-reaction model (Lorentz forces acting along streamlines) gives very reasonable field amplitudes and structures in the saturation regime

Gailitis et al. J. Plasma Phys. 84, 735840301 (2018)

A (not-so-short) diversion into theory...and observation

Any solar dynamo needs:

- some Ω effect to wind up toroidal field from poloidal field
- some α effect to regenerate poloidal field from toroidal field

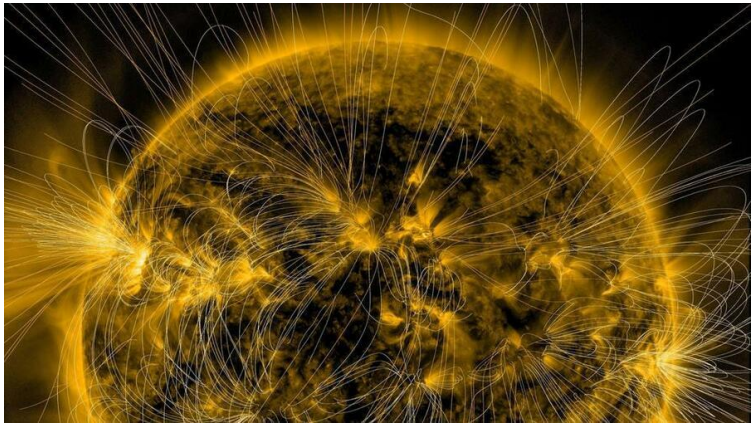

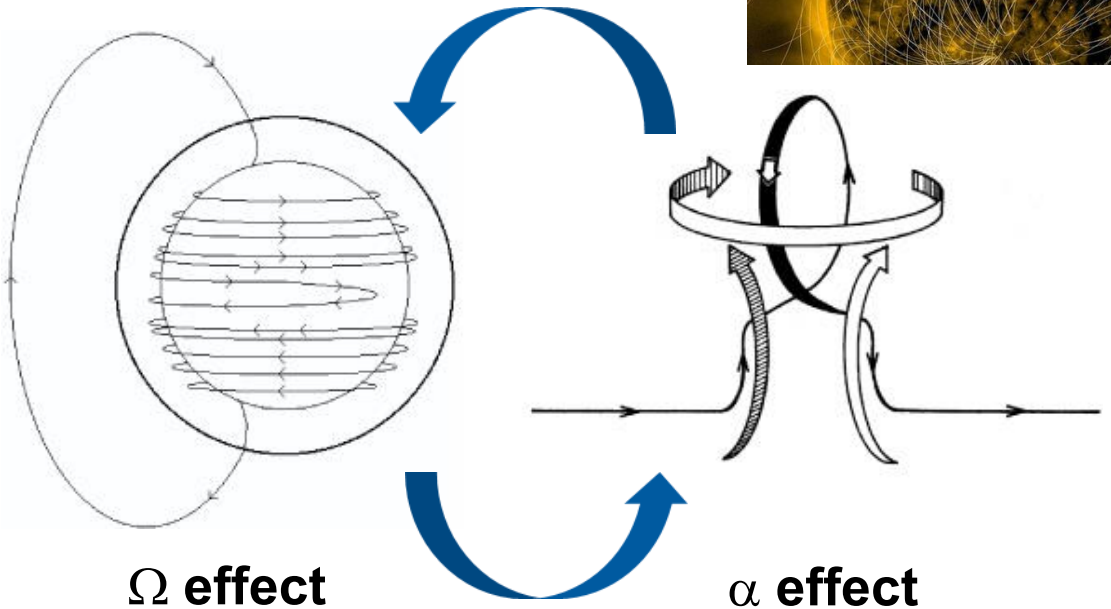

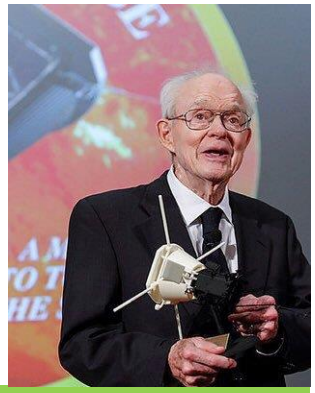

Parker, Astrophys J. 122, 293 (1955)

Solar dynamo: Conventional modelling

With appropriate models, (including meridional circulation), and some parameter fitting, one obtains

- a reasonable period of the Hale cycle (22 years)
- a reasonable shape of the butterfly diagram of sunspots

http://www.solarcyclescience.com/solarcycle.html

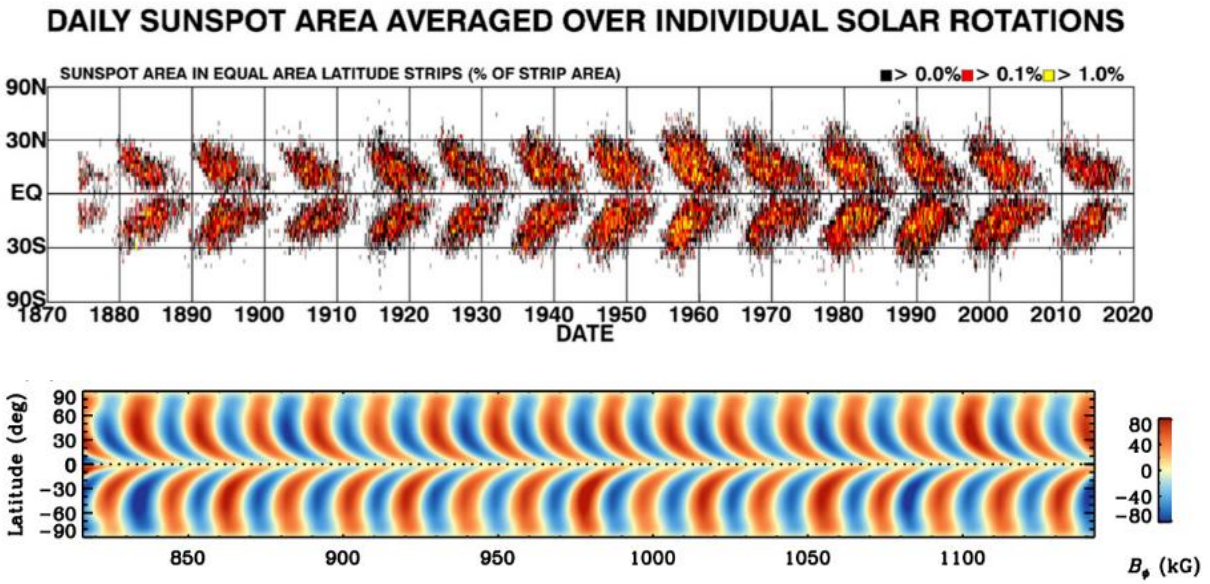

Karak, B.B., Miesch, M., ApJ 847 (2017), 69

Is there a problem at all with the solar dynamo? Perhaps yes…

Conspicious synchronization of the solar Schwabe cycle with the 11.07-yr period of three-planet syzygies of the tidally dominant **Venus-Earth-Jupiter** system (despite weak tidal forces!)

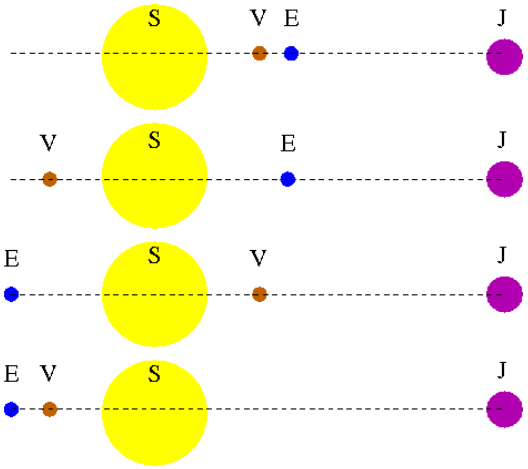

Sunspots

VEJ alignment index

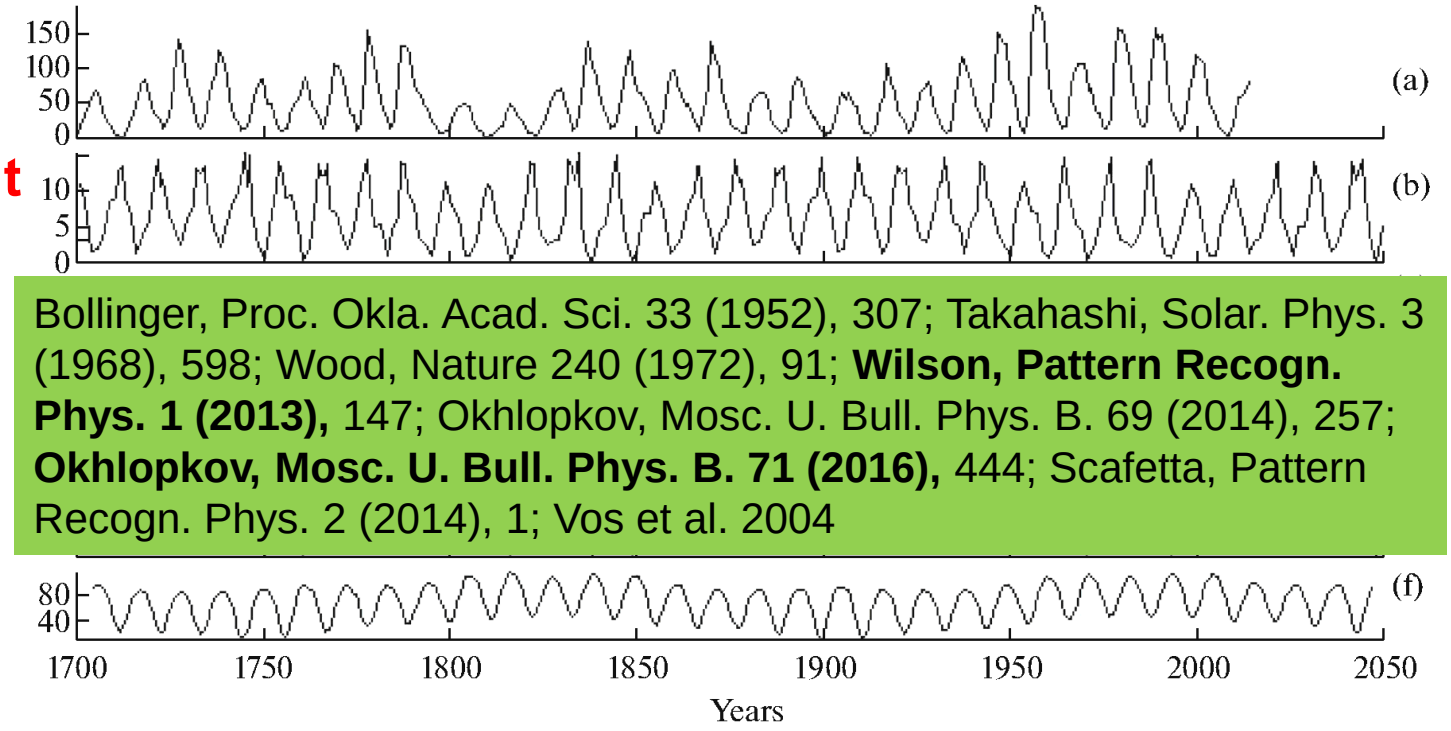

Bollinger, Proc. Okla. Acad. Sci. 33 (1952), 307; Takahashi, Solar. Phys. 3 (1968), 598; Wood, Nature 240 (1972), 91; **Wilson, Pattern Recogn. Phys. 1 (2013),** 147; Okhlopkov, Mosc. U. Bull. Phys. B. 69 (2014), 257; **Okhlopkov, Mosc. U. Bull. Phys. B. 71 (2016),** 444; Scafetta, Pattern Recogn. Phys. 2 (2014), 1; Vos et al. 2004

First indication for phase stability and clocking

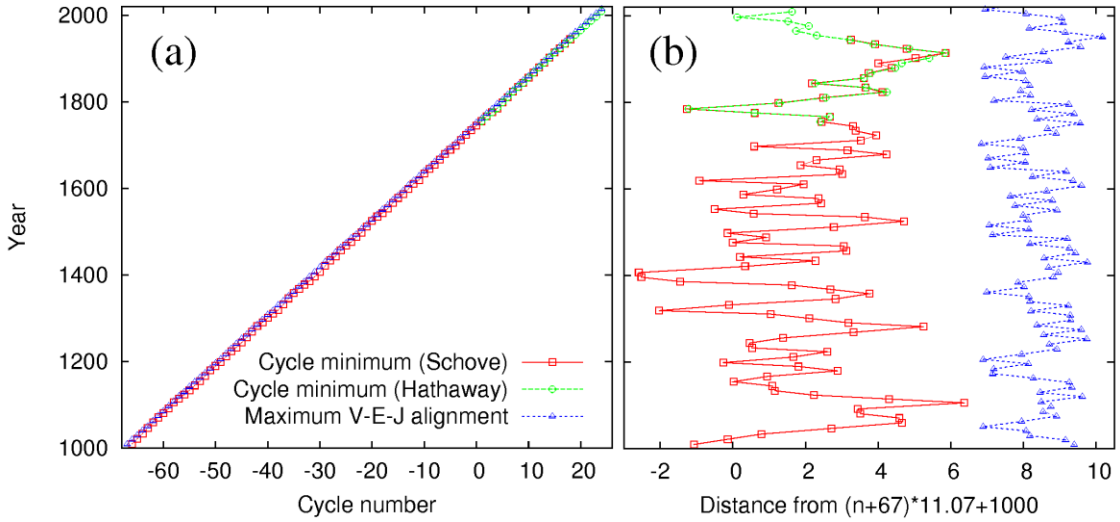

Residuals

Schove, D.J.: J. Geophys. Res. 60 (1955), 127; Hathaway, D.H., Liv. Rev. Sol. Phys. 7 (2010)

Strong indication for a clocked process, in contrast to a random walk process

F. S. et al., Solar Physics 294 (2019)

Schove's data (derived mainly from aurorae borealis) are often criticized ("9 per century rule")

I. Usoskin, Living Rev. Sol. Phys. 14, 3 (2017); H.-C. Nataf, Solar Physics 297 (2022), 107

However: ^{10}Be and ^{14}C data give similar cycles.

F. S. et al., Astron. Nachr. 341 (2020), 600

Dicke´s ratio in dependence on the number N of cycles

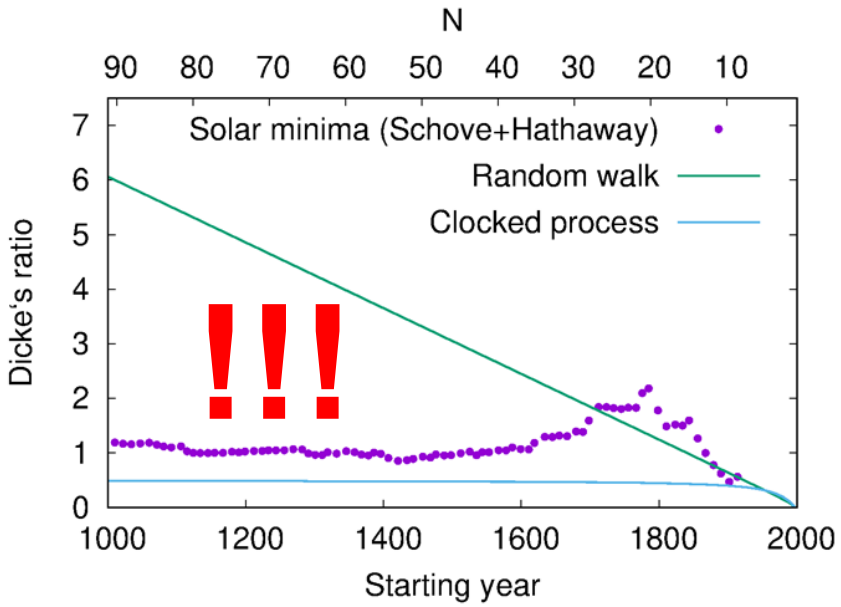

Distinction between random walk (RW) and clocked process (CP) for the instants y_n of sunspot maxima/minima

Residuals: $\delta y_n = y_n - y_0 - p(n-1)$, with p being the mean cycle period

A telling measure for discriminating between RW und CP is DICKE´s RATIO between the variance of δy_n and the variance of $(\delta y_n - \delta y_{n-1})$

	RATIO	Limes N→ infinity
Random walk	$(N+1)(N^2-1)/(3(5N^2+6N-3))$	N/15
Clocked process	$(N^2-1)/(2(N^2+2N+3))$	1/2

Dicke, R.H., Nature 276 (1978), 676

Gough´s ratio in dependence on the number N of cycles

Weisshaar, Cameron, Schüssler, A&A 671, A87 (2023)

…use new ^{14}C data of

N. Brehm et al., Nat. Geosci. (2021); Usoskin et al., A&A (2021)

…to derive the closely related GOUGH´s RATIO between the variance of phase deviations and the variance of cycle periods

	RATIO	Limes N→ infinity
Random walk	N(N+2)/(12(N+1))	N/12
Clocked process	N(7N-2)/(12(N+1)^2)	7/12

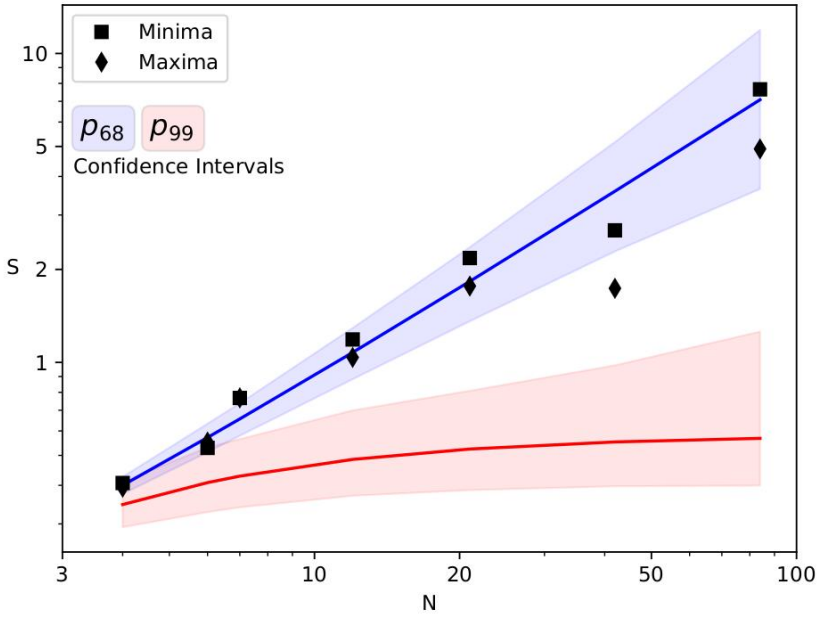

"*The data are consistent with random walk of phase …. while, owing to the much longer data set, clock synchronization is rejected at levels exceeding 99%.*"

This sounds convincing, but…

Weisshaar´s et al. conclusion is premature…

…as it depends heavily on just one additional minimum at 1845 (for which there is no other observational evidence), and another minimum around 1650 (amidst the Maunder minimum) which is also not clear

Further problems occur during the Oort minimum ~1100

F. S., J. Beer, T. Weier, Solar Phys. 298, 83 (2023)

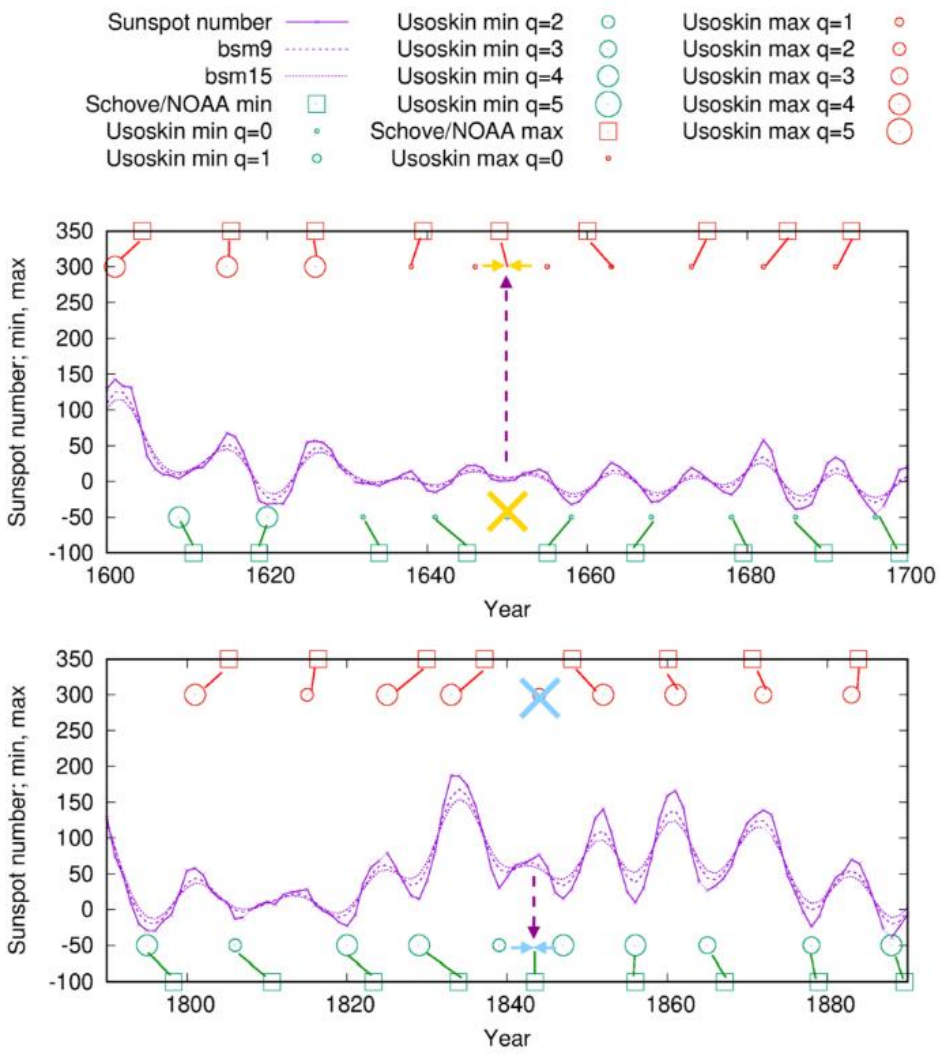

Weisshaar´s et al. conclusion is premature…

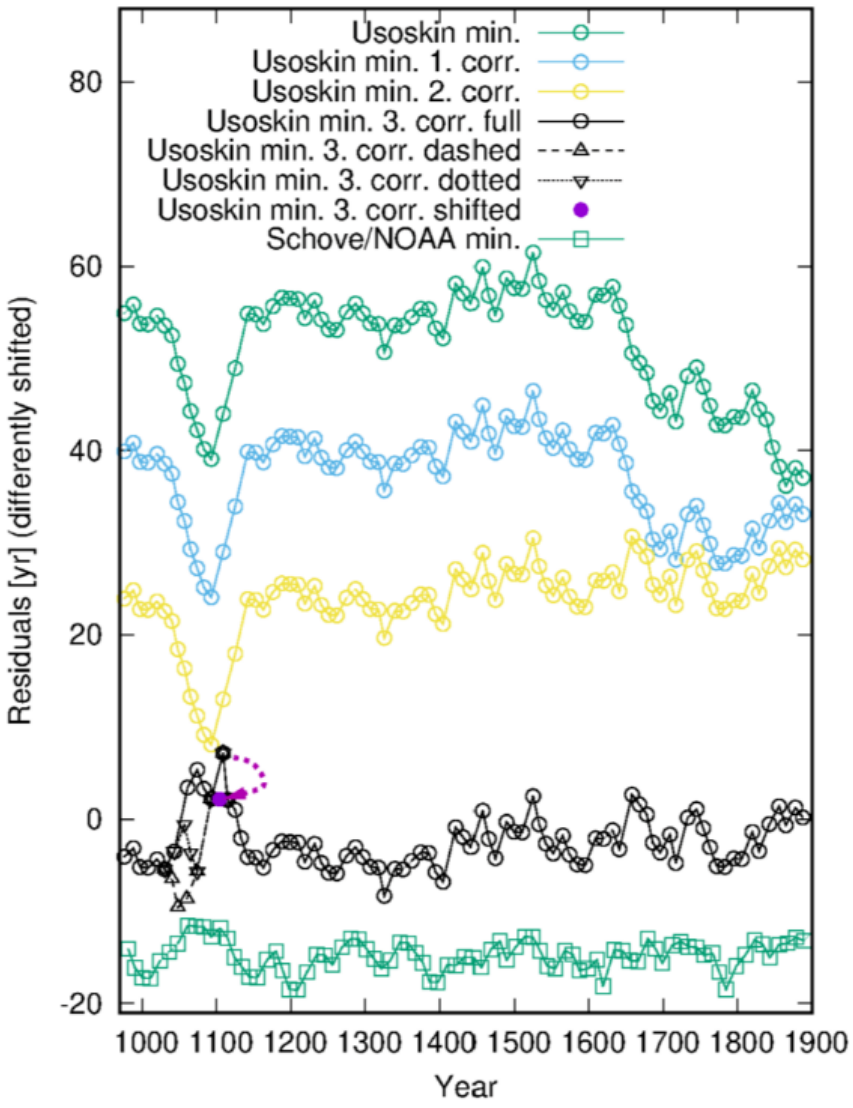

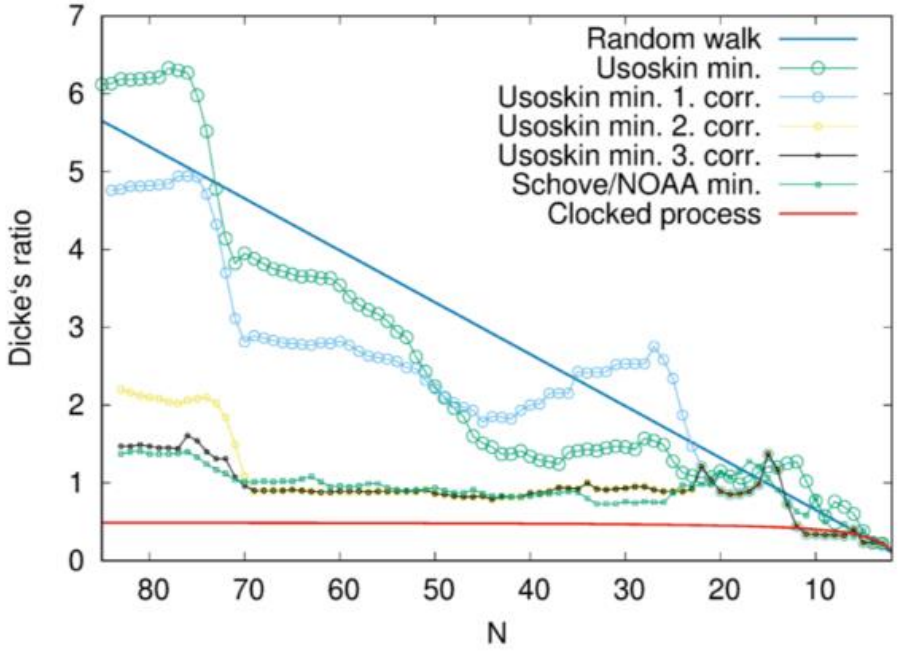

…as with appropriate corrections, the curve of residuals becomes increasingly flat, and Dicke‘s ratio approaches that for a clocked process…

F. S., J. Beer, T. Weier, Solar Phys. 298, 83 (2023)

Second indication for phase stability and clocking

Phase diagrams for algae data from lake Holzmaar und algae-produced Methanesulfonate (MSA) in Greenland ice core GISP2 show 11.04-years cycle with very similar band structures.

Bands are separated by apparent 5.5-years-phase jumps, resulting from nonlinear transfer function (due to optimality condition of algae growth)

Strong evidence for a 11.04(?)-years-cycle, that was phase-stable over 1000 years!

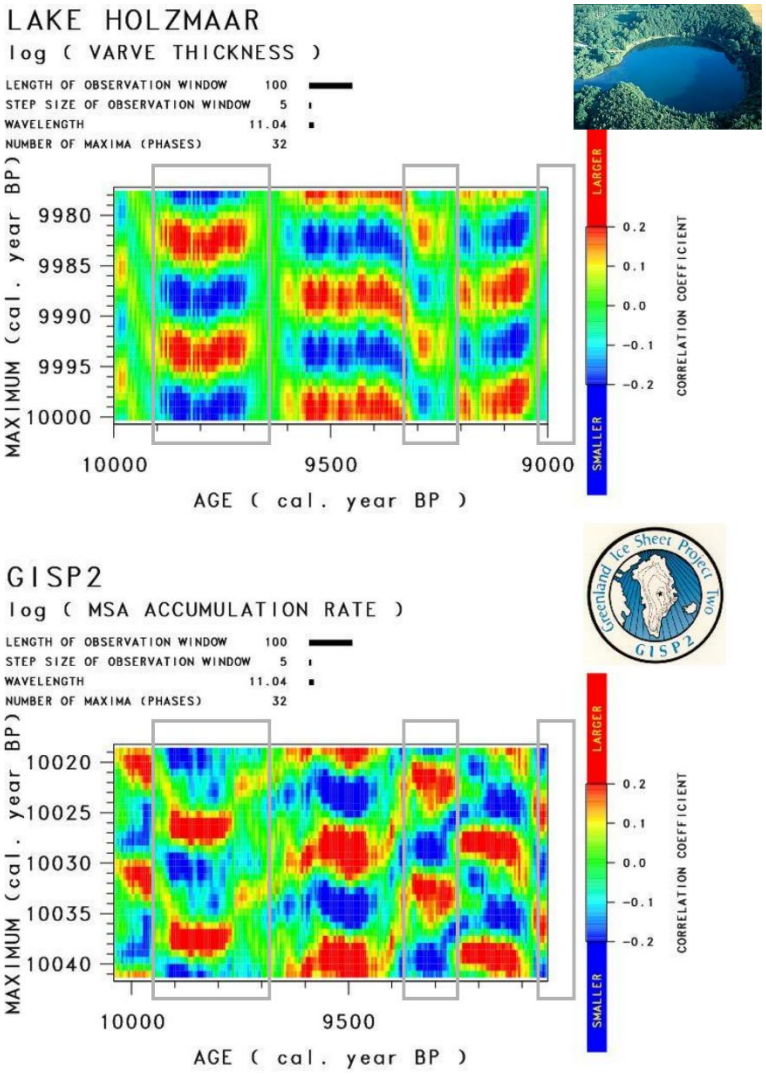

H. Vos et al., in “Climate in Historical Times: Towards a Synthesis of Holocene Proxy Data and Climate Models”, GKSS School of Environmental Research, p. 293 (2004)

F. S. et al., Astron. Nachr. 341 (2020), 600

Original idea: tidal forces might synchronize α to 11.07 years

Current driven **Tayler instability** (with azimuthal wave number m=1) tends to undergo intrinsic helicity oscillations…

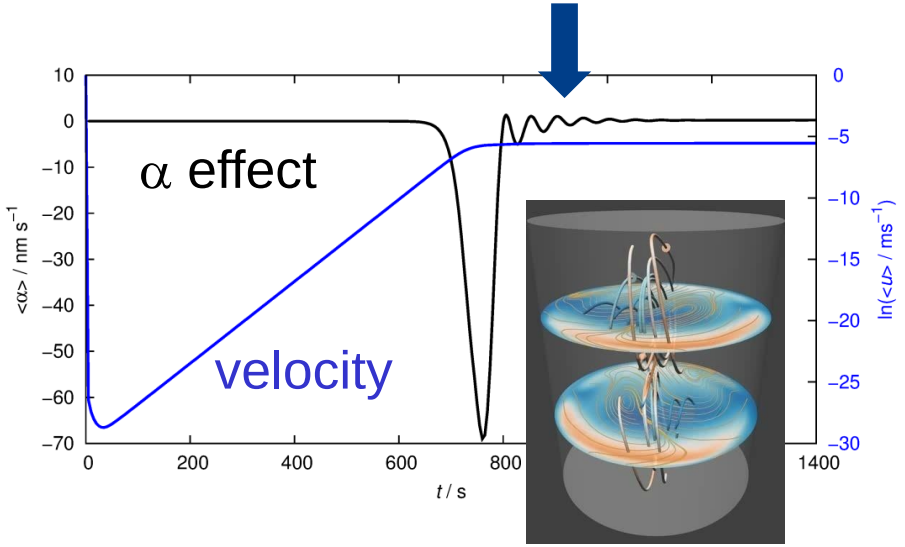

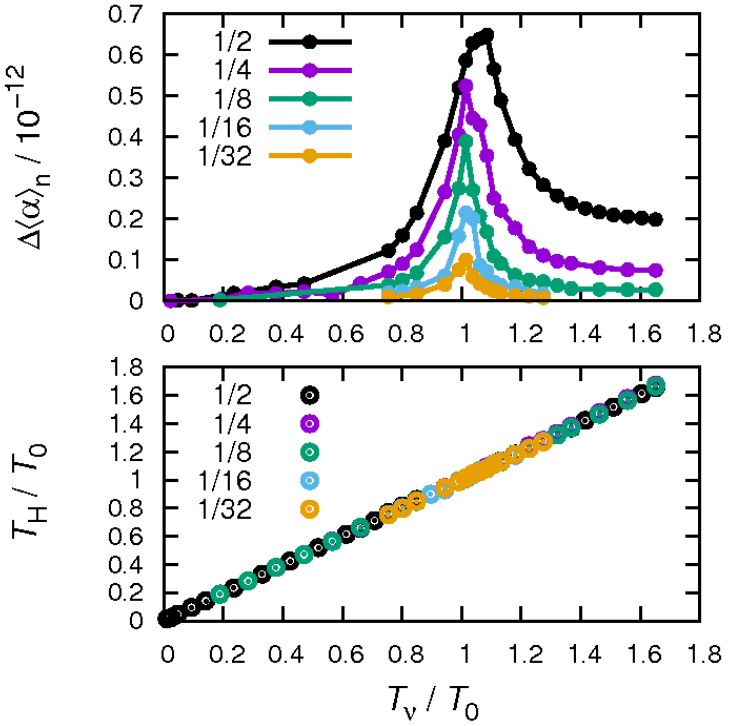

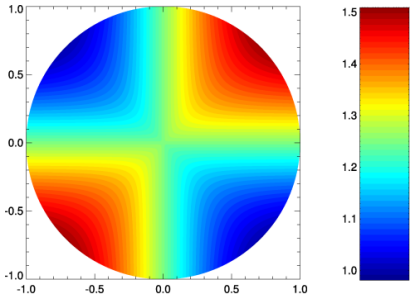

…which can be easily synchronized by tidal (m=2) perturbations (of the VEJ-system)

N. Weber et al., NJP 17 (2015), 113013; F. S. et al., Solar Phys. 291 (2016), 2197; Solar Physics 294 (2019), 60

However: No 11.07-yr peak in the spectrum of tidal potential…

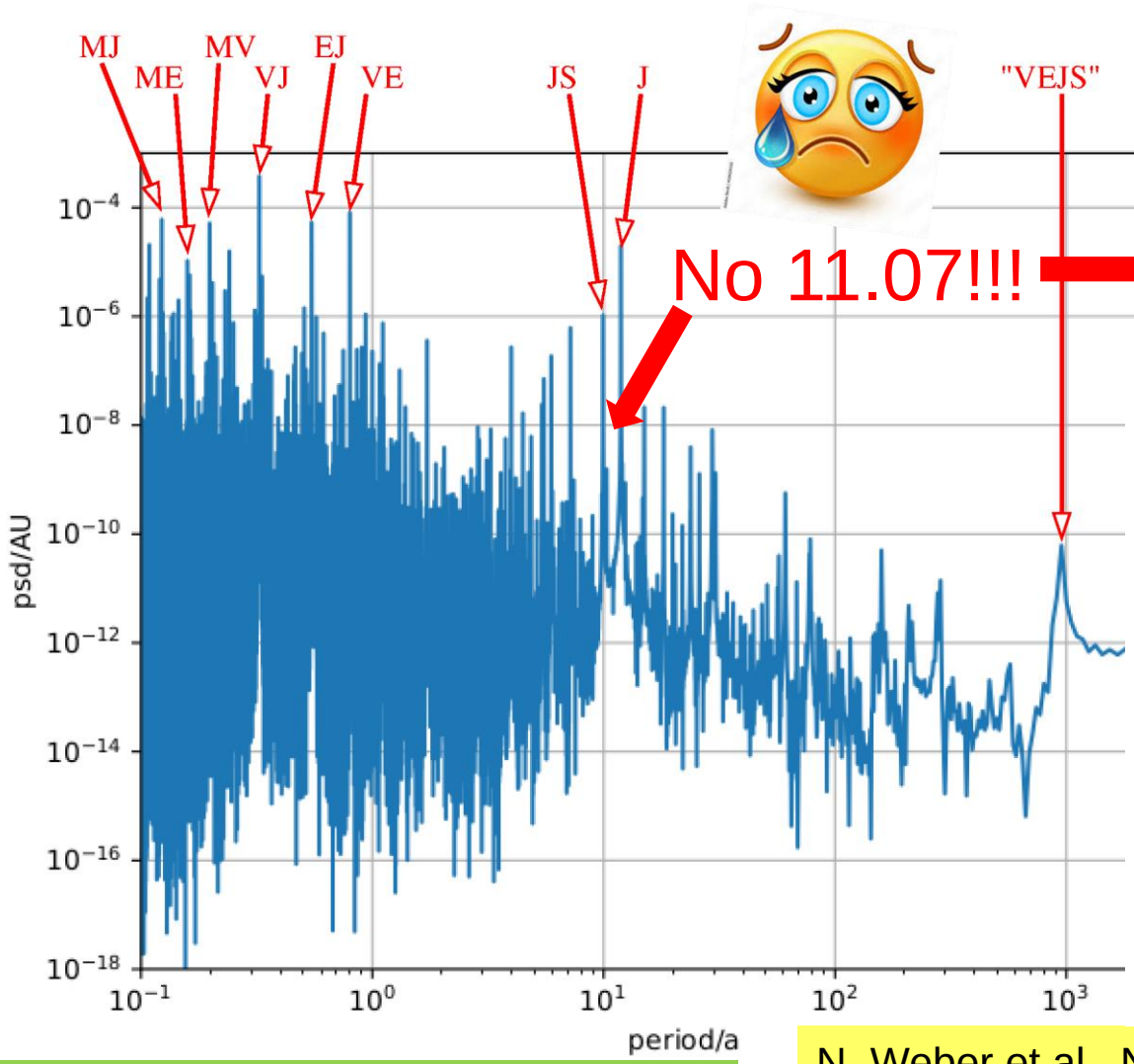

This puts into question the entire concept of **direct helicity synchronization** (e.g., of the Tayler instability) by tidal forces as previously developed in…

H-.C. Nataf, Solar Phys. 297, 107 (2022),
R.G. Cionco et al., Solar Phys. 298, 70 (2023)

N. Weber et al., New J. Phys 17, 113013 (2015); F. Stefani et al. Solar Phys. 291 (2016), 294 (2019), 296 (2021)

However: No 11.07-yr peak in the spectrum of tidal potential…

So, let's first focus on those periods

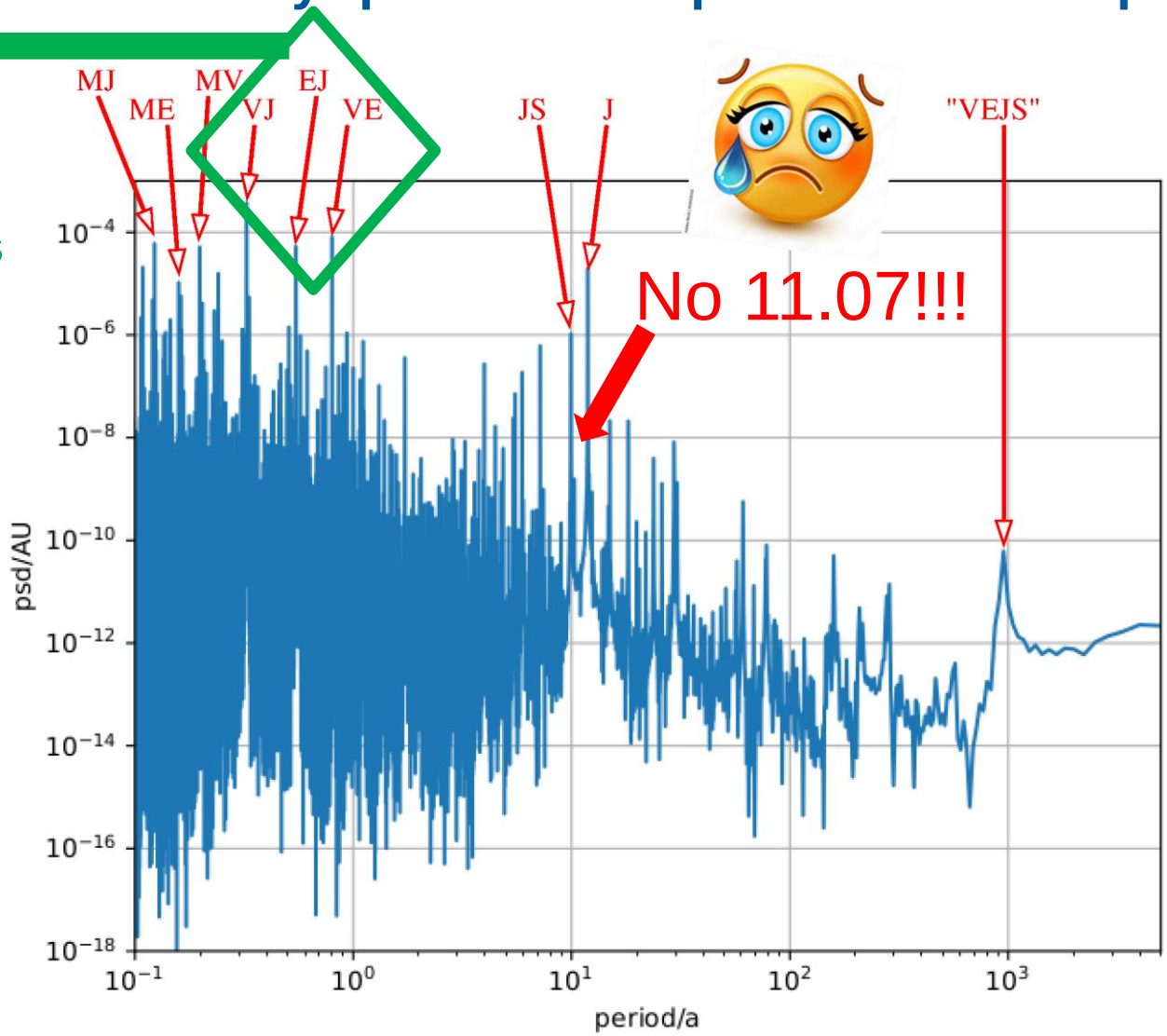

H-.C. Nataf, Solar Phys. 297, 107 (2022),
R.G. Cionco et al., Solar Phys. 298, 70 (2023)

New ansatz: Tidal synchronization of magneto-Rossby waves

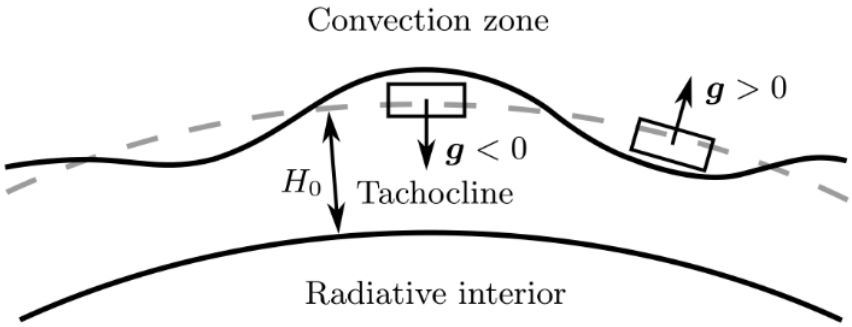

magneto-Rossby waves

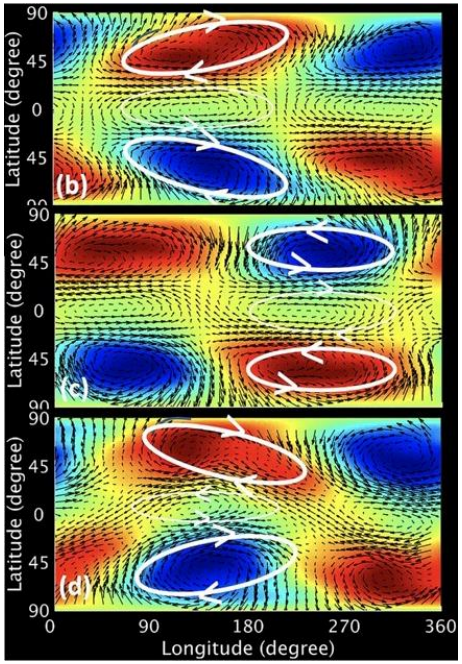

M. Dikpati, S.W. McIntosh, Space Weather 18 (2020), e2018SW002109

Shallow water approximation with azimuthal magnetic field under the influence of tidal forces

G. Horstmann et al., Astrophys. J. 944 (2023), 48; F.S. et al., Solar Physics 299 (2024), 51

New ansatz: Tidal synchronization of magneto-Rossby waves

$$\Box_{v_A}^2 v - C_0^2 \Box_{v_A} \Delta v + f_0^2 \frac{\partial^2 v}{\partial t^2} - C_0^2 \beta \frac{\partial}{\partial x}\frac{\partial v}{\partial t} + 2\lambda \frac{\partial}{\partial t}\Box_{v_A} v - \lambda C_0^2 \Delta \frac{\partial v}{\partial t} + \lambda^2 \frac{\partial^2 v}{\partial t^2} = f_0 \frac{\partial}{\partial x}\frac{\partial^2 V}{\partial t^2} - \lambda \frac{\partial}{\partial y}\frac{\partial^2 V}{\partial t^2} - \frac{\partial}{\partial t}\frac{\partial}{\partial y}\Box_{v_A} V$$
$$= \left[f_0 \Omega + 2\Omega^2 - \frac{2v_A^2}{R_0^2} + \frac{2f_0\Omega}{R_0} y \right] \frac{4K\Omega}{R_0} \sin\left(\frac{2x}{R_0} - 2\Omega t\right) + \frac{4K\lambda\Omega^2}{R_0} \cos\left(\frac{2x}{R_0} - 2\Omega t\right)$$

Rieger-type periods

magneto-Rossby waves

Analytical solution

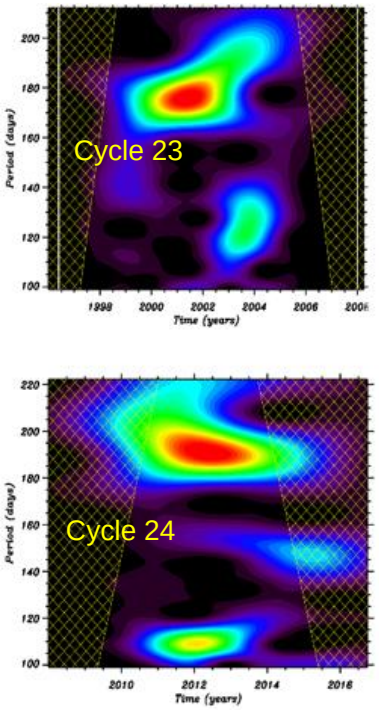

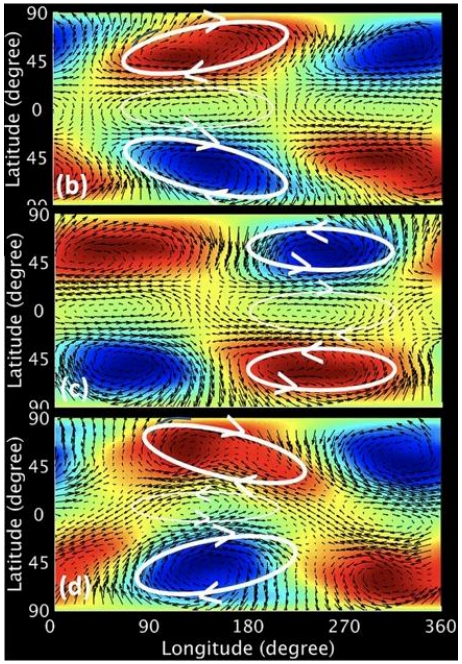

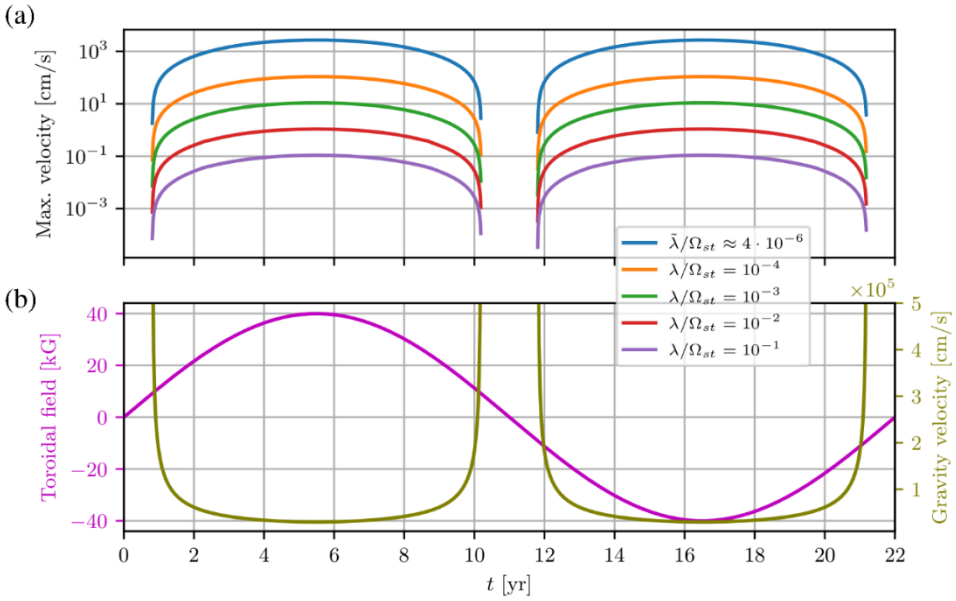

Example: Venus-Jupiter spring tide, period 118 days; wave **velocities of up to 1-100 m/s are possible** for realistic tides

E. Gurgenashvili et al., A&A 653, A146 (2021)

M. Dikpati, S.W. McIntosh, Space Weather 18 (2020), e2018SW002109

New ansatz: Tidal synchronization of magneto-Rossby waves

Venus-Jupiter spring tide with period 118 days

Earth-Jupiter spring tide with period 199 days

Venus-Earth spring tide with period 292 days

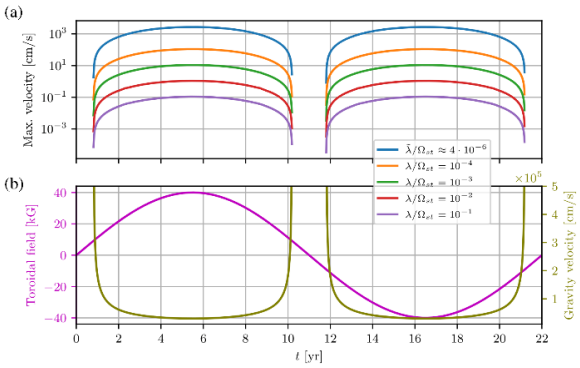

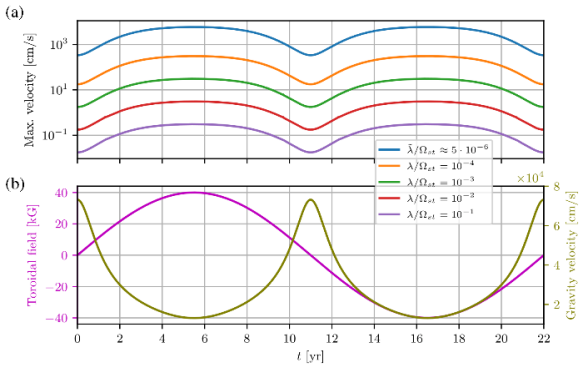

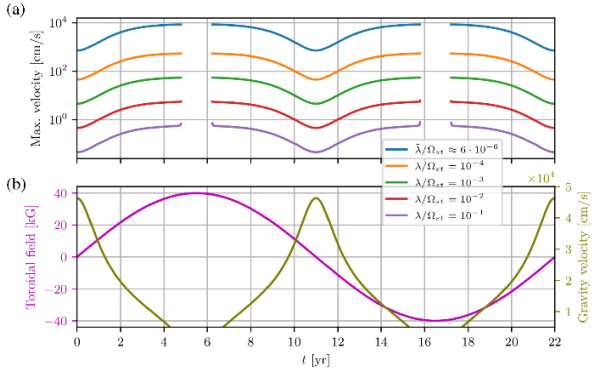

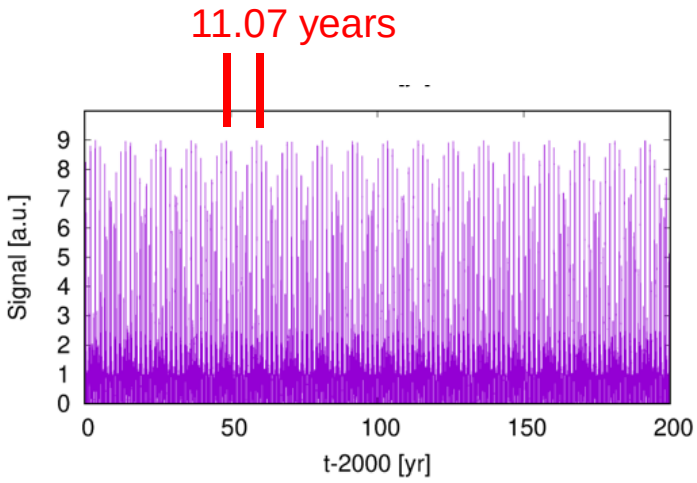

$$s(t) = \left[\cos\left(2\pi \cdot \frac{t - t_{\mathrm{VJ}}}{0.5 \cdot P_{\mathrm{VJ}}}\right) + \cos\left(2\pi \cdot \frac{t - t_{\mathrm{EJ}}}{0.5 \cdot P_{\mathrm{EJ}}}\right) + \cos\left(2\pi \cdot \frac{t - t_{\mathrm{VE}}}{0.5 \cdot P_{\mathrm{VE}}}\right)\right]^2$$

Any dynamo-relevant effect (helicity, α-effect, zonal flow, pressure…) will be a **quadratic functional** of the waves. This comprises a significant part with **11.07-year** period.

F.S. et al., Solar Physics 299 (2024), 51

A „realistic“ 2D α–Ω-dynamo model with meridional circulation…

$$\frac{\partial B}{\partial t} = \tilde{\eta} D^2 B + \frac{1}{s}\frac{\partial (sB)}{\partial r}\frac{\partial \tilde{\eta}}{\partial r} - R_\mathrm{m} s \boldsymbol{u}_\mathrm{p}\cdot\nabla\left(\frac{B}{s}\right) + C_\Omega s(\nabla\times(A\boldsymbol{e}_\phi))\cdot\nabla\Omega\,,$$

$$\frac{\partial A}{\partial t} = \tilde{\eta} D^2 A - \frac{R_\mathrm{m}}{s}\boldsymbol{u}_\mathrm{p}\cdot\nabla(sA) + C_\alpha^\mathrm{c}\alpha^\mathrm{c}B + C_\alpha^\mathrm{p}\alpha^\mathrm{p}B\,,$$

$$C_\Omega = \Omega_\mathrm{eq}\mathrm{R}_\odot^2/\eta_\mathrm{t}\,,$$

$$R_\mathrm{m} = u_0\mathrm{R}_\odot/\eta_\mathrm{t}\,,$$

$$C_\alpha^\mathrm{c} = \alpha_\mathrm{max}^\mathrm{c}\mathrm{R}_\odot/\eta_\mathrm{t}\,,$$

$$C_\alpha^\mathrm{p} = \alpha_\mathrm{max}^\mathrm{p}\mathrm{R}_\odot/\eta_\mathrm{t}\,.$$

$$\Omega(r,\Theta) = C_\Omega\left\{\Omega_\mathrm{c} + \frac{1}{2}\left[1+\mathrm{erf}\left(\frac{r-r_\mathrm{c}}{d}\right)\right](1-\Omega_\mathrm{c}-c_2\cos^2\Theta)\right\}$$

$$\alpha^\mathrm{c}(r,\Theta,t) = C_\alpha^\mathrm{c}\frac{3\sqrt{3}}{4}\sin^2\Theta\cos\Theta\left[1+\mathrm{erf}\left(\frac{r-r_\mathrm{c}}{d}\right)\right]\left[1+\frac{|\boldsymbol{B}(r,\Theta,t)|^2}{B_0^2}\right]^{-1}$$

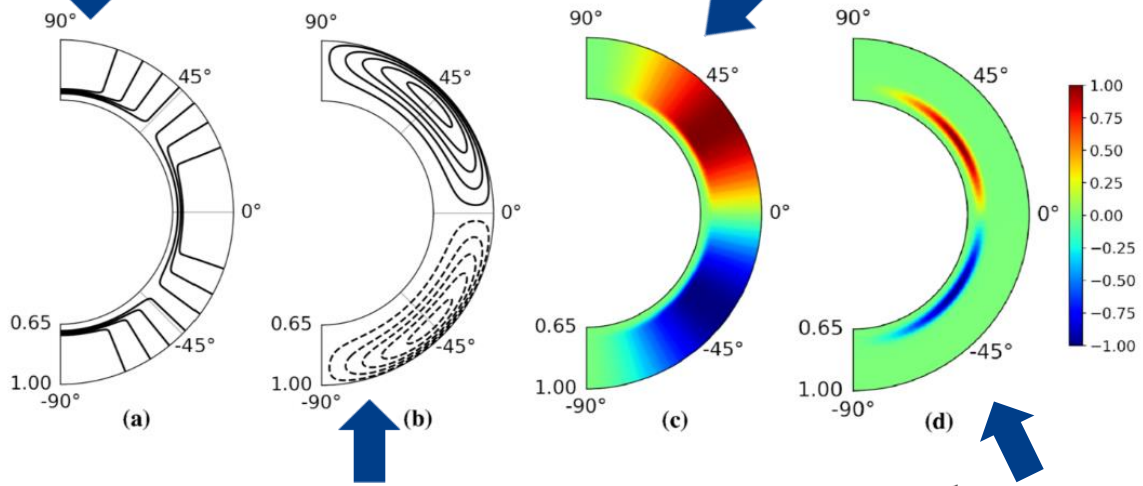

$$\alpha = \alpha^\mathrm{c} + \alpha^\mathrm{p}$$

Assumed to result from wave helicity

$$\boldsymbol{u}_\mathrm{p} = \nabla\times(\psi(r,\Theta)\boldsymbol{e}_\phi)$$

$$\alpha^\mathrm{p}(r,\Theta,t) = C_\alpha^\mathrm{p}\frac{1}{\sqrt{2}}\sin^2\Theta\cos\Theta\left[1+\mathrm{erf}\left(\frac{r-r_\mathrm{c}}{d}\right)\right]\left[1-\mathrm{erf}\left(\frac{r-r_\mathrm{d}}{d}\right)\right]\times$$

$$\psi(r,\Theta) = R_\mathrm{m}\left\{-\frac{2}{\pi}\frac{(r-r_\mathrm{b})^2}{(1-r_\mathrm{b})}\sin\left(\pi\frac{r-r_\mathrm{b}}{1-r_\mathrm{b}}\right)\cos\Theta\sin\Theta\right\}$$

$$\frac{2|\boldsymbol{B}(r,\Theta,t)|^2}{1+|\boldsymbol{B}(r,\Theta,t)|^4}\sin(2\pi t/T_\mathrm{f})\,,$$

11.07 yr

M. Klevs, F. Stefani., L. Jouve, Solar Phys. 298, 90 (2023)

…shows a nice parametric resonance

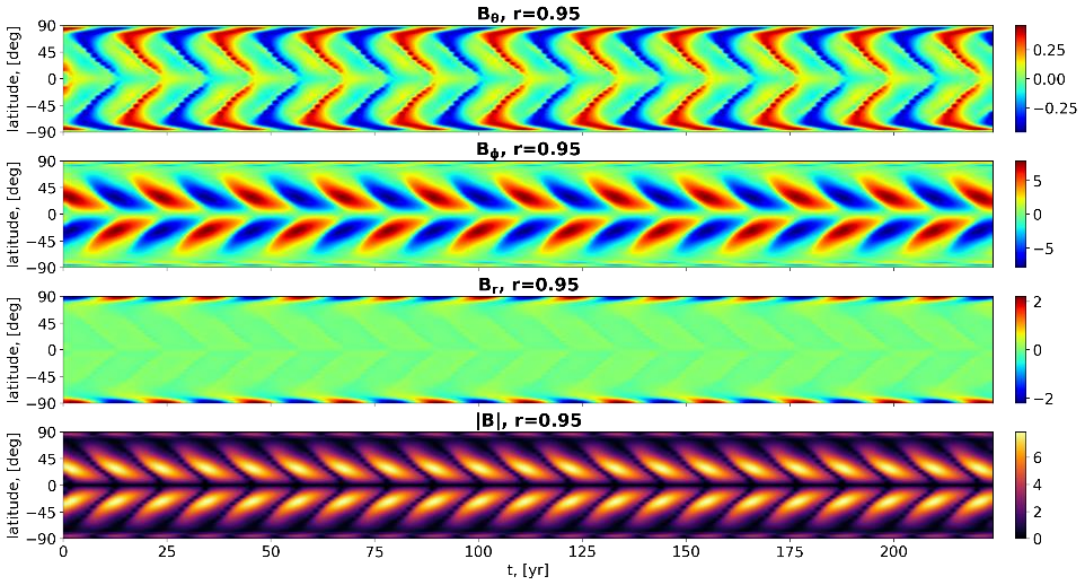

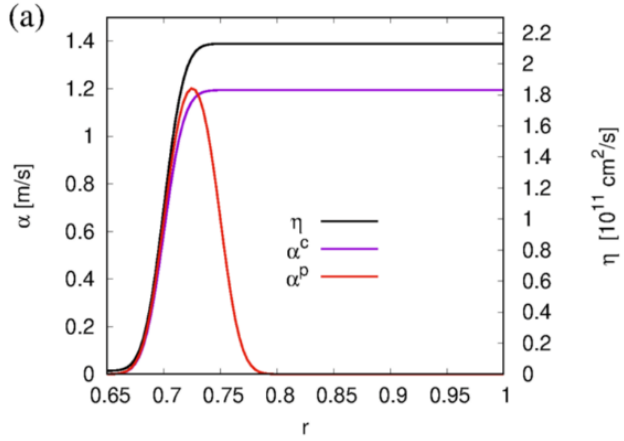

Much higher conductivity in the tachocline than in the convection zone

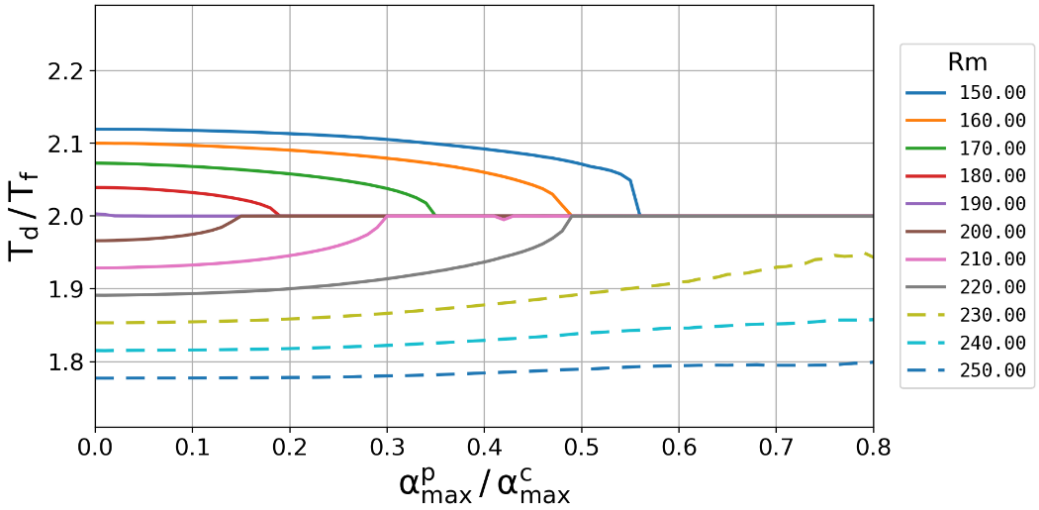

For a reasonable value α_0=1.3 m/s, we need just **some dm/s** for the synchronized α–term to entrain the entire dynamo

Suess/de Vries cycle: A beat period between 22.14 and 19.86 yr ?

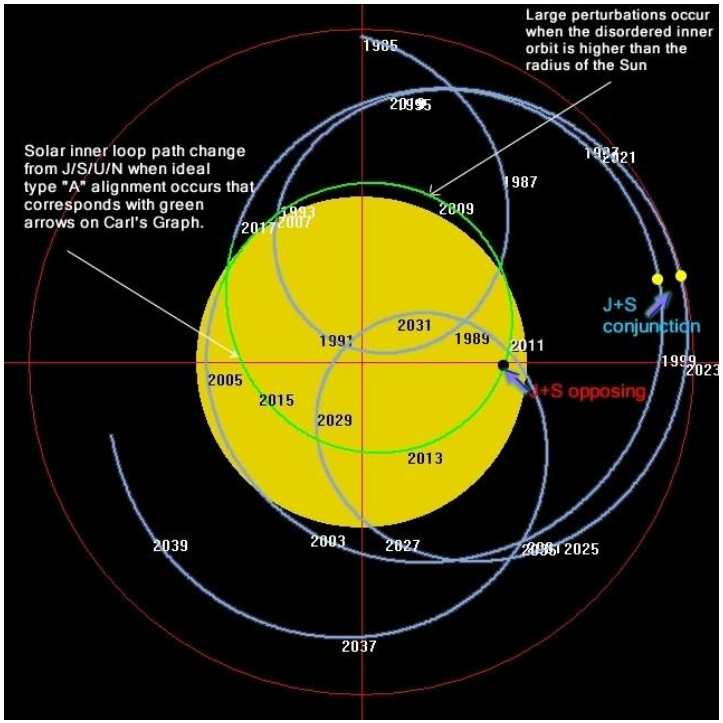

Tidal forcing → **22.14 years**

Sun around barycenter → **19.86 years**

(with unclear spin-orbit coupling ← J. Shirley, arXiv:2309.13076

Beat period: **193 years**

19.86 x 22.14/(22.14-19.86)

193 years: Suess-de Vries cycle

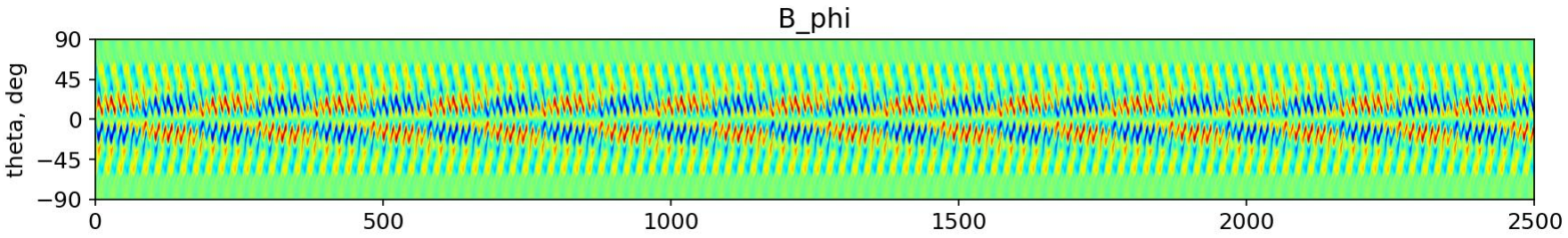

Comparison: numerical results - sediment data (Lake Lisan)

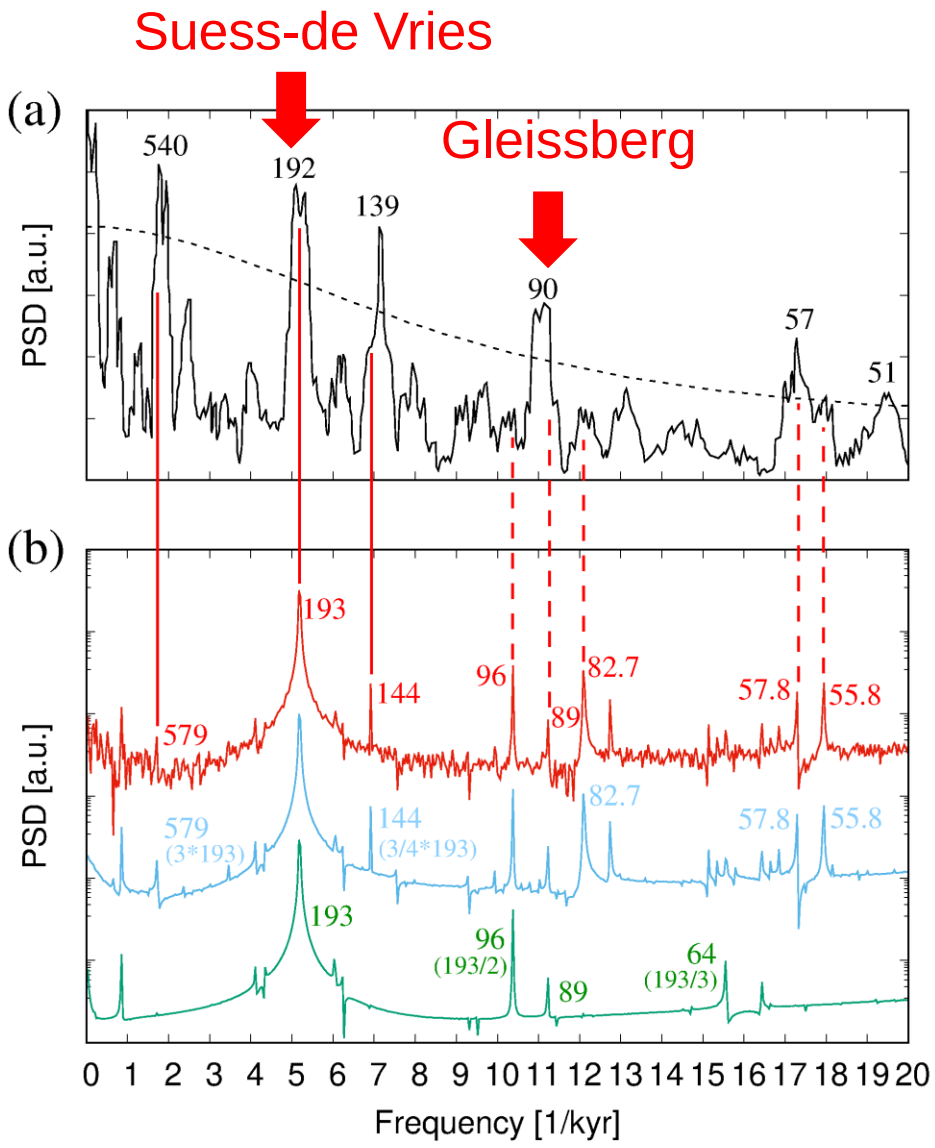

Yearly sediment thicknesses over 8500 years (climate archive)

S. Prasad et al., Geology 32, 581 (2004)

1D α–Ω-dynamo model

…with some noise

…all planets

…only Jupiter and Saturn

F.S. et al., Solar Physics 296, 88 (2021); 299, 51 (2024)

Very fresh: Quasi-biennial oscillation (QBO)….

…with typical periods of 1.5-1.8 years shows up in many data of solar activity. One example:

Monthly data of sunspot area, and 7-months average

7-months average and 25-months average

Difference between 7-months and 25-months average (+ Gnevyshev-Gap)

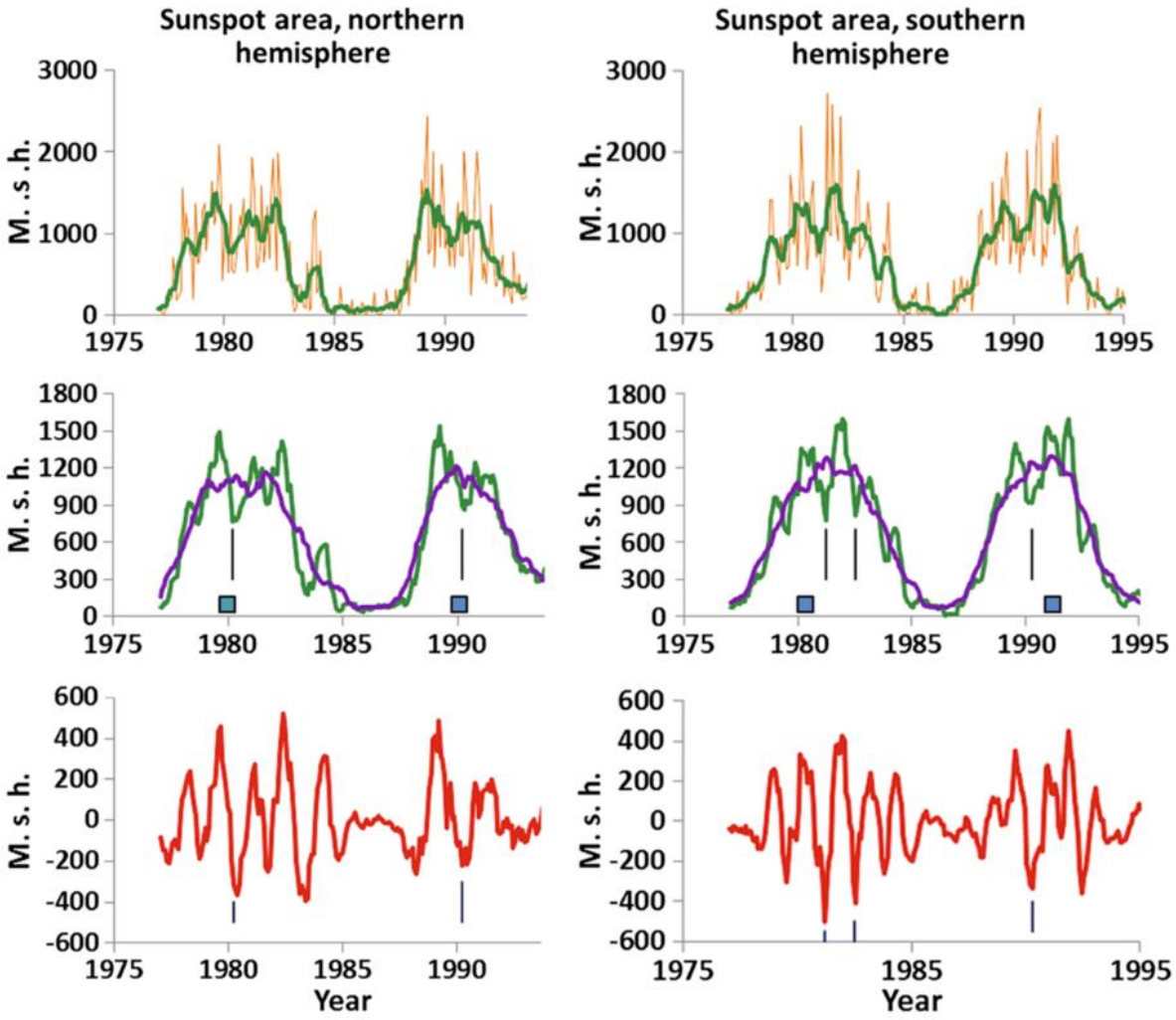

G. Bazilevskaya et al., Space Sci. Rev. 186, 359 (2014)

Very fresh: Quasi-biennial oscillation (QBO)

Sum of waves with periods of 118, 199, 292 day

Square of that sum

Axi-symmetric part of the square

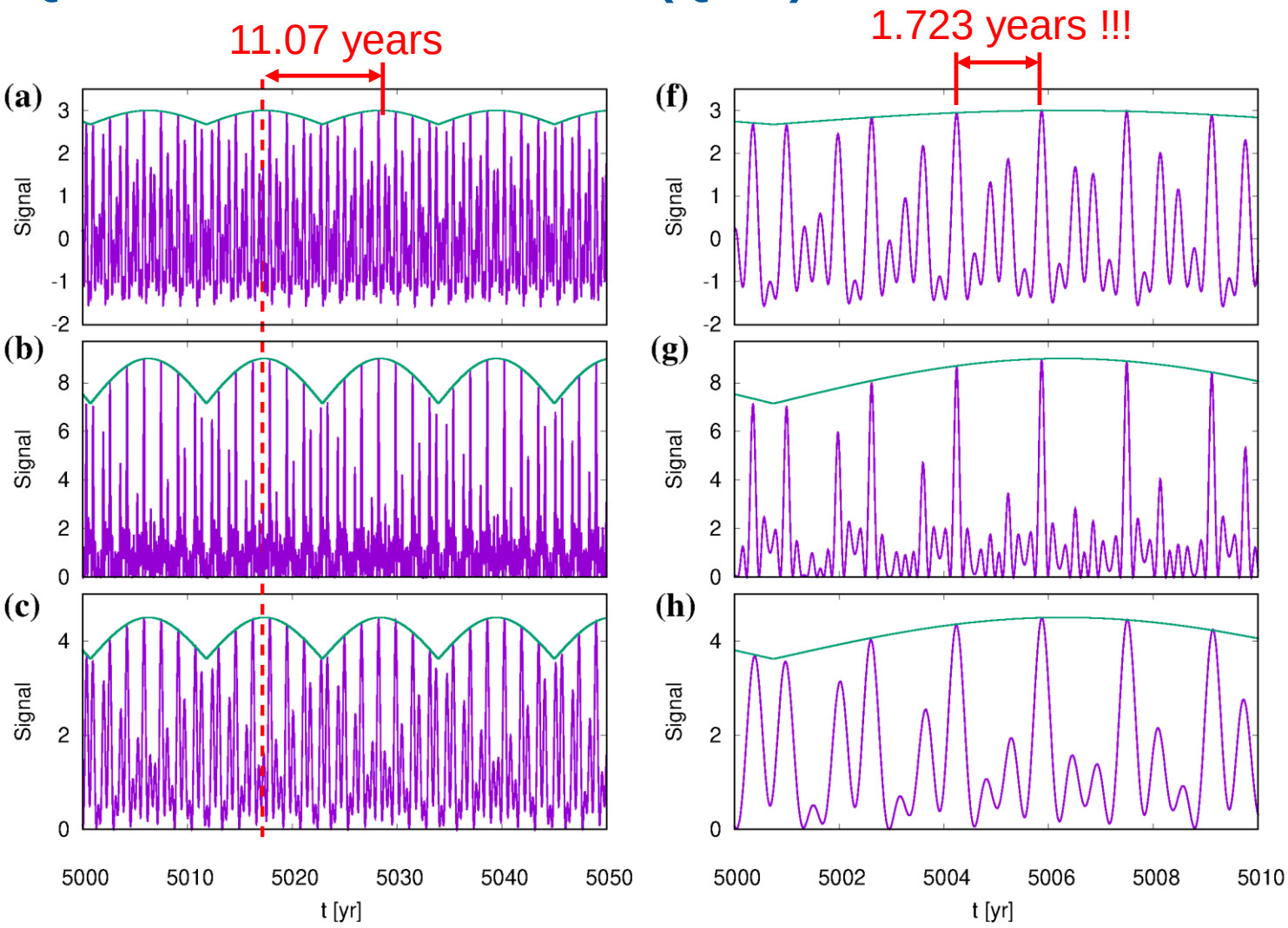

F. S. et al., Adding further pieces to the synchronization puzzle: QBO, bimodality, and phase jumps, Solar Physics (accepted); arXiv:2503.22337

The QBO in our model…

…emerges quite naturally when implementing the full axi-symmetric part into the dynamo model. Fortunately, the 22.14-year Hale cycle remains!

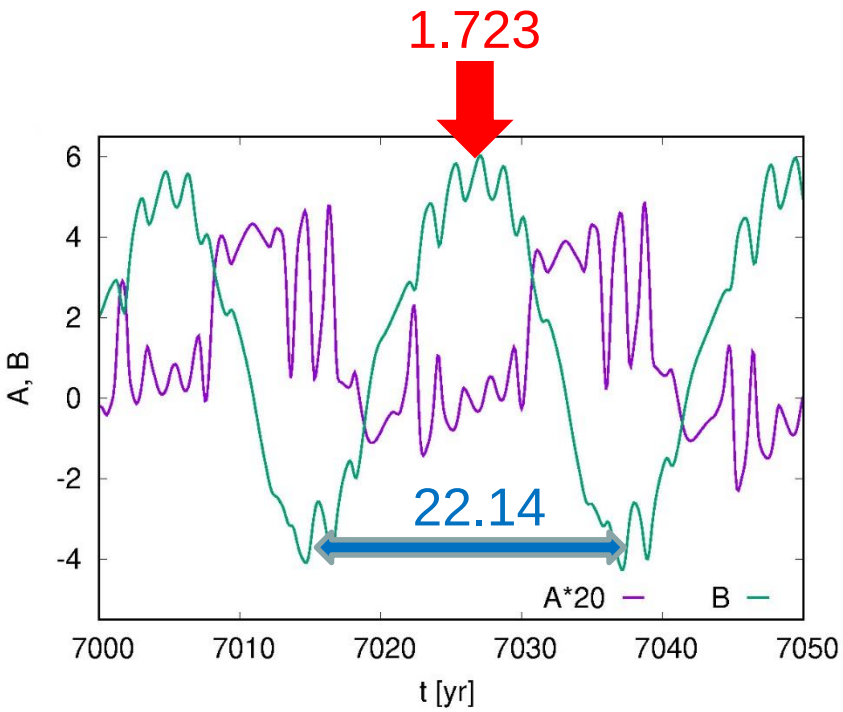

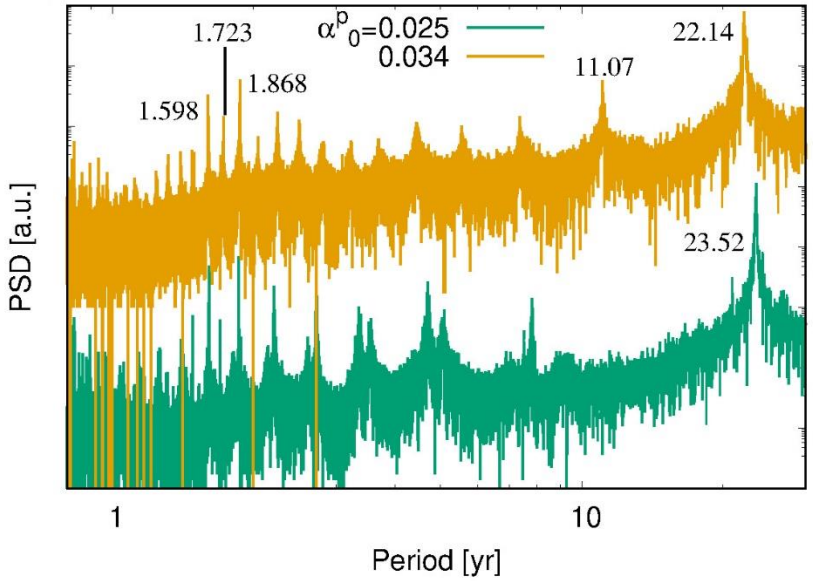

Reconsidering Ground-Level Enhancement Events (GLEE)…

Originally identified in

V.M. Velasco Herrera et al., New Astron. 60, 7 (2018)

as 1.73 years.

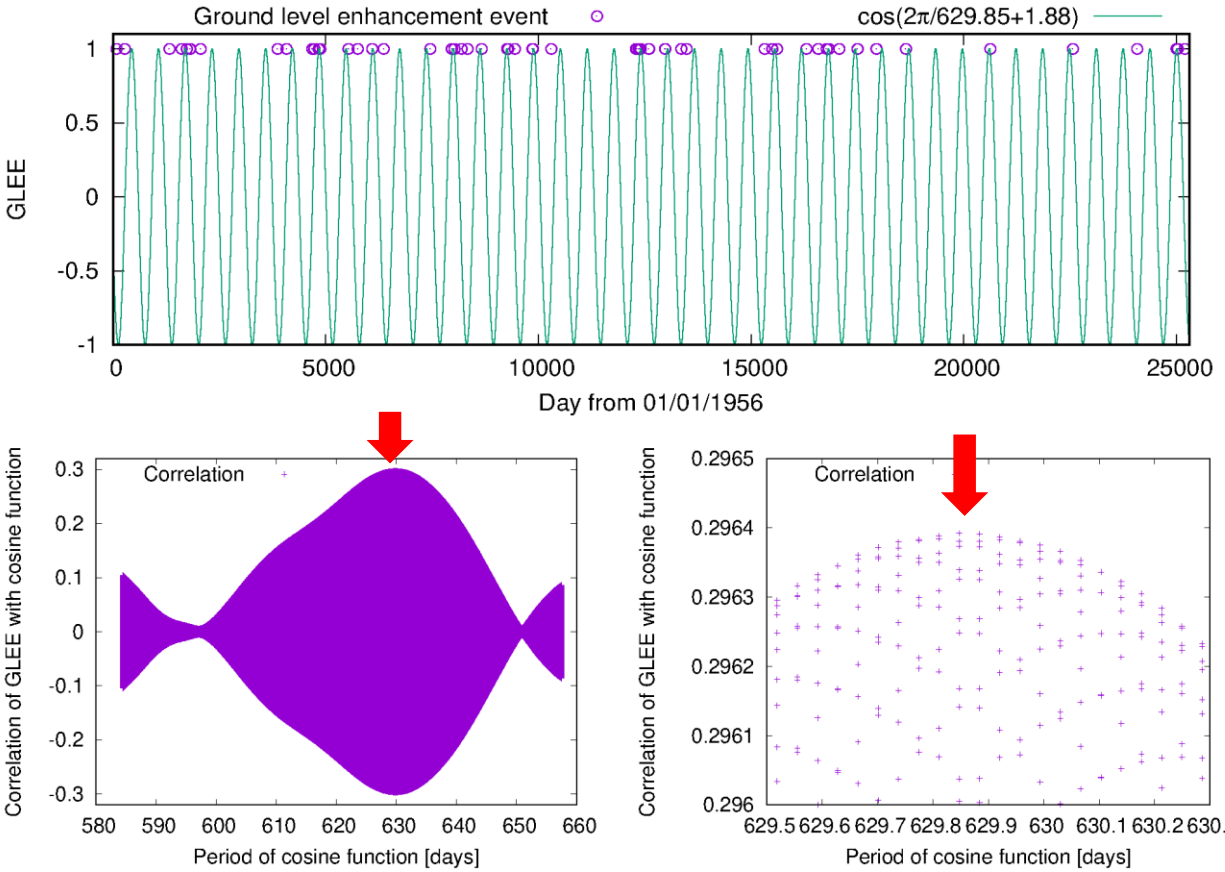

- New analysis with longer data → Maximum of correlation at period of 229.85 days = 1.724 years
- Our dynamo model gave 1.723 Jahre
- Difference is smaller than 0.1 Prozent

Consistent model of QBO, Schwabe/Hale, Suess-Vries

When taking into account spin-orbit coupling, we regain also the Suess-de Vries cycle of 193 years.

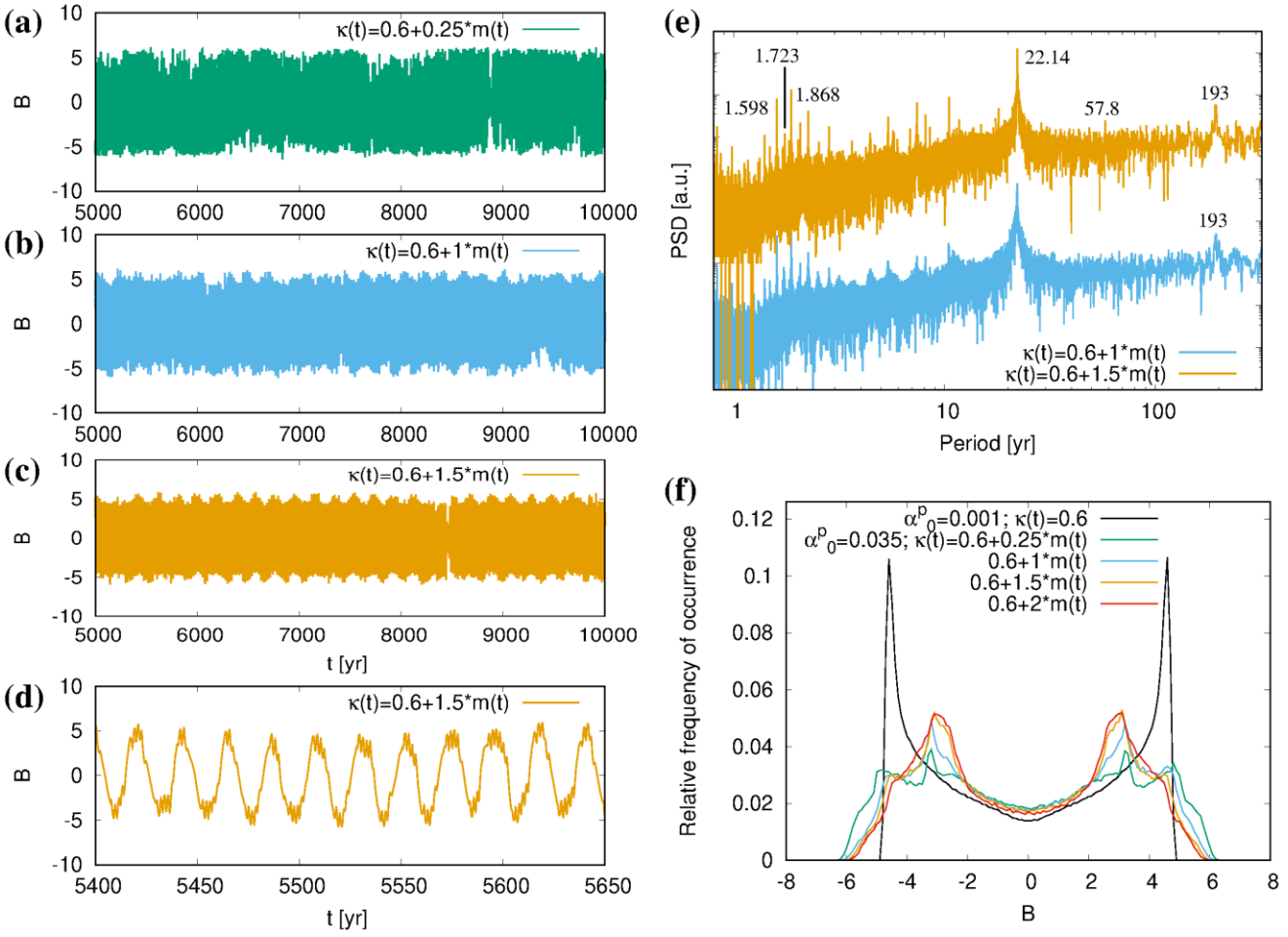

Consistent model of QBO, Schwabe/Hale, Suess-Vries

When taking into account spin-orbit coupling, we regain also the Suess-de Vries cycle of 193 years.

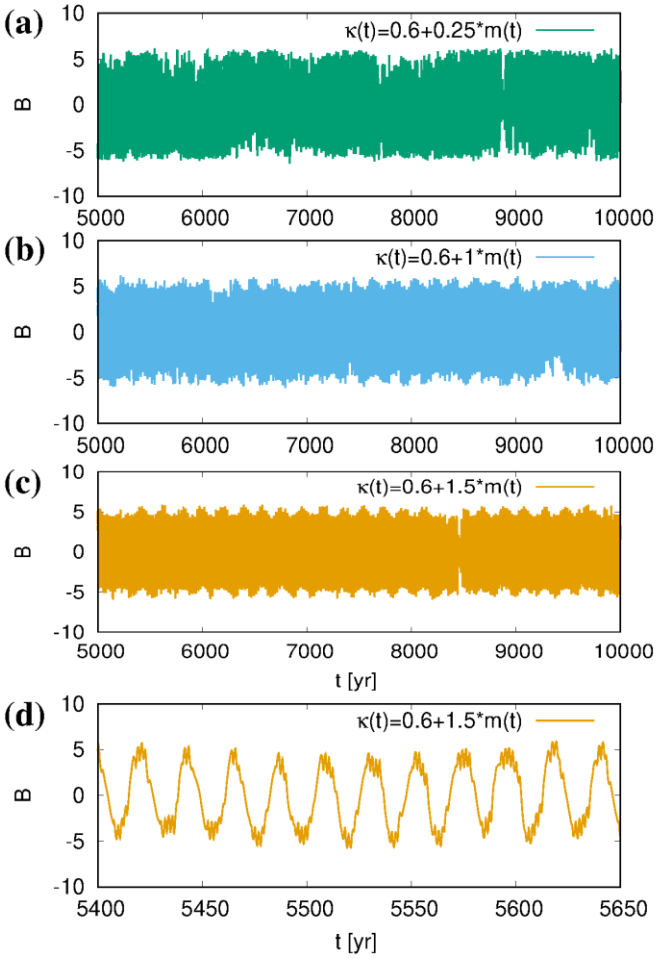

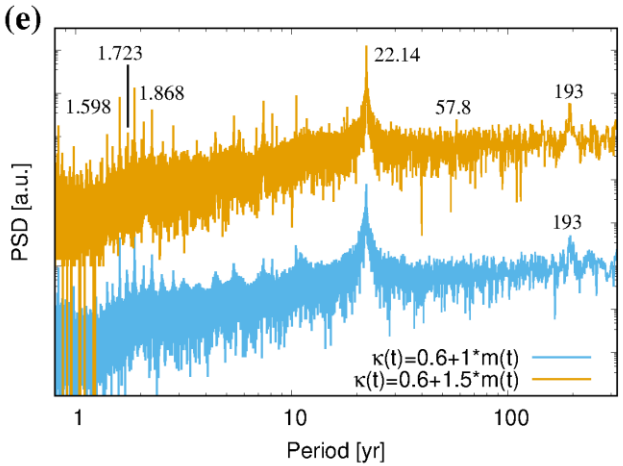

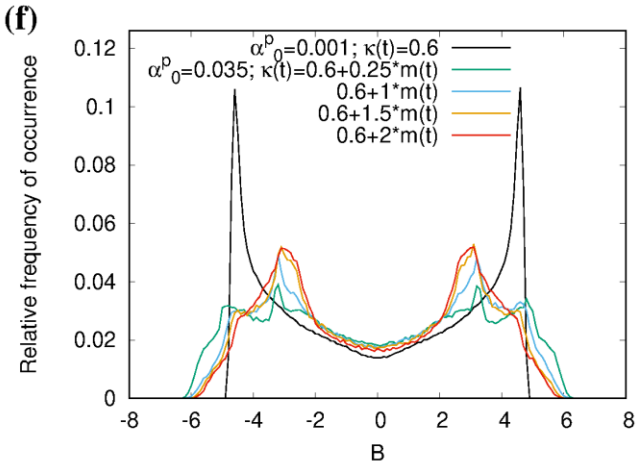

?

The QBO in our model …

…provides a typical double peak in the distribution function

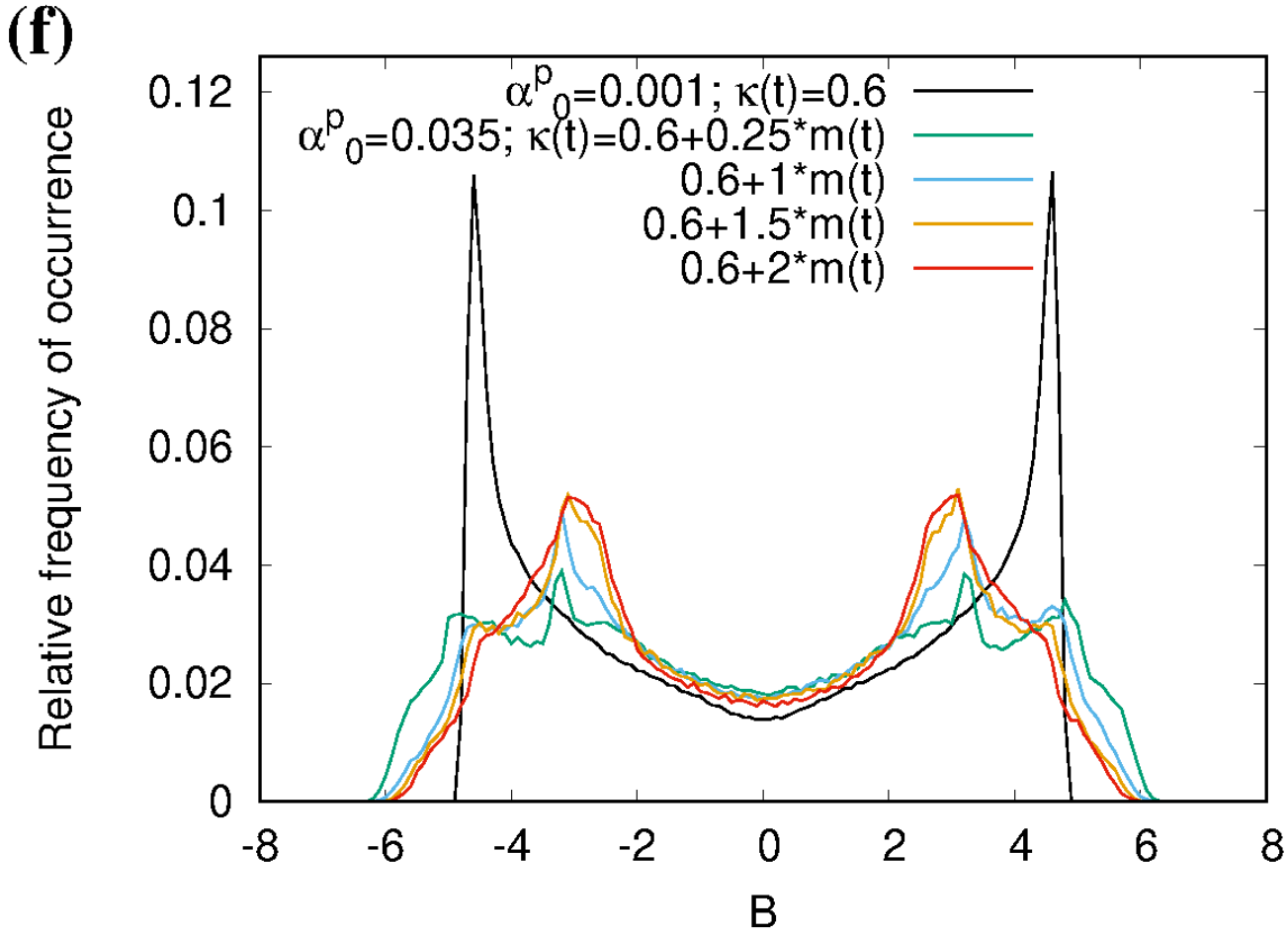

…which is well-known in the literature

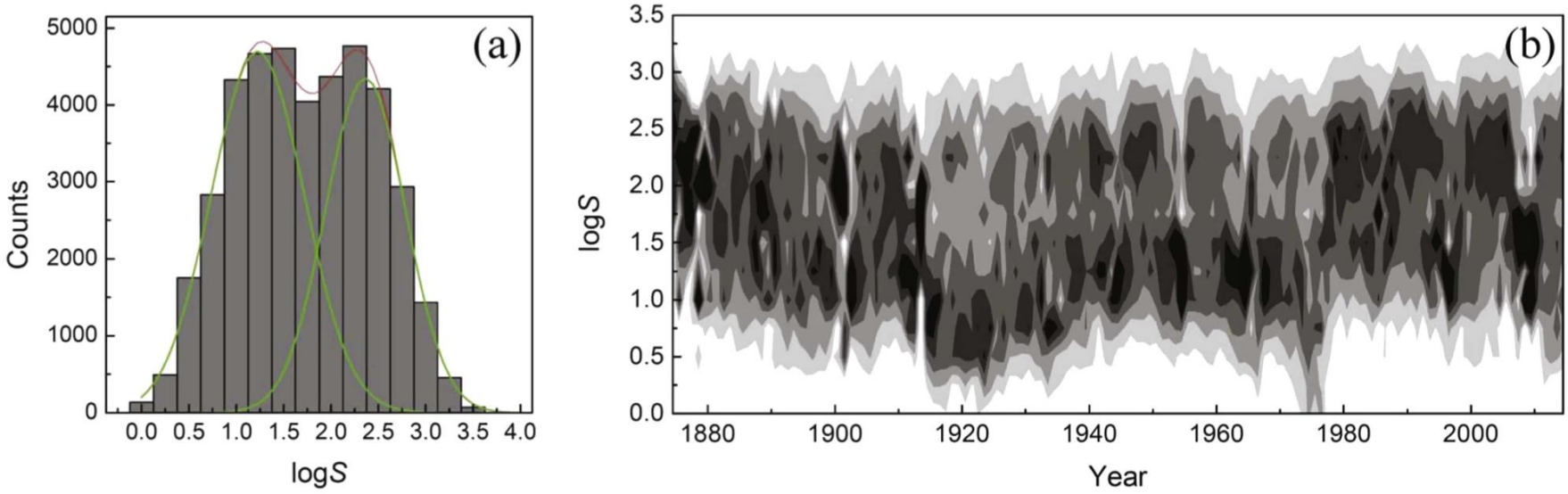

Y. A. Nagovitsyn, A. A. Pevtsov, Astrophys. J. 833, 94 (2016)

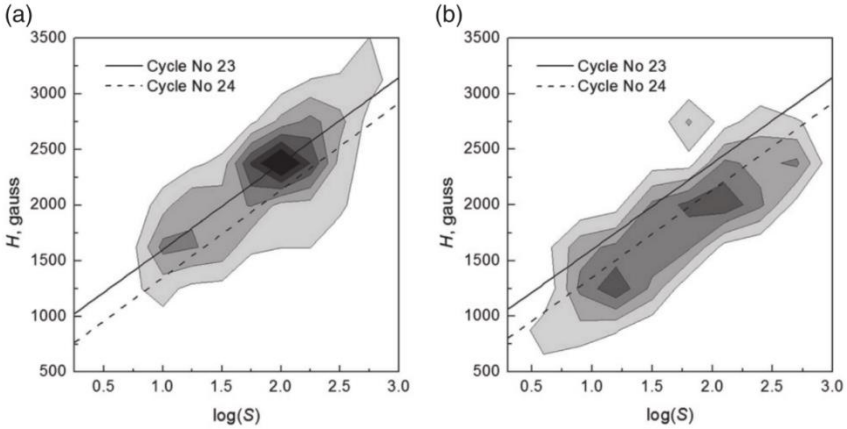

Y. A. Nagovitsyn, A. A. Pevtsov, A. A. Osipova, Astron. Nachr. 338, 26 (2017)

The QBO in our model …

…also leads to a remarkable “sedation” of the dynamo (it “sits” much longer at lower field strenghts)

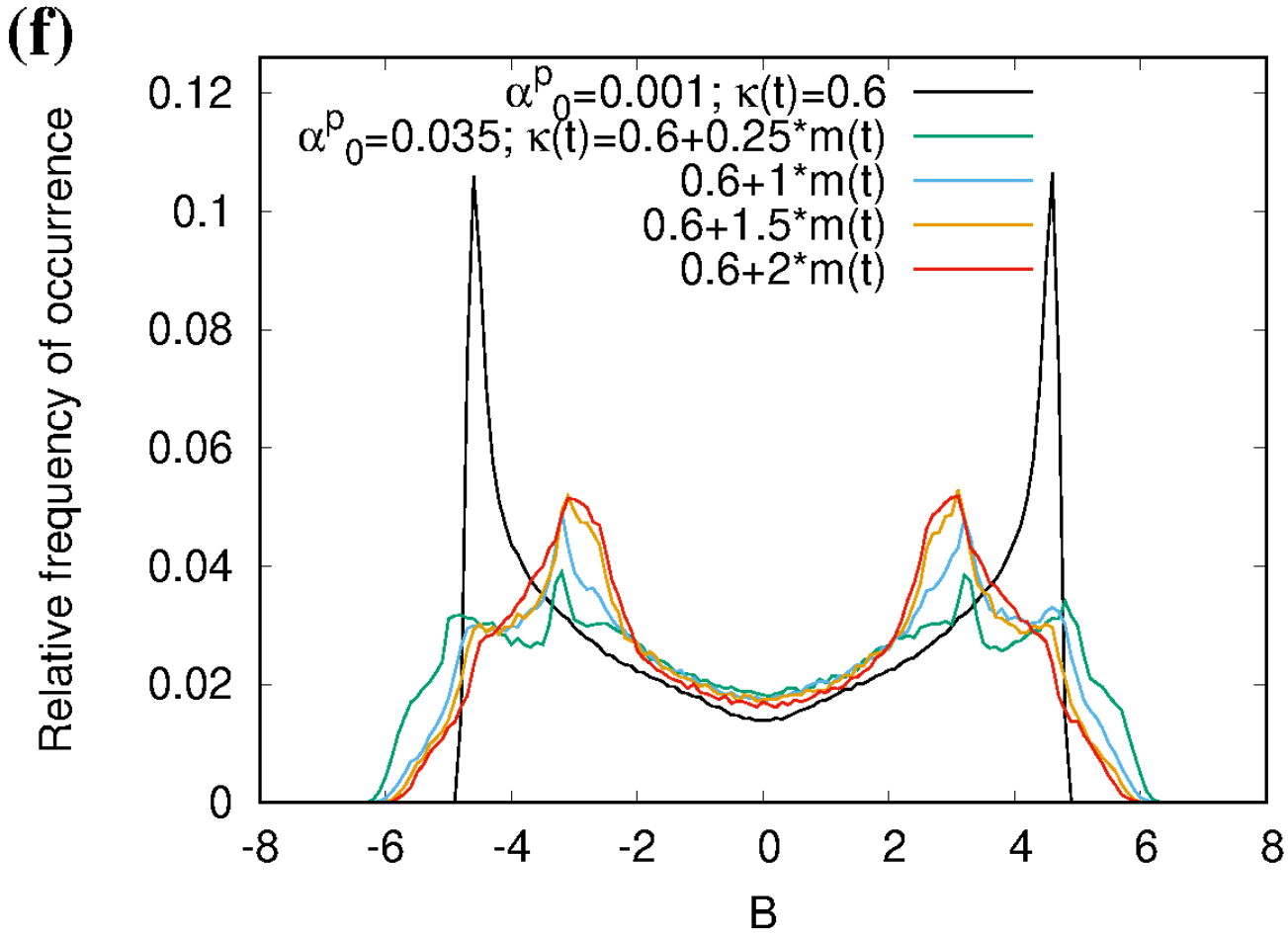

…which might explain why…

…the variability of solar activity is about 5 times lower than that of other solar-like (periodic) stars.

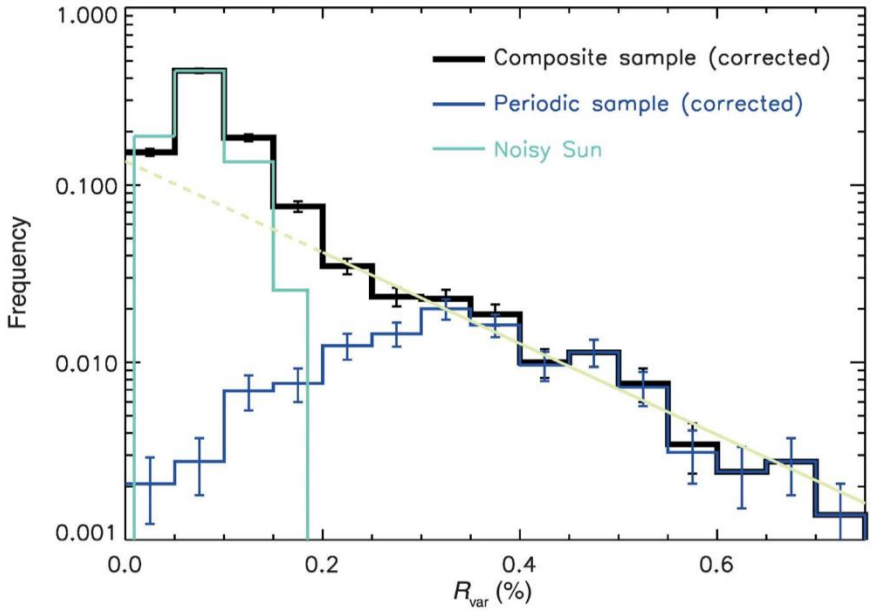

T. Reinhold et al., Science 368, 518–521 (2020)

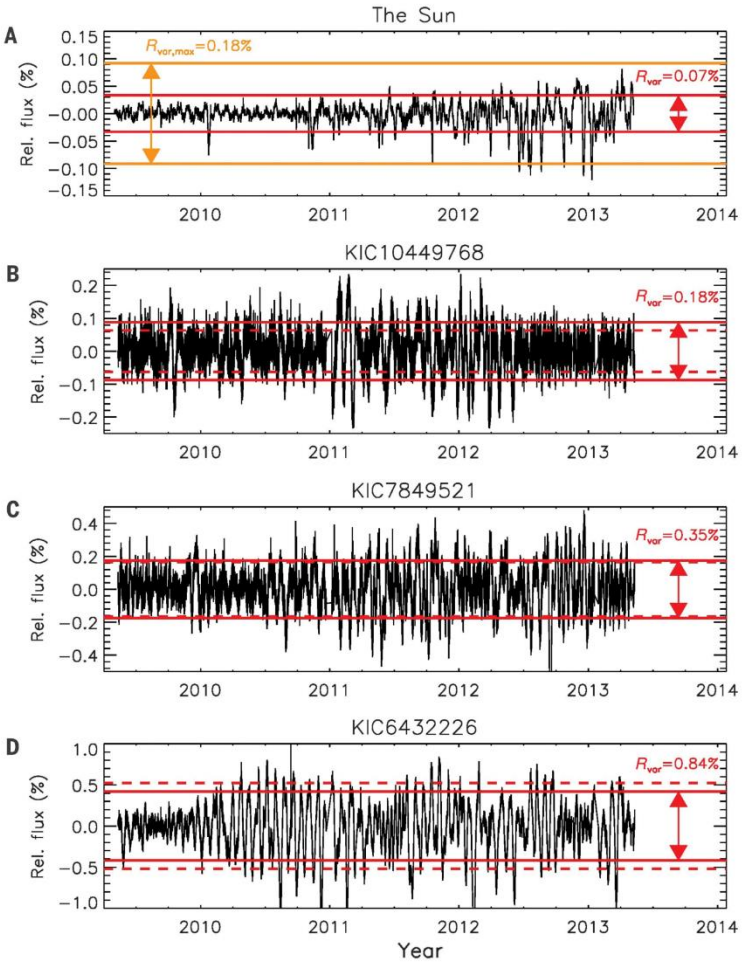

…which might explain why…

…the variability of solar activity is about 5 times lower than that of other solar-like (periodic) stars.

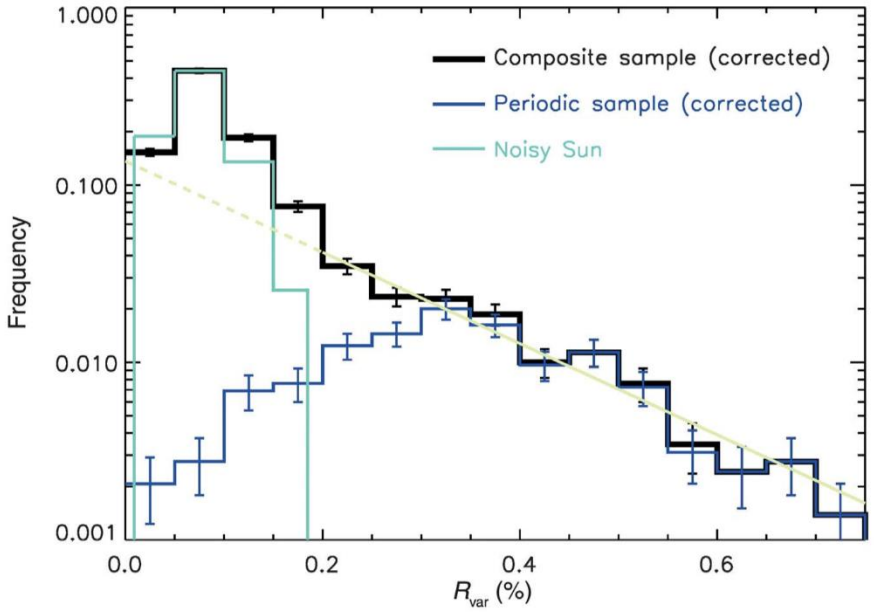

T. Reinhold et al., Science 368, 518–521 (2020)

"The work by Reinhold et al. raises the possibility that the Sun is in an **uncharacteristically subdued state of activity** compared to the peers to which it is commonly compared, even though it is not currently in a state like the Maunder Minimum"

E.W. Cliver et al., Liv. Rev. Solar Phys. (2022), 19, 2

Speaking about uncharacteristically low values…

…what about the **particularly** low values of ^{7}Li?

M. Carlos et al., The Li-age correlation: the Sun is unusually Li deficient for its age, MNRAS 485, 4052 (2019)

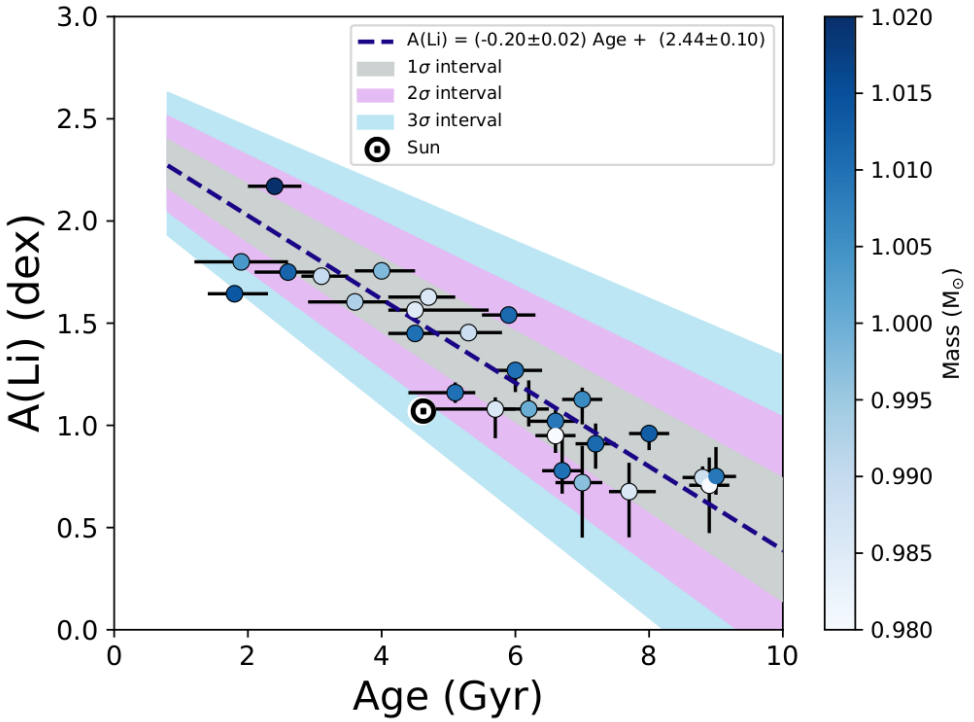

Could the enhanced Rossby waves be responsible for that?

“One solution to erase this disagreement is to introduced macroscopic transport at the base of the envelope…”

G. Buldgen et al., A&A 669, L9 (2023)

Summary of our synchronized solar dynamo model

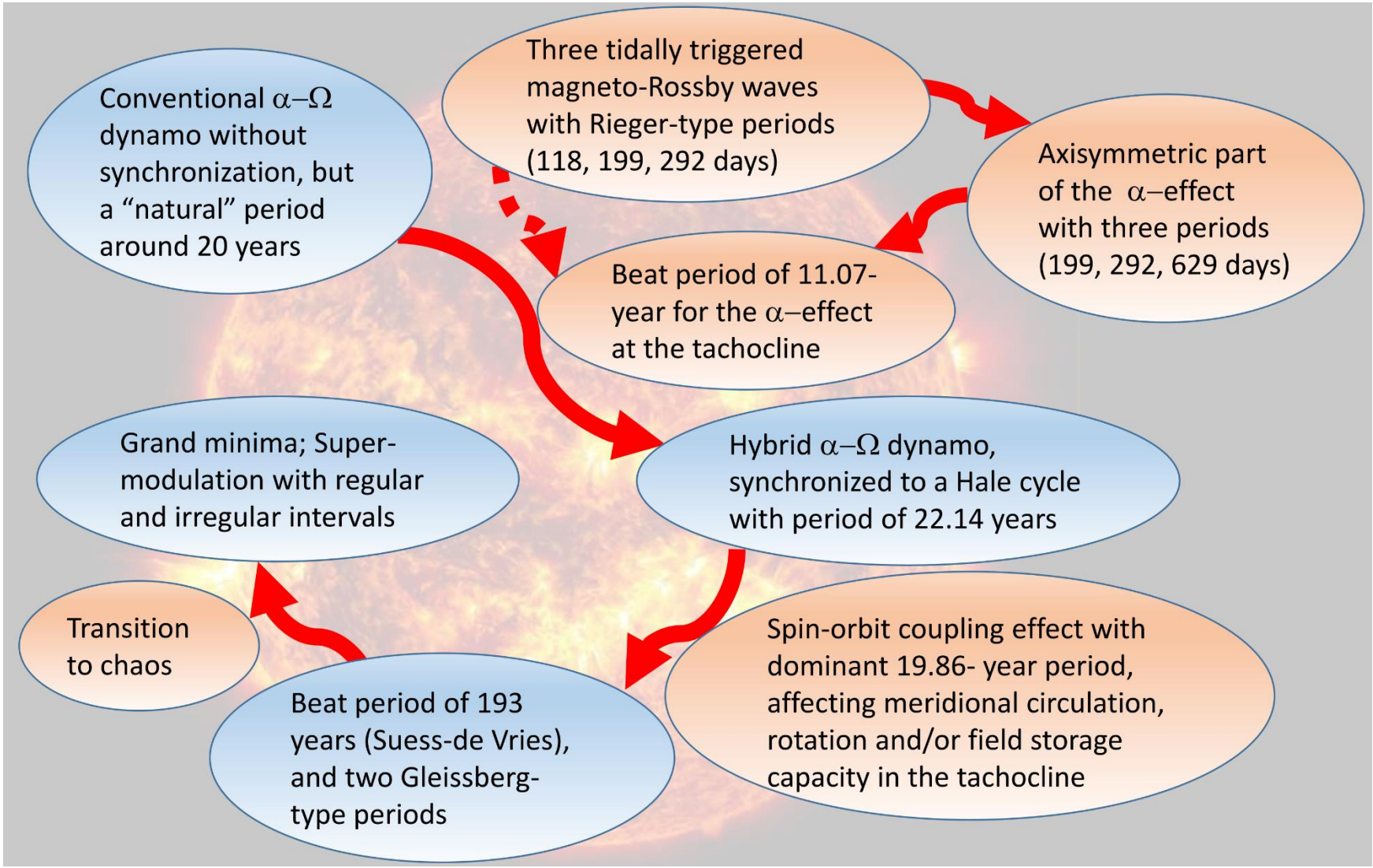

Summary of our synchronized solar dynamo model

- General principle: Energy is „harvested“ on the shortest possible time-scales
- **Various dynamo periods emerge as beat periods**
- Three tidally triggered magneto-Rossby waves on Rieger-type time-scale → **QBO + Schwabe/Hale**
- Hale+Barycentric motion → **Suess-de Vries** (+Gleissberg)
- **Self-consistency**: **The sharp Suess-de Vries peak at 193 years could hardly be explained without phase-stability of the primary Hale cycle at 22.14 years**

Precession driven DRESDYN dynamo: Two motivations

Influence of Milankovic cycles (precession, nutation, ellipticity) on the geodynamo

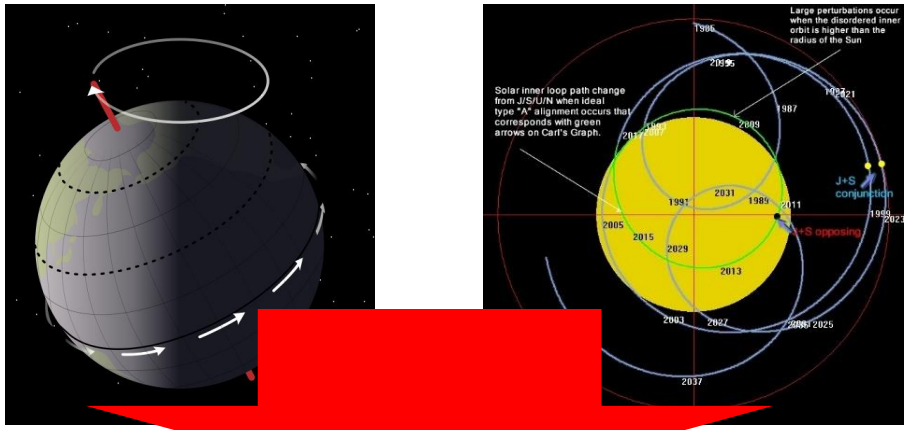

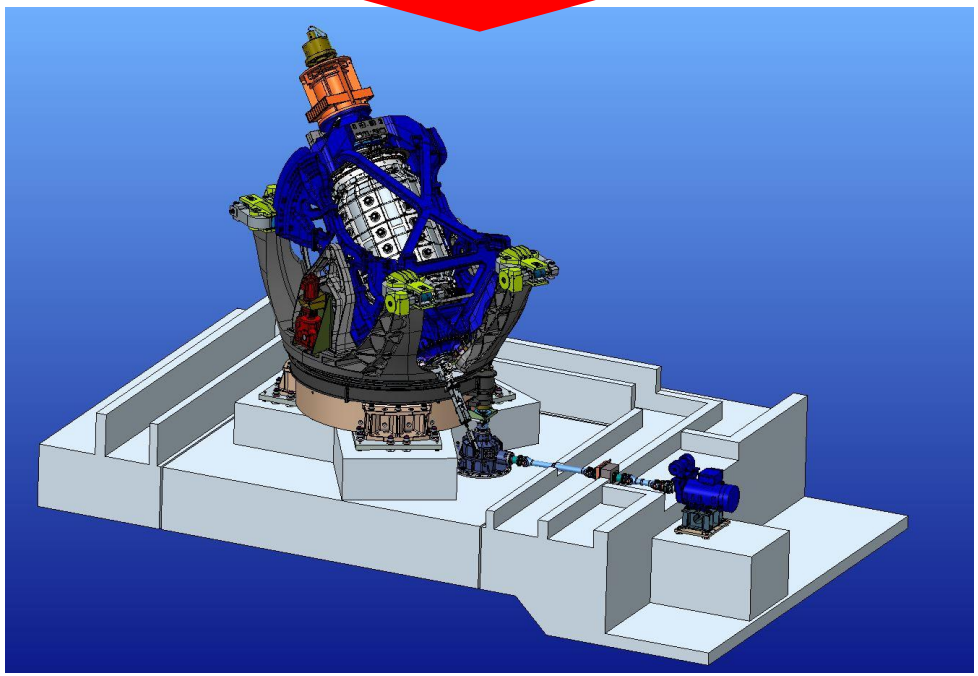

Influence of rosette-like motion on solar dynamo (spin-orbit coupling)

Precession driven dynamo within the DRESDYN project

Key parameters:

- Cylinder with 2 m diameter and 2 m height, 8 tons of liquid sodium
- Cylinder rotation: 10 Hz (will need some 800 kW motor power)
- Turntable rotation: 1 Hz
- Magnetic Reynolds number ~ 700
- Gyroscopic torque onto the basement: 8 MNm !

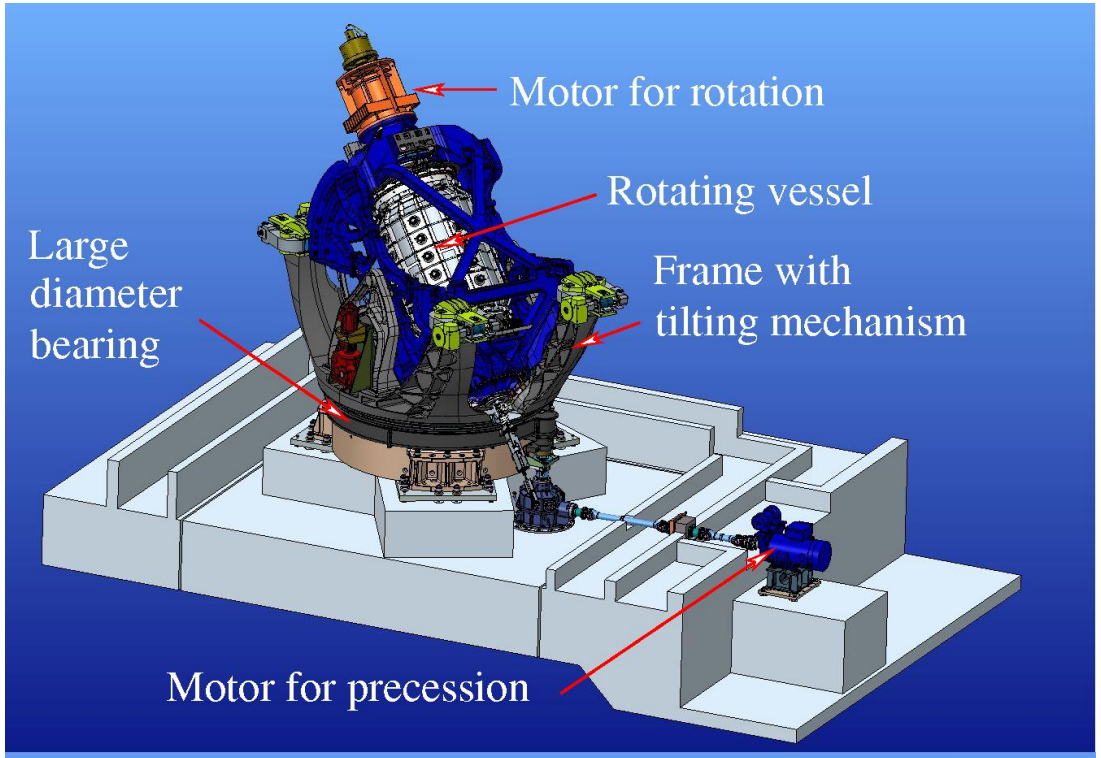

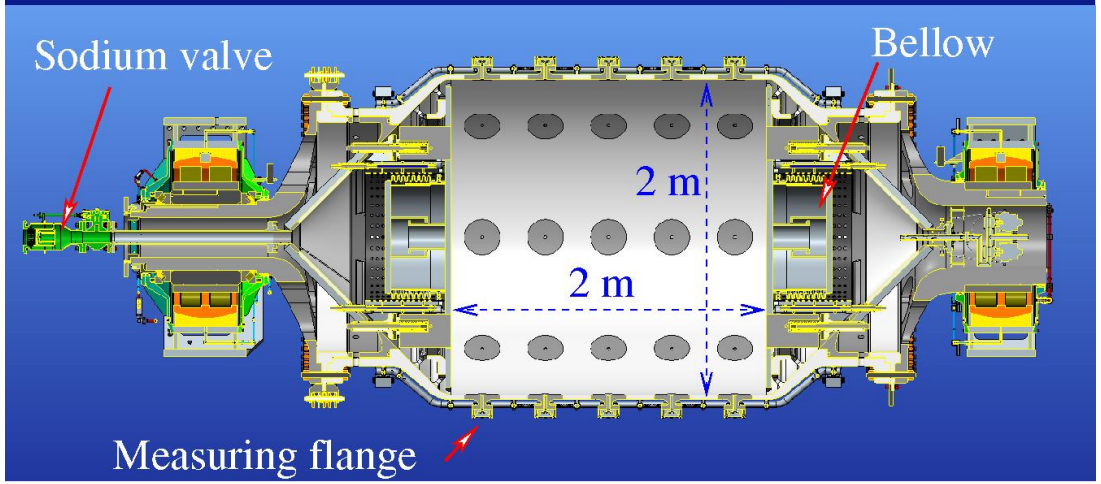

“Fundamental” problems due to huge gyroscopic torque

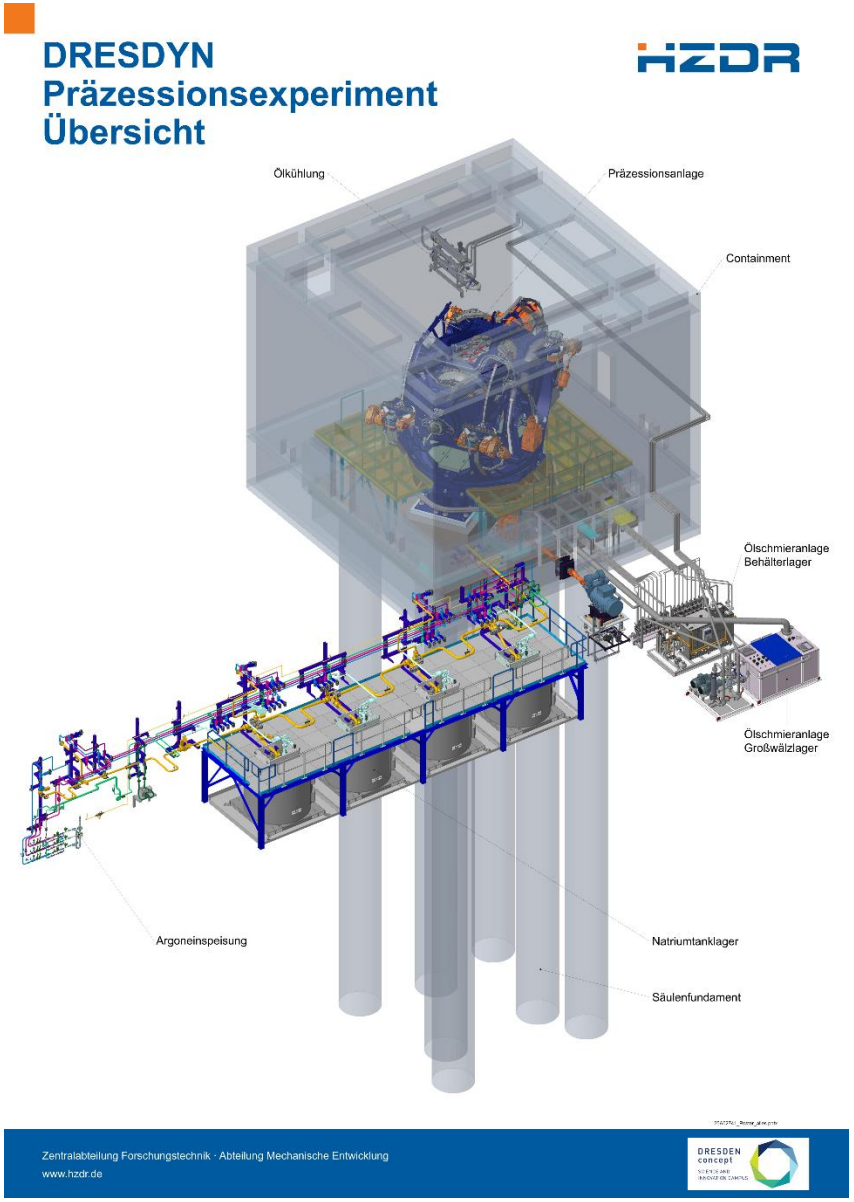

7 pillars going 22 m deep into the granite bedrock

DRESDEN concept

HZDR

“Fundamental” problems due to huge gyroscopic torque

April 2013: drilling 7 holes (22 m deep)

July 2013: Constructing the ferroconcrete basement

May 2015: The tripod for the dynamo within the containment (with stainless steel “wallpaper”)

Large ball bearing installed (12/2018)

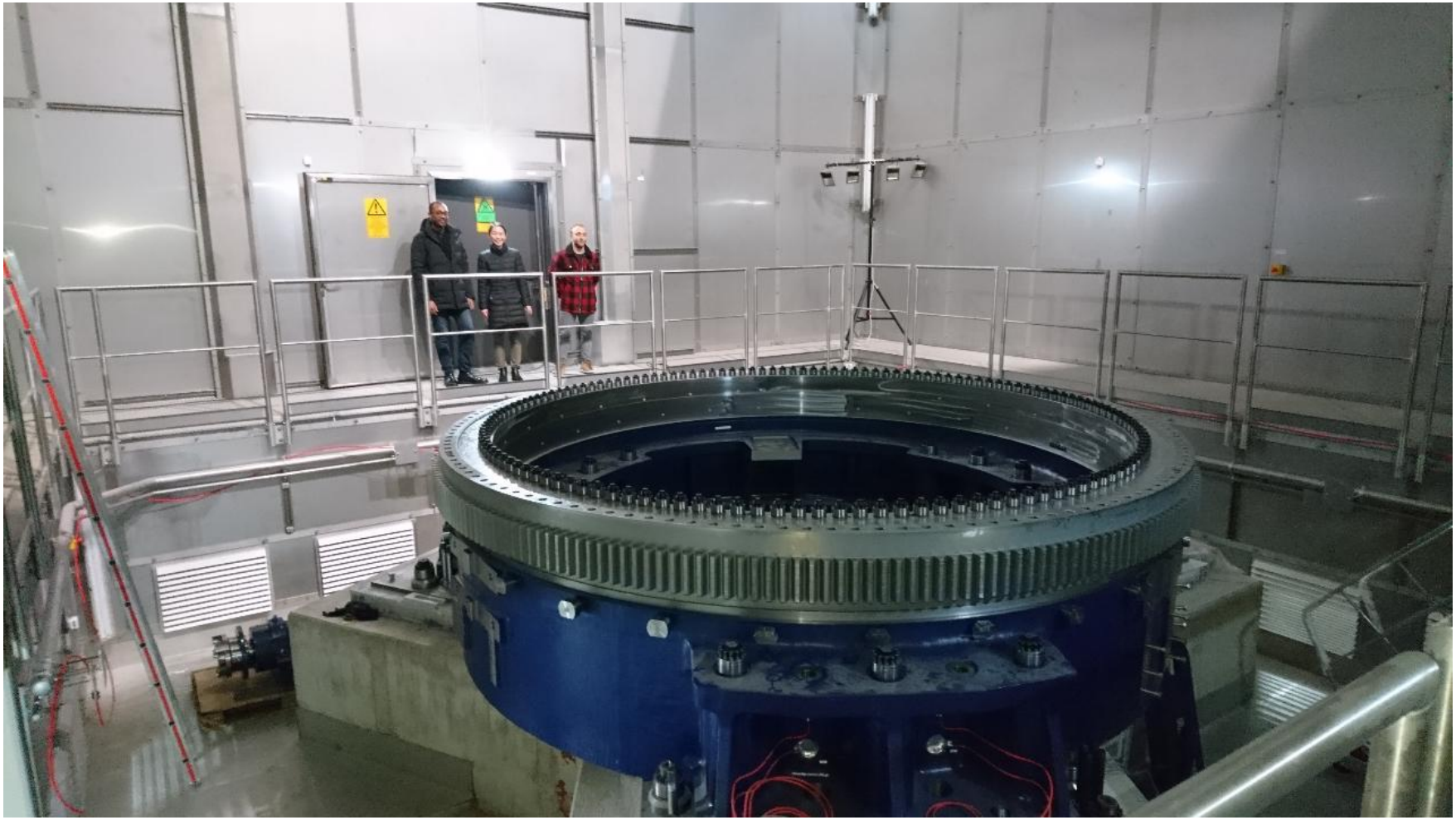

Traverse and pylons (01/2019)

Test assembly of the tilting frame (07/2019)

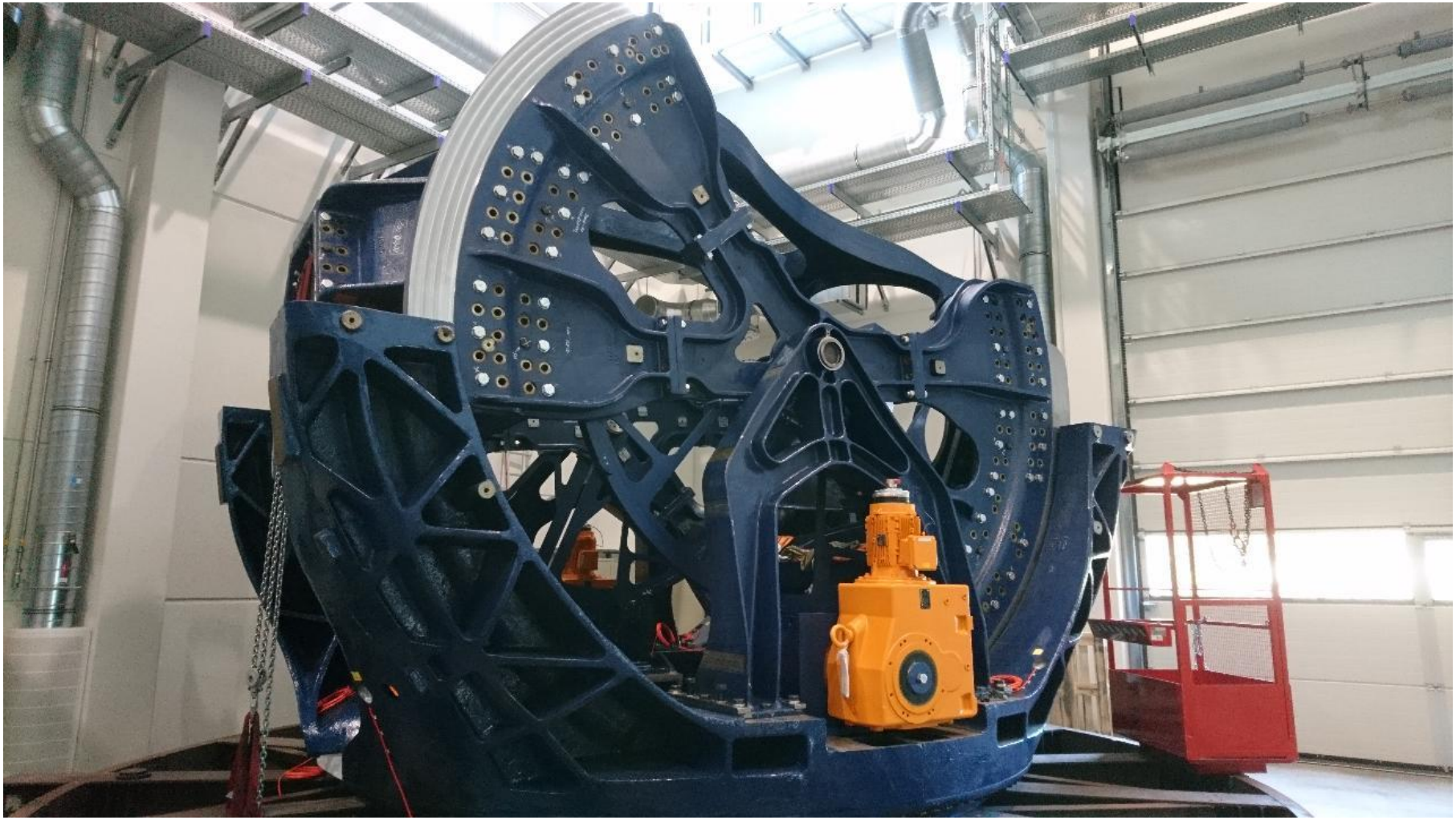

Pylons transferred to the containment (11/2019)

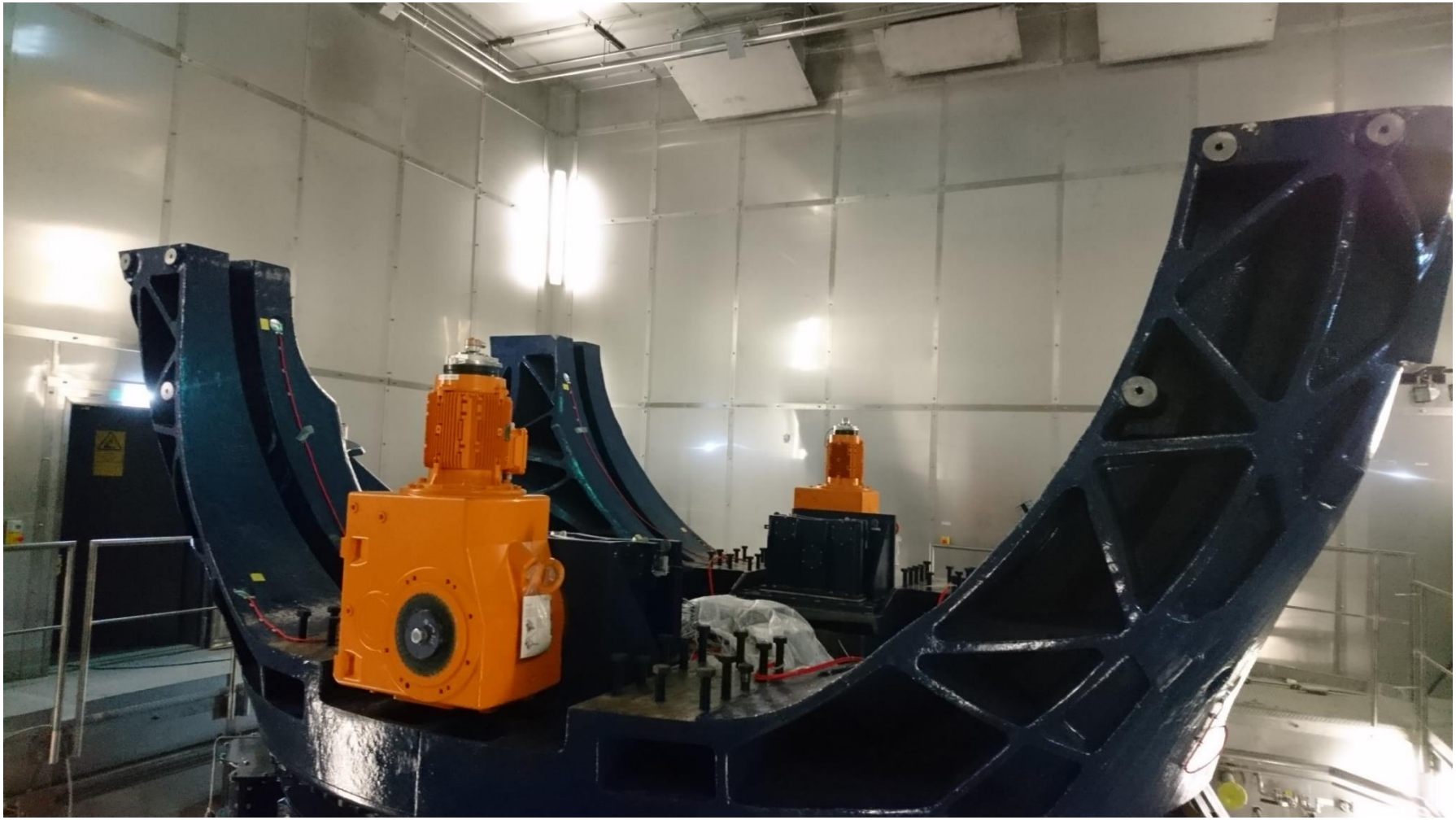

Pylons with central rotary connection (for 1 MW power and oil)

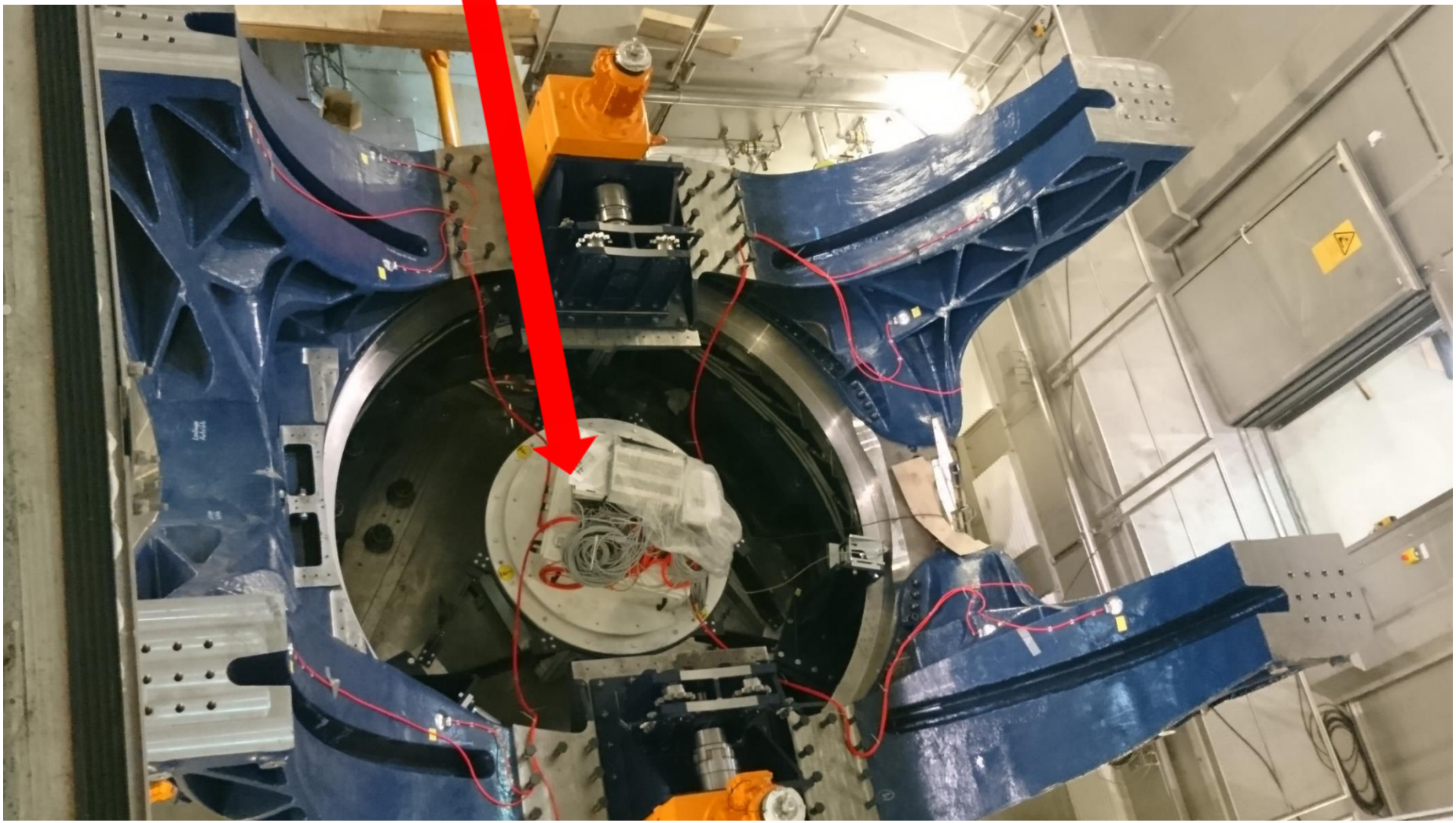

Rotation vessel with bearings

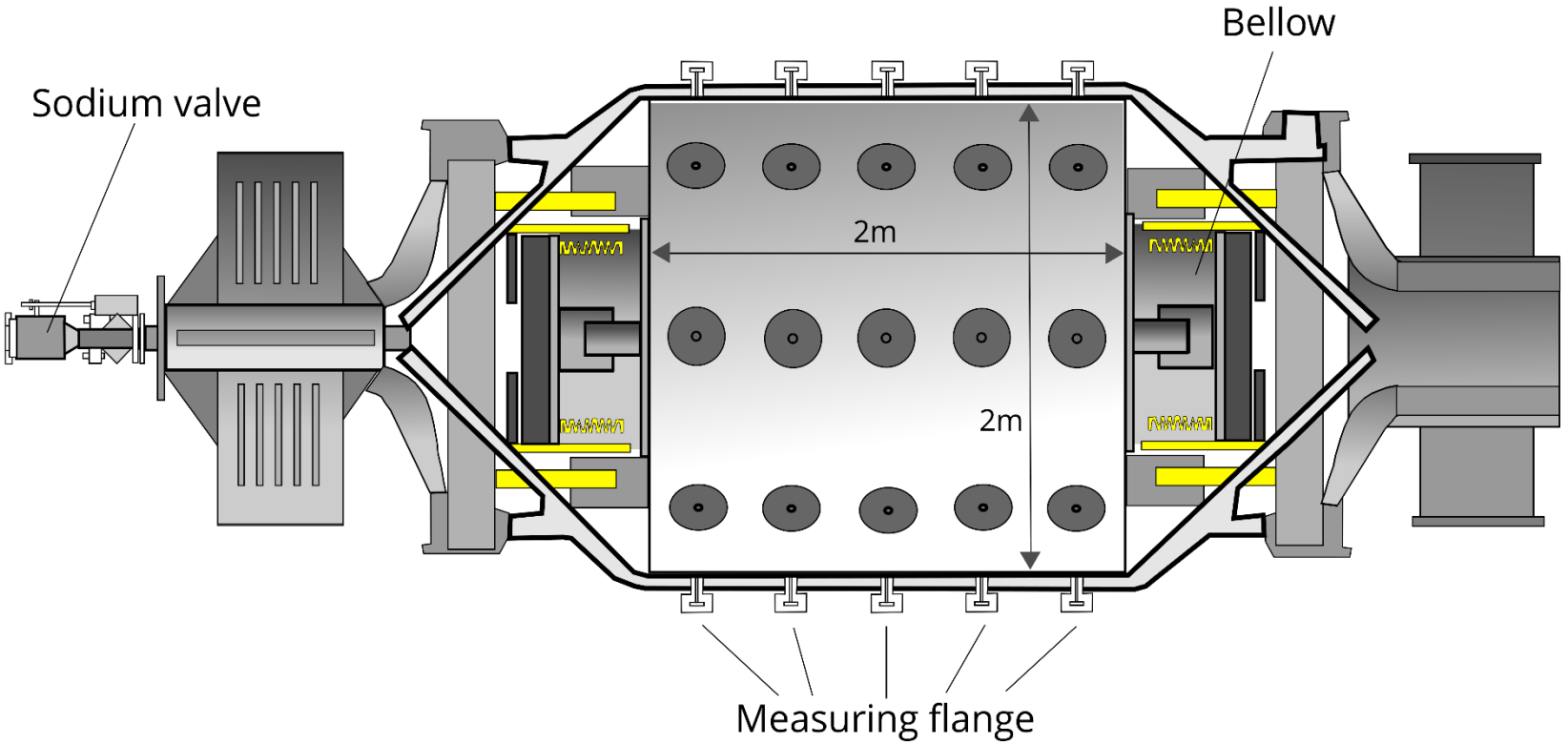

Pressure test (with 35 bar) of the rotation vessel (3/2019)

The vessel arrives at HZDR (July 3, 2020)

Assembly of the first conical end and the bearing (May 2022)

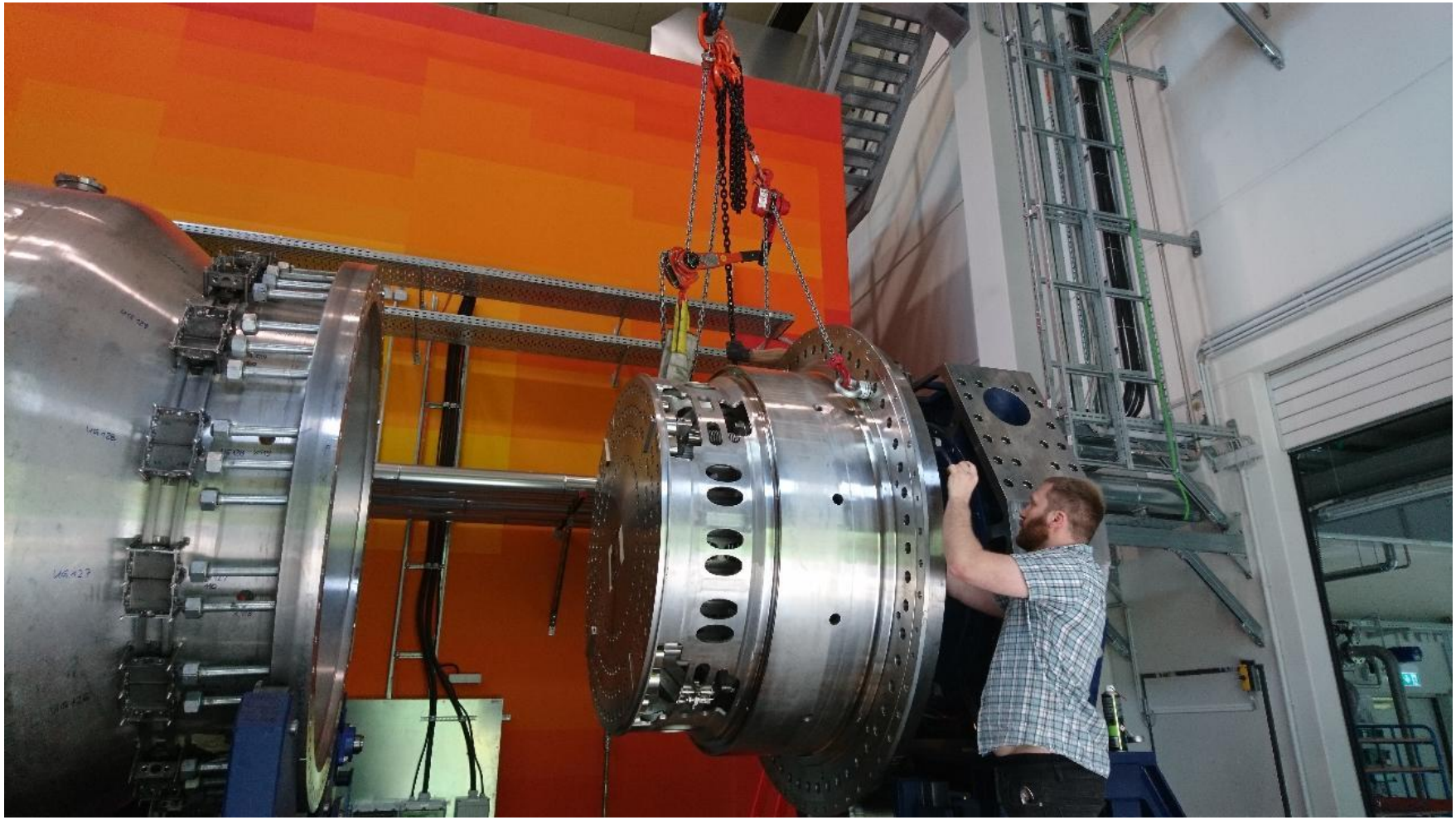

The “hell machine” in some detail

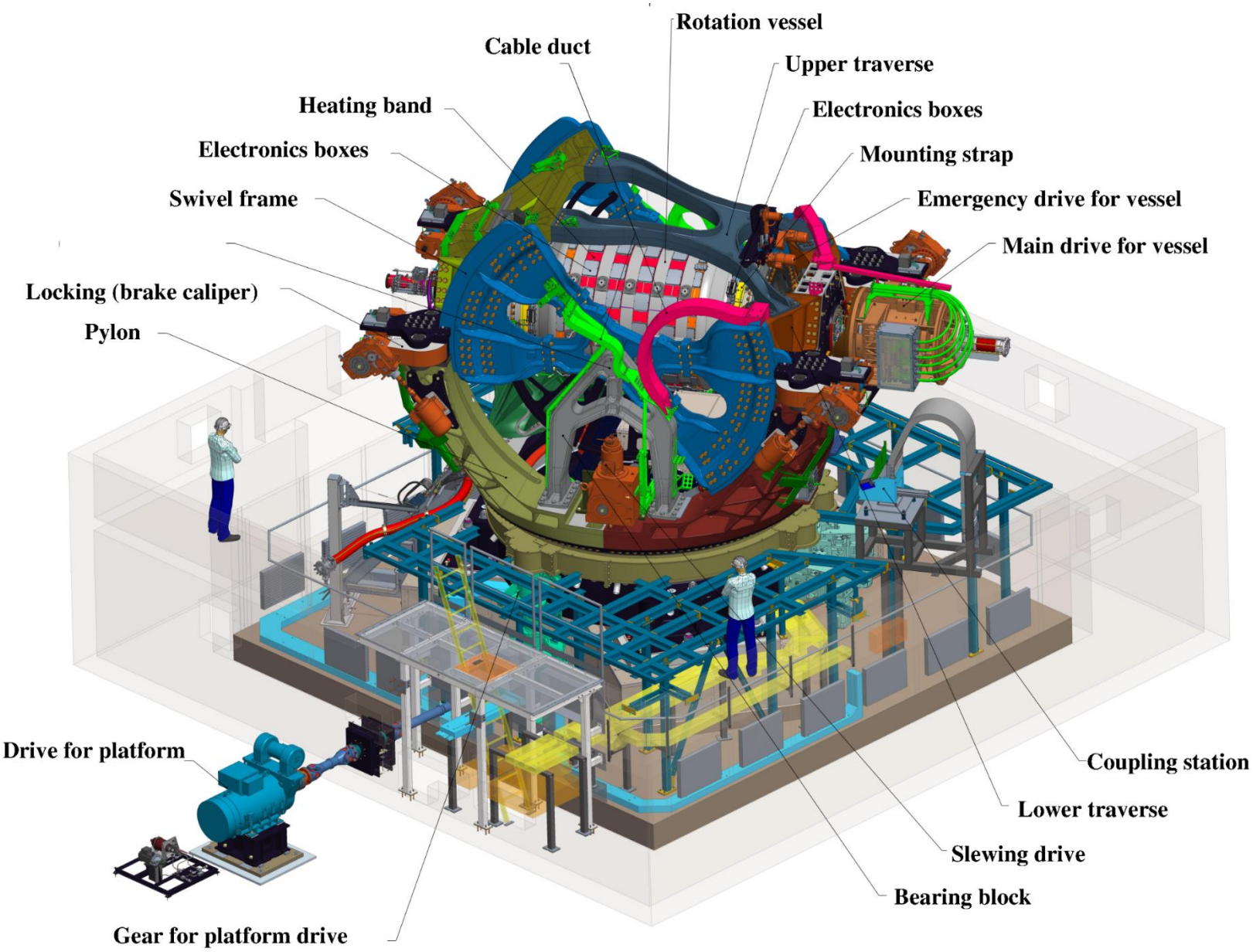

28. November 2024: The first water experiment (at 1 Hz)

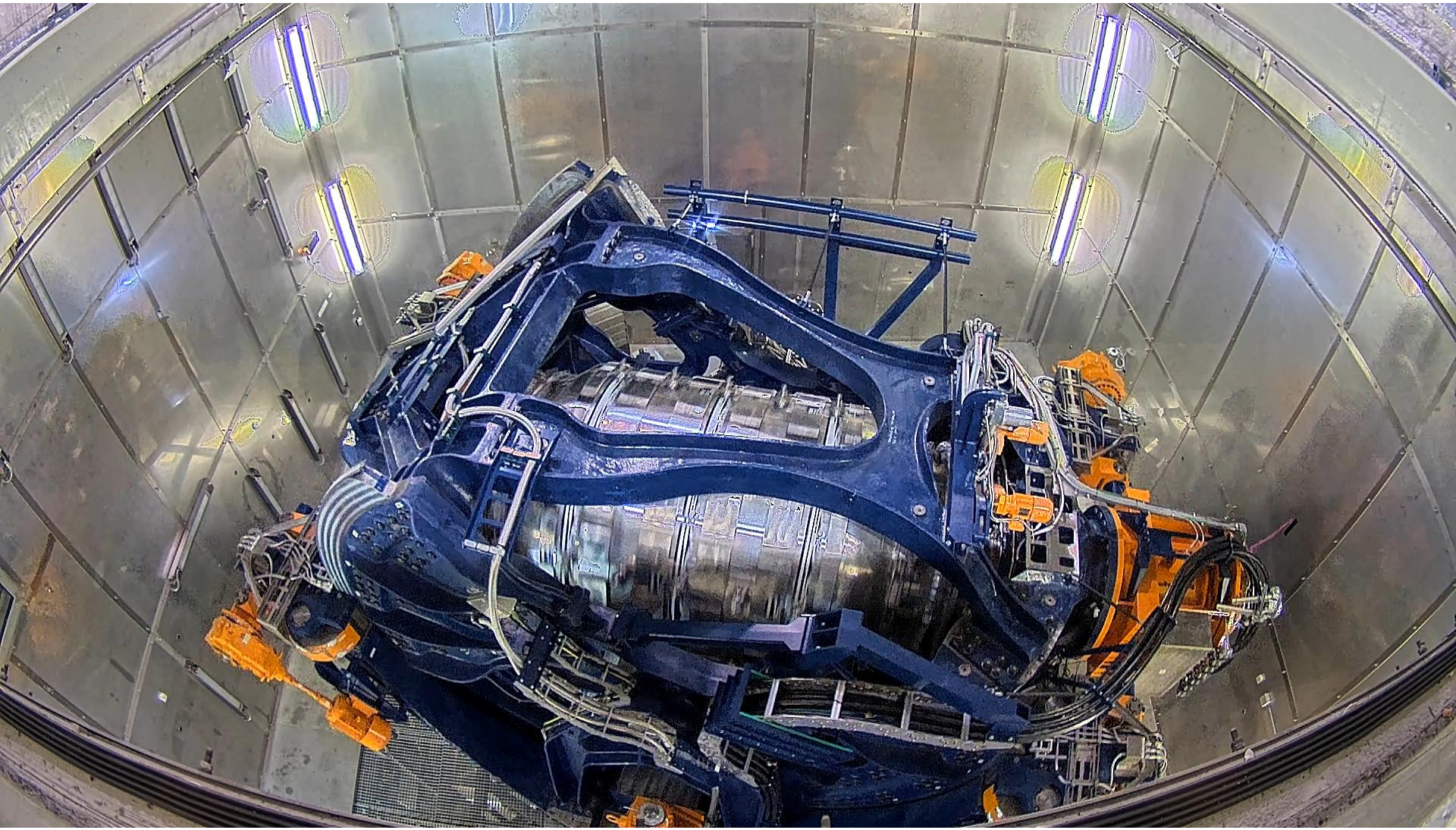

First runs with water (at 1 Hz) on 28 November 2024

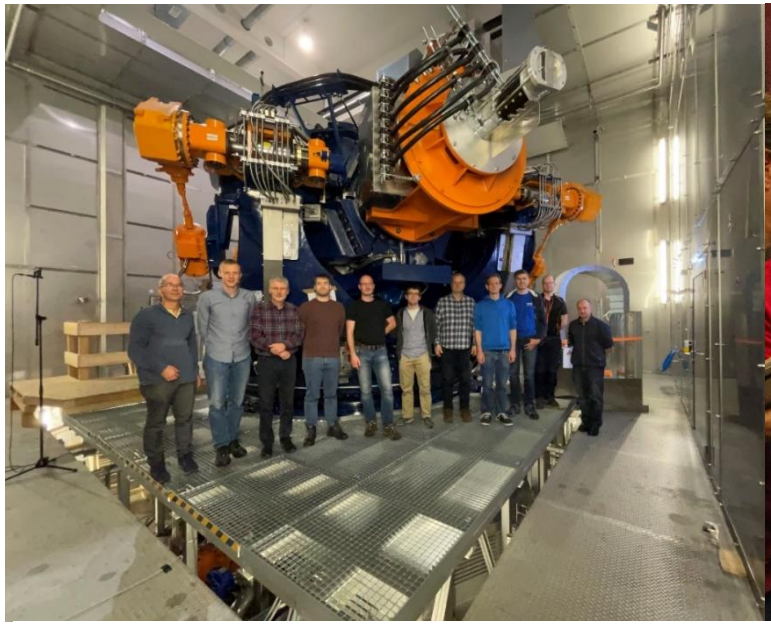

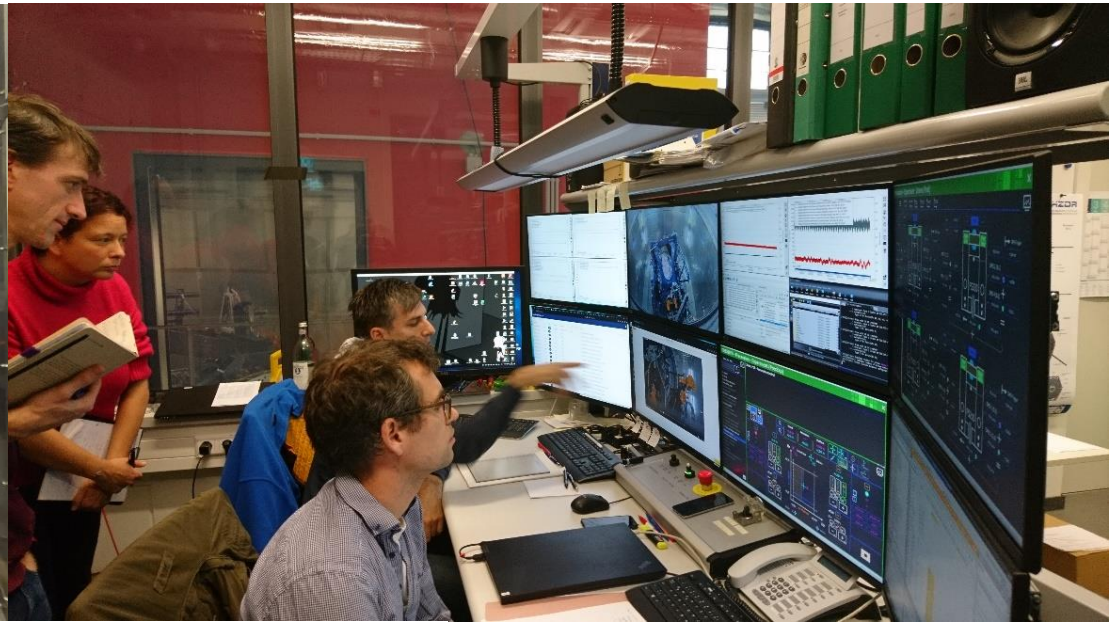

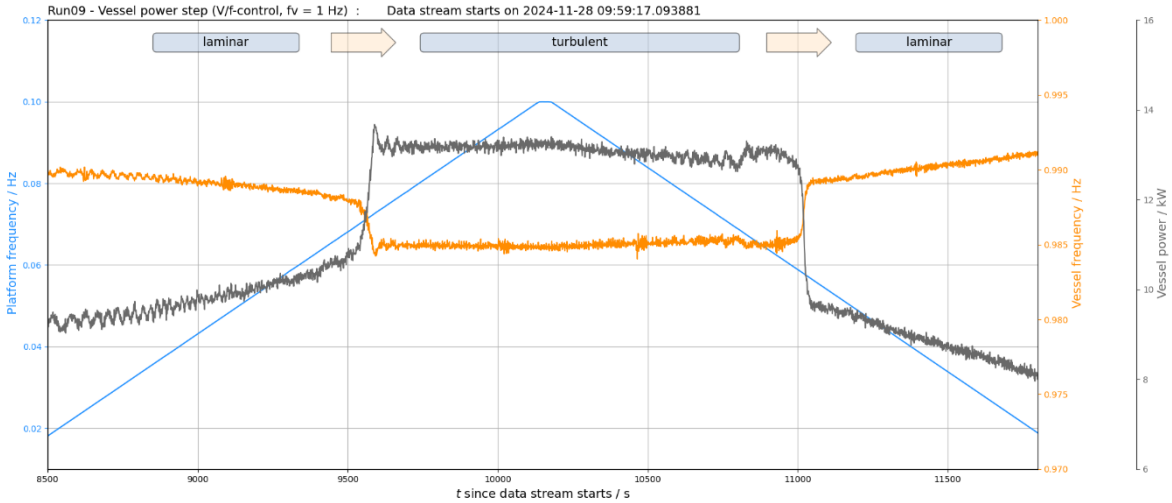

Transition laminar-turbulent observed at the expected precession ratio (with slight hysteres)

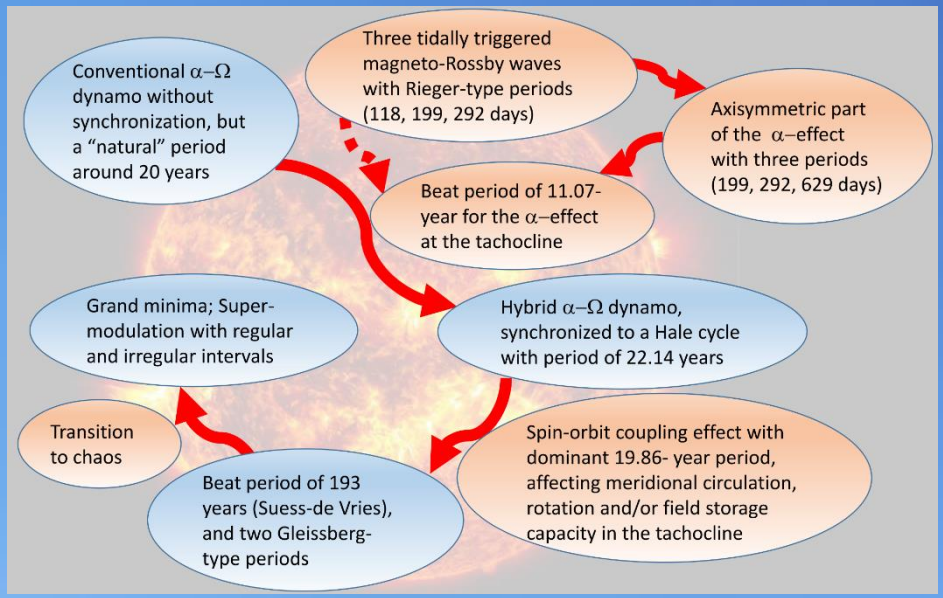

Thank you for your attention!